Missouri S&T Library and Learning Resources

Scholars' Mine

Doctoral Dissertations | Student Theses and Dissertations

1978

The effects of certain impurities and their interactions on zinc electrowinning

Donald R. Fosnacht

Follow this and additional works at: https://scholarsmine.mst.edu/doctoral_dissertations

Part of the Metallurgy Commons

Department: Materials Science and Engineering

Recommended Citation

Fosnacht, Donald R., "The effects of certain impurities and their interactions on zinc electrowinning" (1978). *Doctoral Dissertations*. 343.
https://scholarsmine.mst.edu/doctoral_dissertations/343

This thesis is brought to you by Scholars' Mine, a service of the Missouri S&T Library and Learning Resources. This work is protected by U. S. Copyright Law. Unauthorized use including reproduction for redistribution requires the permission of the copyright holder. For more information, please contact scholarsmine@mst.edu.

THE EFFECTS OF CERTAIN IMPURITIES AND THEIR INTERACTIONS ON ZINC ELECTROWINNING

By

DONALD RALPH FOSNACHT, 1950-

A DISSERTATION

Presented to the Faculty of the Graduate School of the

UNIVERSITY OF MISSOURI-ROLLA

In Partial Fulfillment of the Requirements for the Degree

DOCTOR OF PHILOSOPHY

in

METALLURGICAL ENGINEERING

1978

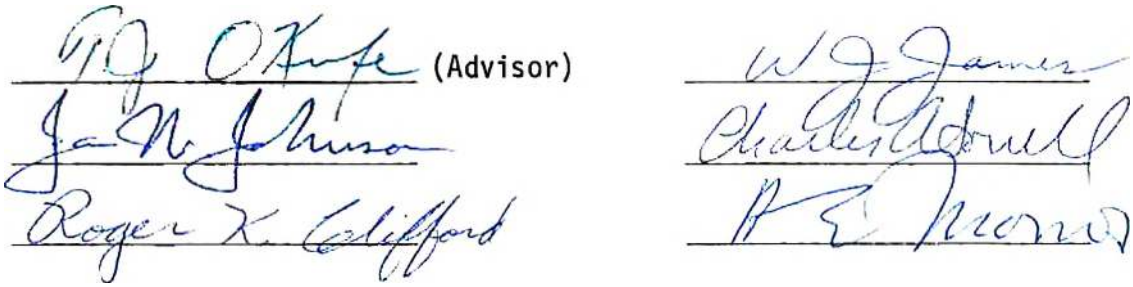

PUBLICATION THESIS OPTION

This thesis has been prepared in the style utilized by Metallurgical Transactions B. Pages 1-122 will be presented for publication in that Journal. Appendices A, B, C, D, E, F, G, H, and I have been added for purposes normal to thesis writing.

SYNOPSIS

The effects of germanium, antimony, arsenic, cobalt, glue, and free acid concentration were studied on both commercial and synthetic electrolytes. The effects of a single factor and the combined effects of multiple factors were elucidated. The temperature, zinc concentration, and current density were also varied. It was found that the acid concentration was the most critical factor when impurity levels were at normal plant solution concentrations. The ranges where the effect of the impurity became apparent were: greater than 20 ppb for antimony; 40 ppb for germanium; 120 ppb for arsenic; and 7-8 mg/l for cobalt for a solution containing 65 g/l zinc and 100 g/l free sulfuric acid. At higher levels of acid, the acceptable level of impurity declined markedly. Glue additions were found to counteract the effects of antimony and germanium, but did little to counteract the effects of cobalt and arsenic. The level of acid was found to be especially critical when cobalt and arsenic were in the electrolyte. Cobalt and arsenic exhibited synergism and lower current efficiencies were obtained for arsenic-cobalt combinations than expected. A factorially designed experiment was conducted to quantify the effects observed by one factor at a time testing. The effects of the various factors on electrode polarization were examined using cyclic voltammetry. Levels as low as 0.02 mg/l Ge and Sb and 0.1 mg/l Co cause measurable changes in polarization. The polarization characteristics of combinations of impurities and glue can be used to determine the optimum levels of glue addition. The structure of the deposits was examined using x-ray diffraction and scanning electron microscopy.

ACKNOWLEDGEMENTS

This work is dedicated to my wife, Vicki, whose sacrifice, encouragement, and patience helped make it possible.

I would like to express my appreciation to all the members of my committee for all their constructive criticisms and useful discussions that were invaluable during the course of my research. A special debt of gratitude is owed to Dr. Thomas J. O'Keefe, my advisor, who provided keen insight and guidance throughout the course of this research effort. I would also especially like to thank Dr. Roger K. Clifford for the many fruitful discussions concerning the use of statistical designs and Dr. William J. James whose incessant wisdom and experience greatly aided in the evaluation of the results and in preparing the final manuscript. I would like to acknowledge Dr. Yar-Ming Wang for his helpful advice and assistance concerning this study. The technical assistance provided by Messrs. Harlan Rice, Kenny Allison, Jack Smart, and Ms. Laura Jean Blaser is also greatly appreciated.

I wish to acknowledge the financial assistance provided by the AMAX Foundation, New York, NY, and the technical assistance provided by Cominco Ltd., Trail, British Columbia, Canada, and AMAX Zinc Company, Sauget, IL. I would also like to thank ASARCO, Inc., Hillsboro, IL, for providing the French process zinc oxide used in this study.

Finally, a great deal of thanks is owed to Ms. Nina Haas for her efforts in typing the manuscript.

TABLE OF CONTENTS

Page

PUBLICATION THESIS OPTION..... ii

SYNOPSIS..... iii

ACKNOWLEDGEMENTS..... iv

LIST OF FIGURES..... x

LIST OF TABLES..... xvii

The Effects of Certain Impurities and Their Interactions on Zinc Electrowinning..... 1

Abstract..... 1

Introduction..... 2

Experimental..... 4

Factorial Design..... 4

Solution Preparation..... 4

Electrode Preparation..... 7

Electrolysis..... 8

Results and Discussion..... 9

Current Efficiency Tests..... 9

Statistical Analysis..... 9

Effect of Current Density..... 12

Effect of the Design Variables..... 14

Acid Effects..... 15

Antimony, Arsenic, and Germanium Effects..... 15

Cobalt Effects and Interactions with Acid..... 19

Interaction of Arsenic, Antimony and Germanium with Acid..... 21

Table of Contents (Continued)

Page

Effects of Temperature..... 24

The Effects of Glue Addition..... 24

Interactions Among Impurities..... 30

Summary of the Results..... 34

Development of the Statistical Model..... 34

Deposit Morphologies..... 39

Addition-free Electrolyte..... 41

Arsenic-Containing Solutions..... 41

Solutions Containing Glue..... 41

Solutions Containing Antimony, Germanium, or Cobalt.. 43

Solutions Containing Germanium and Glue Combinations. 45

Conclusions..... 51

Acknowledgements..... 52

References..... 53

List of Figures..... 57

Evaluation of Zinc Sulfate Electrolytes Containing Certain Impurities and Additives by Cyclic Voltammetry and Electron Microscopy..... 60

Abstract..... 60

Introduction..... 61

Experimental..... 63

Solution Preparation..... 63

Cyclic Voltammetry..... 65

Results and Discussion..... 68

Voltammograms for No-Addition Electrolytes..... 68

Table of Contents (Continued)

Page

Voltammograms for Electrolytes Containing Germanium of Cobalt Additions..... 73

Factors Affecting the Co and Ge Voltammograms..... 83

Zinc Concentration..... 83

Acid Concentration..... 83

Surface Roughness..... 83

Impurity Concentration and Temperature..... 88

Test Time..... 88

Apparent Mechanism of Germanium and Cobalt Interaction at the Working Electrode..... 92

Voltammogram for Electrolytes Containing Antimony..... 94

Voltammograms for Electrolytes Containing Glue..... 99

Effects of Glue-Impurity Combinations on Zinc Polarization Behavior..... 102

Antimony-Glue Combinations..... 102

Combinations of Glue With Germanium or Cobalt..... 103

Possible Applications of this Technique..... 113

Conclusions..... 115

Acknowledgements..... 116

References..... 117

List of Figures..... 120

VITA..... 123

APPENDICES..... 124

A. Literature Review..... 124

A. Importance of the Zinc Electrowinning Process..... 124

Table of Contents (Continued)

Page

B. Effects of the Main Process Parameters..... 124

1. Acid and Zinc Levels..... 125

2. Temperature and Current Density..... 126

3. Agitation..... 127

C. Importance of Solution Purity..... 128

1. General Characteristics..... 128

2. Mechanisms of Impurity Interaction..... 130

3. Cathodic Polarization and Deposit Morphology..... 137

4. Review of General Impurity Effects..... 140

5. Individual Impurity Characteristics..... 140

a. Antimony..... 140

b. Arsenic..... 143

c. Cadmium..... 144

d. Cobalt..... 145

e. Copper..... 149

f. Germanium..... 150

g. Iron..... 152

h. Manganese..... 153

i. Nickel..... 155

j. Action of Additives..... 157

k. Lead and Anode Factors..... 160

D. Commentary of Past and Future Research..... 162

B. Bibliography..... 166

C. Experimental Values for the Current Efficiency Tests..... 176

D. Calculated Factor Effects for the Experimental Design.... 214

Table of Contents (Continued)

Page

E. Statistical Evaluation of the Fit of the Model to the Experimental System for the Factorial Design and Determination of Curvature..... 220

F. Method of Computation Used to Determine the Factor Effects and Calculated Current Efficiencies for the Statistically-Designed Experiment..... 221

G. Determination of Zinc Concentration by EDTA Titration..... 223

H. Analysis of Zinc Oxide Powder Used to Prepare Neutral Purified Solution..... 225

I. Possible Future Research..... 226

LIST OF FIGURES

The Effects of Certain Impurities and Their Interactions on Zinc Electrowinning

Figures — Page

1. Current Efficiency vs Current Density for Industrial Electrolytes Containing 60 g/ℓ Zn and 200 g/ℓ H_2SO_4. T = 40°C..... 13
2. Current Efficiency vs Acid Concentration for Industrial Electrolytes Containing 60 g/ℓ Zn. T = 40°C; Current Density = 40 mA/cm^2..... 16
3. Current Efficiency vs Impurity Concentration for Prepared Electrolytes Containing 65 g/ℓ Zn and 200 g/ℓ H_2SO_4. T = 45°C; Current Density = 40 mA/cm^2..... 18
4. Current Efficiency vs Cobalt Concentration for Prepared Electrolytes Containing 65 g/ℓ Zn and Various Acid Concentrations. T = 45°C; Current Density = 40 mA/cm^2..... 20
5. Current Efficiency vs Antimony Concentration for Prepared Electrolytes Containing 65/ℓ Zn and Various Acid Concentrations. T = 45°C; Current Density = 40 mA/cm^2.. 22
6. Current Efficiency vs Germanium Concentration for Prepared Electrolytes Containing 65 g/ℓ Zn and Various Acid Concentrations. T = 45°C; Current Density = 40 mA/cm^2..... 23
7. Current Efficiency vs Acid Concentration for Prepared Electrolytes Containing 65 g/ℓ Zn and 80 ppb As. T = 45°C; Current Density = 40 mA/cm^2..... 25

List of Figures (Continued)

Figures Page

8. Current Efficiency vs Organic Additive Concentration for Prepared Electrolytes Containing 65 g/ℓ Zn and 100 g/ℓ H_2SO_4. T = 45°C; Current Density = 40 ma/cm^2... 27

9. Current Efficiency vs Glue Concentration for Prepared Electrolytes Containing 65/ℓ Zn, 100 g/ℓ H_2SO_4 and Constant Amounts of Impurity Addition. T = 45°C; Current Density = 40 mA/cm^2..... 29

10. Current Efficiency vs Cobalt Concentration for Prepared Electrolytes Containing 65 g/ℓ Zn and 100 g/ℓ H_2SO_4 With and Without 28 ppb Sb. T = 45°C; Current Density = 40 mA/cm^2..... 31

11. Current Efficiency vs Germanium Concentration for Prepared Electrolytes Containing 65 g/ℓ Zn and 100 g/ℓ H_2SO_4 With and Without 5 mg/ℓ Co. T = 45°C; Current Density = 40 mA/cm^2..... 33

12. Calculated Current Efficiency vs Experimental Current Efficiency for Results of the Factorial Design..... 37

13. Deposit Obtained for a No-addition Electrolyte. T = 45°C; Current Density = 40 mA/cm^2. (1000x)..... 42

14. Deposit Obtained for an Electrolyte Containing 0.1 mg/ℓ As. T = 45°C; Current Density = 40 mA/cm^2. (1000x).... 42

15. Deposit Obtained for an Electrolyte Containing 21 mg/ℓ Glue. T = 45°C; Current Density = 40 mA/cm^2. (1000x).. 44

16. Deposit Obtained for an Electrolyte Containing 0.026 mg/ℓ Sb. T = 45°C; Current Density = 40 mA/cm^2. (1000x) 44

List of Figures (Continued)

Figures Page

17. Deposit Obtained for an Electrolyte Containing 5 mg/ℓ Co. T = 45°C; Current Density = 40 mA/cm^2. (1000x).... 46

18. Deposit Obtained for an Electrolyte Containing 0.1 mg/ℓ Ge. T = 45°C; Current Density = 40 mA/cm^2. (1000x).... 46

19. Deposit Obtained for an Electrolyte Containing 0.1 mg/ℓ Ge and 6 mg/ℓ Glue. T = 45°C; Current Density = 40 mg/ℓ cm^2. (1000x)..... 48

20. Deposit Obtained for an Electrolyte Containing 0.1 mg/ℓ Ge and 13 mg/ℓ Glue. T = 45°C; Current Density = 40 mA/cm^2. (1000x)..... 48

21. Deposit Obtained for an Electrolyte Containing 0.1 mg/ Ge and 21 mg/ Glue. T = 45°C; Current Density = 40 mA/cm^2. (1000x)..... 49

LIST OF FIGURES

Evaluation of Zinc Sulfate Electrolytes Containing Certain Impurities and Additives by Cyclic Voltammetry and Electron Microscopy

Figures — Page

1. Schematic of Equipment Used for the Cyclic Voltammetry Experiments. [C = Working Electrode (Al); R = Mercurous Sulfate Reference Electrode; A = Auxiliary Electrode (Pt); V = Voltage Monitoring Terminals; and I = Current Supply Terminals]..... 66
2. Voltammogram for No-Addition Electrolyte. T = 45°C; Scan Rate = 0.5 mV/sec..... 70
3. Hydrogen Current Density vs Electrode Potential for Electrolytes Containing 200 g/ℓ H_2SO_4 and the Indicated Additions. T = 45°C; Scan Rate = 0.5 mV/sec..... 72
4. Voltammogram Obtained for Electrolytes Containing Germanium or Cobalt Additions. T = 45°C; Scan Rate = 0.5 mV/ℓ sec..... 74
5. Sequence of Changes that Occur at Points i and ai as the Impurity Concentration Increases for Electrolytes Containing Germanium or Cobalt Additions..... 75
6. Peak Current Density vs Cobalt Content. Scan Rate = 0.5 mV/sec..... 76
7. Zinc Deposit Obtained for Electrolyte Containing 65 g/ℓ Zn and 200 g/ℓ H_2SO_4. Potential Held at Point D for 1 Minute. (3000x)..... 80

List of Figures (Continued)

Figures Page

8. Zinc Deposit Obtained for Electrolyte Containing 65 g/ℓ Zn, 200 g/ℓ H_2SO_4, and 100 ppb Ge. Potential Held at Point D for 1 Minute. (3000x)..... 81

9. Zinc Deposit Obtained for Electrolyte Containing 65 g/ℓ Zn, 200 g/ℓ H_2SO_4, and 8 mg/ℓ Co. Potential Held at Point D for 1 Minute. (3000x)..... 82

10. Peak Current Density vs Zinc Concentration. Scan Rate = 0.5 mV/sec; T = 45°C..... 84

11. Peak Current Density vs Acid Concentration. Scan Rate = 0.5 mV/sec; T = 45°C..... 85

12. Hydrogen Current Density vs Electrode Potential for Electrolytes Containing 6.5 g/ℓ Zn and Various H_2SO_4 Concentrations. Scan Rate = 0.5 mV/sec; T = 45°C..... 86

13. Peak Current Density vs Cobalt Concentration for Working Electrodes Having Different Surface Preparation. Scan Rate = 0.5 mV/sec; T = 45°C..... 87

14. Peak Current Density vs Germanium Concentration. Scan Rate = 0.5 mV/sec; T = 45°C..... 89

15. Peak Current Density vs Cobalt Concentration for Various Temperatures. Scan Rate = 0.5 mVsec..... 90

16. Peak Current Density vs Cobalt Concentration. Fast Scan (5 mV/sec) to Point D then Slow Scan (0.5 mV/sec) back to Starting Potential..... 91

17. Voltammogram Obtained for Electrolytes Containing Antimony Additions. T = 45°C; Scan Rate = 0.5 mV/sec..... 95

List of Figures (Continued)

Figures Page

18. Zinc Deposit Obtained for Electrolyte Containing 65 g/ℓ Zn, 200 g/ℓ H_2SO_4, and 104 ppb Sb. Potential Held at Point D for 1 Minute. (3000x)..... 98

19. Voltammogram Obtained for Electrolytes Containing Glue Additions. T = 45°C; Scan Rate = 0.5 mV/sec..... 100

20. Zinc Deposit Obtained for Electrolyte Containing 65 g/ℓ Zn, 200 g/ℓ H_2SO_4, and 10 mg/ℓ Glue. Potential Held at Point D for 1 Minute. (3000x)..... 101

21. Voltammogram Obtained for Electrolytes Containing Glue and Cobalt or Germanium Additions. T = 45°C; Scan Rate = 0.5 mV/sec..... 104

22. Potential at Point X vs Glue Concentration for Electrolytes Containing Germanium Additions. T = 45°C; Scan Rate = 0.5 mV/sec..... 105

23. Potential at Point X vs Glue Concentration for Electrolytes Containing Cobalt Additions. T = 45°C; Scan Rate = 0.5 mV/sec..... 106

24. Peak Current Density vs Glue Concentration for Electrolytes Containing Germanium Additions. T = 45°C; Scan Rate = 0.5 mV/sec..... 107

25. Peak Current Density vs Glue Concentration for Electrolytes Containing Cobalt Additions. T = 45°C; Scan Rate = 0.5 mv/sec..... 108

List of Figures (Continued)

Figures Page

26. Zinc Deposit Obtained for Electrolyte Containing 65 g/ℓ Zn, 200 g/ℓ H_2SO_4, and 8 mg/ℓ Co. Potential Held at -0.785 V vs S.H.E. for 1 Minute. (3000x)..... 110

27. Zinc Deposit Obtained for Electrolytes Containing 65 g/ℓ Zn, 200 g/ℓ H_2SO_4, 8 mg/ℓ Co, and 10 mg/ℓ Glue. Potential Held at -0.785 V vs S.H.E. for 1 Minute. (3000x)..... 111

LIST OF TABLES

The Effects of Certain Impurities and Their Interactions on Zinc Electrowinning

Tables		Page
I.	Factors Used in the Design	5
II.	Analyses of Neutral Purified Solutions (mg/ℓ)	6
III.	Factors Shown to be Significant for Confidence Level = 0.99	10
IV.	Calculated Factor Effects for Antimony, Germanium, and Arsenic	17
V.	Coded Factors Used in the Model	35
VI.	Comparison of Calculated and Experimentally Obtained Current Efficiencies for Other Factor Levels	38
VII.	Zinc Deposit Crystallographic Orientations	40

LIST OF TABLES

Evaluation of Zinc Sulfate Electrolytes Containing Certain Impurities and Additives by Cyclic Voltammetry and Electron Microscopy

Tables		Page
I.	Analysis of Neutral Purified Solution (mg/ℓ).....	64
II.	Possible Reactions Occurring at the Working Electrode.....	69
III.	Comparison of Zinc Deposition Potential and Potential at Point x for Electrolytes With and Without Impurity Addition.....	79
IV.	Comparison of Current Densities Obtained for 200 g/ℓ H_2SO_4 Electrolytes With and Without 104 ppb Sb.....	96

LIST OF TABLES

Appendices

Tables		Page
I.	Composition of Cell Feed for a Zinc Electrolysis Circuit as Reported in the Literature.[159]	131
II.	Estimated Reversible Potentials Based on Concentrations Approximating Commercial Practice.[159] pH = 0	132
III.	Effect of Antimony and Glue Additions on Crystal Orientation and Polarization	139
IV.	Current Efficiency Results for the Factorial Design	176
V.	Current Efficiencies for the Center Points and Analysis of Variance for the Factorial Design	183
VI.	Current Efficiency Results for 12 hour Deposits at 45°C from the Base Electrolyte	184
VII.	Current Efficiency Results for 12 hour Deposits at 40°C from Industrial Electrolyte Containing 60 g/ℓ Zn and 200 g/ℓ H_2SO_4	185
VIII.	Current Efficiency Results for 12 hour Deposits at 40°C from Industrial Electrolytes Containing 60 g/ℓ Zn and Various Concentrations of H_2SO_4	186
IX.	Current Efficiency Results for 12 hour Deposits at 45°C from Electrolytes Containing Antimony and 100 g/ℓ H_2SO_4	187
X.	Current Efficiency Results for 12 hour Deposits at 45°C Electrolytes Containing Antimony and 150 g/ℓ H_2SO_4	188

Appendices (Continued)

Tables Page

XI. Current Efficiency Results for 12 hour Deposits at 45°C from Electrolytes Containing Arsenic and 100 g/ℓ H_2SO_4 189

XII. Current Efficiency Results for 12 hour Deposits at 45°C from Electrolytes Containing Arsenic and Varying Acid Concentrations 190

XIII. Current Efficiency Results for 12 hour Deposits at 45°C from Electrolytes Containing Cobalt and 100 g/ℓ H_2SO_4 191

XIV. Current Efficiency Results for 12 hour Deposits at 45°C from Electrolytes Containing Cobalt and 150 g/ℓ H_2SO_4 192

XV. Current Efficiency Results for 12 hour Deposits at 45°C from Electrolytes Containing Germanium and 100 g/ℓ H_2SO_4 193

XVI. Current Efficiency Results for 12 hour Deposits at 45°C from Electrolytes Containing Germanium and 150 g/ℓ H_2SO_4 195

XVII. Current Efficiency Results for 12 hour Deposits at 45°C from Electrolytes Containing Glue and 100 g/ℓ H_2SO_4 196

XVIII. Current Efficiency Results for 12 hour Deposits at 45°C from Electrolytes Containing Gum Arabic and 100 g/ℓ H_2SO_4 197

Appendices (Continued)

Tables

		Page
XIX.	Current Efficiency Results for 12 hour Deposits at 45°C from Electrolytes Containing Chloride and 100 g/ℓ H_2SO_4	198
XX.	Current Efficiency Results for 12 hour Deposits at 45°C from Electrolytes Containing Antimony and Germanium and 100 g/ℓ H_2SO_4	199
XXI.	Current Efficiency Results for 12 hour Deposits at 45°C from Electrolytes Containing Antimony and Glue and 100 g/ℓ H_2SO_4	200
XXII.	Current Efficiency Results for 12 hour Deposits at 45°C from Electrolytes Containing Antimony and Gum Arabic and 100 g/ℓ H_2SO_4	201
XXIII.	Current Efficiency Results for 12 hour Deposits at 45°C from Electrolytes Containing Cobalt and Antimony and 100 g/ℓ H_2SO_4	202
XXIV.	Current Efficiency Results for 12 hour Deposits at 45°C from Electrolytes Containing Cobalt, Antimony, and Glue and 100 g/ℓ H_2SO_4	203
XXV.	Current Efficiency Results for 12 hour Deposits at 45°C from Electrolytes Containing Cobalt and Germanium and 100 g/ℓ H_2SO_4	204
XXVI.	Current Efficiency Results for 12 hour Deposits at 45°C from Electrolytes Containing Cobalt, Germanium, and Glue and 100 g/ℓ H_2SO_4	205

Appendices (Continued)

Tables		Page
XXVII.	Current Efficiency Results for 12 hour Deposits at 45°C from Electrolytes Containing Cobalt and Glue and 100 g/ℓ H_2SO_4	206
XXVIII.	Current Efficiency Results for 12 hour Deposits at 45°C from Electrolytes Containing Germanium and Glue and 100 g/ℓ H_2SO_4	207
XXIX.	Current Efficiency Results for 12 hour Deposits at 45°C from Electrolytes Containing Glue and Chloride and 100 g/ℓ H_2SO_4	208
XXX.	Current Efficiency Results for 12 hour Deposits at 45°C from Electrolytes Containing Gum Arabic and Chloride and 100 g/ℓ H_2SO_4	209
XXXI.	Current Efficiency Results for 24 hour Deposits at 45°C from Electrolytes Containing Various Impurities and 100 g/ℓ H_2SO_4	210
XXXII.	Current Efficiency Results for 12 hour Deposits at 45°C from Electrolytes Containing Arsenic and Other Impurities and 100 g/ℓ H_2SO_4	211
XXXIII.	Current Efficiency Results for 12 hour Deposits at 35°C from Electrolytes Containing Various Impurities and 100 g/ℓ H_2SO_4	212
XXXIV.	Current Efficiency Results for 12 hour Deposits at 35°C from Electrolytes Containing Various Impurities and 200 g/ℓ H_2SO_4	213

Appendices (Continued)

Table Page

XXXV. Factors and Factor Effects for the Factorial Design... 214

The Effects of Certain Impurities and Their Interactions on Zinc Electrowinning

Donald R. Fosnacht and Thomas J. O'Keefe

Abstract

The effects of germanium, antimony, arsenic, cobalt, glue, and free acid concentration were studied on both commercial and synthetic electrolytes. The effects of a single factor and the combined effects of multiple factors were elucidated. The temperature, zinc concentration, and current density were varied. It was found that the acid concentration was the most critical factor when impurity levels were at normal plant solution concentrations. The ranges where the effect of the impurity became apparent were: greater than 20 ppb for antimony; 40 ppb for germanium; 120 ppb for arsenic; and 7-8 mg/l for cobalt for a solution containing 65 g/l zinc and 100 g/l free sulfuric acid. At higher levels of acid, the acceptable level of impurity declined markedly. Glue additions were found to counteract the effects of antimony and germanium, but did little to counteract the effects of cobalt and arsenic. The level of acid was found to be especially critical when cobalt and arsenic were in the electrolyte. Cobalt and arsenic exhibited synergism and lower current efficiencies were obtained for arsenic-cobalt combinations than expected. A factorially designed experiment was conducted to quantify the effects observed by one factor at a time testing. The structure of the deposits was examined using x-ray diffraction and scanning electron microscopy.

Introduction

The presence of impurities in the electrolyte is a major problem for the zinc electrowinning industry. Many investigations have been conducted to determine the impurity interactions occurring at the cathode and the maximum level of each impurity that can be tolerated in the electrolyte (1-31). Neutral purification eliminates the bulk of the impurities, but in certain instances their concentrations may still be high enough to cause difficulties in zinc deposition. Impurity behavior is not well understood and many questions remain regarding the acceptable limits of impurities for efficient operation of a zinc electrolysis circuit. In addition, synergism among impurities may occur which further complicates the process and causes unpredictable behavior (56-57). Factors such as acid level, zinc concentration, time of electrolysis, agitation, current density, and temperature also influence the magnitude of the impurity effects.

It is well documented that zinc deposition is very sensitive to small quantities of certain impurities. Previous studies have indicated that levels in the parts per billion range for antimony, arsenic, and germanium can greatly reduce the current efficiency (3-21). For cobalt, the parts per million range is critical (22-31). A complicated purification process is used to try and reach these low levels in actual practice (1,2,58).

The effects of an impurity are often directly attributable to such factors as acid concentration and the temperature of the system involved. Thus, the maximum allowable levels of the impurities must be considered in relation to the process parameters. In addition to

current efficiency, deposit morphology and cathodic polarization are also influenced by the levels of impurities and addition agents in the electrolyte. Profound changes in both these features have been reported (17-19,55)

Organic agents such as glue are often added to the electrolyte to aid in process control. Improvements in deposit appearance and current efficiency may occur when glue is added to the electrolyte, but optimum levels do exist and must not be exceeded or certain deleterious effects can result (17-19).

Since impurity interactions can create severe operating problems, it would be desirable to determine the basis for many of their interactions and make the process more predictable.

This study examines the effects of antimony, arsenic, cobalt, germanium, and glue on current efficiency and deposit morphology at various temperatures and acid concentrations. In order to evaluate the effects of these variables simultaneously, a factorially designed set of experiments was conducted. High and low levels of each parameter were chosen to approximate industrial conditions (1,2). A total of 128 tests were conducted using all possible combinations of the seven factors and the results were used to establish the relative importance of each factor and also determine what important interactions may exist. Once these were established, additional tests were performed to confirm the trends. In addition, a model was generated using these results which allows prediction of the effects of the chosen variables at other levels.

Experimental

Factorial Design

The factors chosen and the two levels of each factor as well as their symbols are given in Table I. The concentration levels indicated are in addition to the concentrations of the impurities already in the base electrolyte. The analysis of the neutral solution used for the base electrolyte is given in Table II.

One replicate of the experimental design consisting of 128 tests was conducted. In addition, 13 center point tests and a select number of duplicate tests were conducted to estimate the experimental variance of the system. The tests were randomized using a table of random numbers in order to eliminate the systematic error involved in the experiment.

Solution Preparation

A stock solution of neutral (pH = 4.0 - 4.5) purified zinc sulfate solution was prepared by using high purity, French process zinc oxide powder and reagent grade sulfuric acid. The zinc sulfate solution was purified by adding 0.1 to 0.2 ml/l of 0.1 N $KMnO_4$; heating to near the boiling point with vigorous stirring; settling of the precipitates for 30 minutes at 80 to 85°C and then filtering. The filtrate was then purified by adding 2 g/l of zinc dust; heating to the boiling point with stirring for 30 to 45 minutes and then filtering to remove excess zinc dust.

A volume of neutral purified solution, sufficient to yield a base electrolyte concentration of 65 g/l, was used.

A stock solution containing 13 mg/l of antimony was prepared by dissolving antimony potassium tartrate in distilled water. Cobalt

Table I. Factors Used in the Design.

	Symbol	Low Level*	High Level*
Temp. (°C)	t	35	45
H_2SO_4 (g/l)	a	100	200
Ge (mg/l)	g	0	0.04
Sb (mg/l)	s	0	0.026
Co (mg/l)	c	0	2.4
As (mg/l)	r	0	0.04
Glue (mg/l)	o	6	20

*For the impurity concentrations, these are the additional levels of impurity over and above those already in the base electrolyte.

Table II. Analysis of Neutral Purified Solution (mg/ℓ).

	Prepared	Industrial
Zn	130,000	170,000
Mn	<0.1	3,500
Cd	1.3	1.7
Sb	0.01	--
As	<0.04	--
Sb + As	--	0.04
Ge	0.002	0.004
Co	<0.1	0.1
Ni	<0.05	<0.05
Fe	0.4	5.9
Cu	0.08	0.3
F^-	0.1	1.0
Cl^-	1.0	370

solution was prepared by dissolving cobaltous sulfate in distilled water to a level of 800 mg/l. Stock solutions of germanium and arsenic of 10 mg/l were also prepared. The germanium was dissolved in sulfuric acid after GeO_2 was fused with K_2CO_3 and Na_2CO_3. As_2O_3 was used to prepare the arsenic solution. All of the stock solutions were analyzed by using atomic absorption analysis. The solutions of the impurities were stored in plastic bottles and analyzed periodically.

Stock solutions of glue (Swift--EZ TPC #3) and gum arabic of 1 g/l were prepared by dissolving the organic in distilled water and storing under refrigeration to minimize degradation.

Test solutions were prepared by taking the required amount of neutral purified, reagent grade sulfuric acid, impurity solution and organic addition agent, and placing them in a 1 liter volumetric flask. The volume was adjusted to one liter by adding distilled water.

Electrode Preparation

Two anodes, consisting of platinum wire gauze, and one cathode of type 3003 aluminum were used for electrolysis. The aluminum cathodes were prepared by polishing with 320 grit paper then rinsing with tap water and distilled water and finally drying in hot air. The electrodes were weighed and then placed in a Plexiglass electrode assembly which maintained the same electrode spacing for each experiment. The anodes had a slightly larger area than the cathodes. The area of cathode exposed to the electrolyte was adjusted to maintain a constant current of 800 mA over a 12 hour deposition period.

Electrolysis

The cells were connected in series in a controlled temperature water bath (±0.5°C). A constant current power supply (HP6284A) was used and the total number of coulombs passed during electrolysis was recorded by an amp-time meter (Pulsco Model 20) which had been calibrated with a copper coulometer. An ammeter was used to adjust the current to the desired value. During the electrolysis, solution levels were maintained by adding distilled water at set intervals. No mechanical stirring was employed, but natural convection due to gas evolution provided some natural stirring.

After electrolysis, the cathodes were rinsed with both tap water and distilled water, and then dried and weighed. The current efficiency was calculated based on the recorded weight and the total amount of coulombs passed. The morphology and crystal orientations of the deposits were then checked by scanning electron microscopy and x-ray diffraction.

Results and Discussion

Current Efficiency Tests

Statistical Analysis The calculated cathode efficiencies were statistically analyzed using a digital computer according to the "table of signs" method (32). The use of the experimental design permits the estimation of the factor effects more precisely than one-factor at a time testing because of hidden replication in the design. The size of the design employed reduces the effects of variations of single observations on the calculated factor effects. The variability of the calculated factor effects is only 0.18 that of a single observation as calculated by the precision ratio ($\sigma_{FE}/\sigma_{OBS} = 0.18$).

In order to determine the variability of the observations, 13 center point tests were conducted along with duplication of 6 of the factorial tests. The factorial tests duplicated were chosen at random. The pooled standard deviation in the current efficiency for the tests was 4.86%. The current efficiencies obtained for the experimental design ranged from 0 to 94 percent.

The significance of the factor effects and the curvature of the system were analyzed by calculating the minimum significant effect statistics (32). If a computed factor effect is larger than the calculated statistic, it can be concluded that the true effect is non-zero. The magnitude of the calculated factor effect gives an indication of the importance of the factor for the system. The larger the magnitude, the greater the importance of the factor. Since the design has a great deal of hidden replication, a significance level of 0.99 was used to calculate the minimum significant

Table III. Factors Shown to be Significant for Confidence Level = 0.99.

Factor	Calculated Factor Effect
Mean	58.99
a	-37.275
c	-23.603
t	-16.475
so	13.815
o	13.284
g	-11.322
ac	-11.287
r	-9.631
asc	9.437
s	-9.190
go	6.678
cr	-6.331
as	5.106
ts	-4.844
tco	-4.525
gscro	4.375
agscro	4.316
tago	-4.166
cro	-4.125
ar	-3.884
gr	3.744

Table III (Continued)

Factor	Calculated Factor Effect
aro	-3.641
acro	-3.509
ta	-3.275
ao	3.119
ags	3.094
acr	-3.041
tgo	-3.100
tgscr	-3.009
tsro	-3.003
tgcro	2.953
asco	-2.844
gs	-2.703
co	2.591
ag	-2.587
tac	2.541
tso	-2.506
gso	2.497
tg	-2.481
tao	-2.478
tagso	-2.397
agso	-2.381
agro	-2.272
agco	2.262

effect statistics. The "t" statistic used in the calculation was $t_{0.99} = 2.55$ for 18 degrees of freedom (33). At this confidence level, the minimum significant factor effect was found to be 2.2 and the minimum significant curvature effect was determined to equal to 4.1. Therefore, for a factor to be considered significant it must exceed 2.2 and for the system to have significant curvature, the curvature factor must exceed 4.1.

The effect of current density was not measured in the factorial study, but was examined in other tests and will be considered later. The significant factors and the calculated factor effects determined by using the factorial design appear in Table III. Before a detailed discussion of the results of the factorial analysis is given, the effect of variation of current density on current efficiency will be discussed.

Effect of Current Density Figure 1 illustrates the effects of increasing the current density. A commercial plant electrolyte containing 60 g/l Zn and 200 g/l H_2SO_4 was used for this study. The cell temperature was maintained at 40°C. As can be seen, the greatest change occurs from 30 to 40 mA/cm^2. After this point the current efficiency continues to increase, but to a lesser extent. It must be recognized that if other factors such as temperature, morphology, dendrite growth, etc. which depend on the current density are not controlled, an adverse effect on the current efficiency may occur upon increasing the current density. However, if these factors are controlled, there are a number of reasons why increasing the current density should improve the current efficiency. First, the overvoltage of hydrogen discharge increases at a faster rate than that of

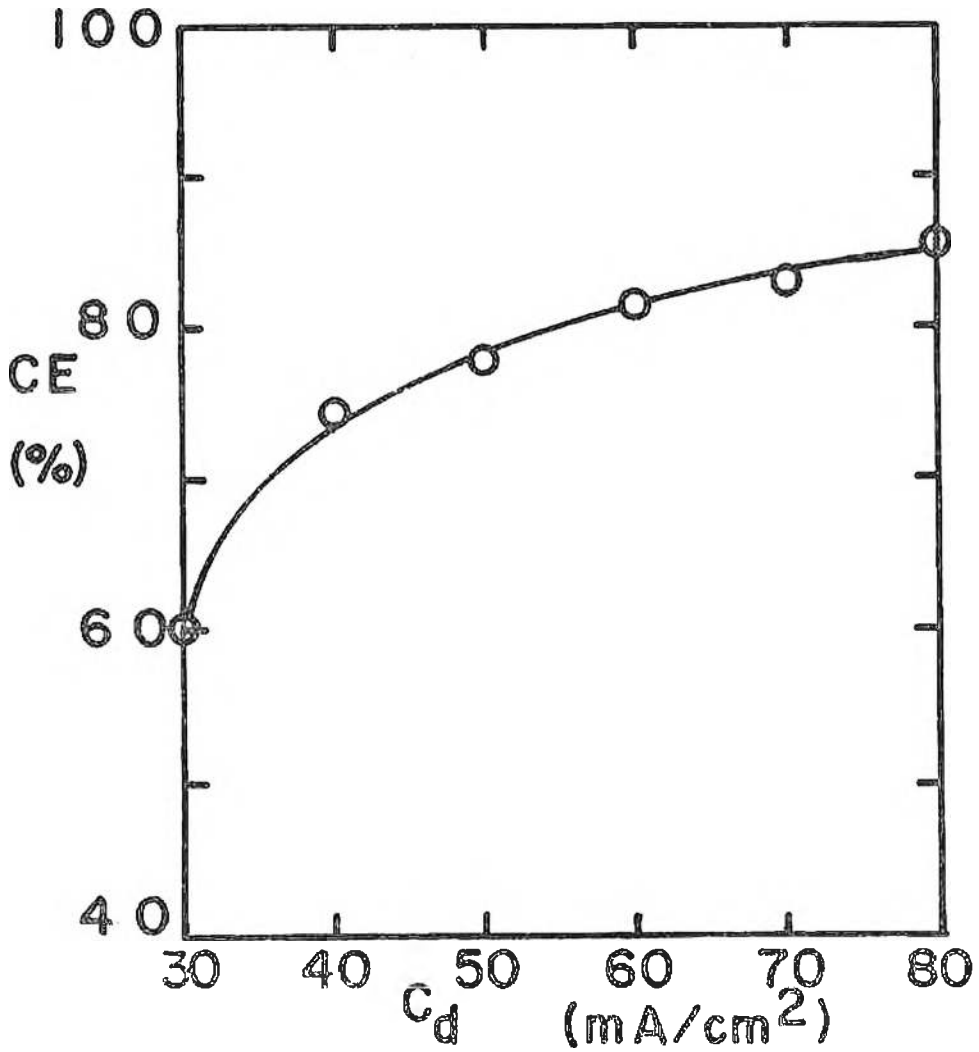

Figure 1. Current Efficiency vs Current Density for Industrial Electrolytes Containing 60 g/ℓ Zn and 200 g/ℓ H_2SO_4. T = 40°C.

zinc discharge as the current density increases, which enables the zinc ions to utilize a greater percentage of the applied current (34). Also, the effect of the impurities in the electrolyte is lessened, because the relative amount of impurities depositing with the zinc decreases because their rate of deposition is diffusion controlled and the zinc deposition rate is not (35). Finally, at very low current densities, the cathodic protection of the deposited zinc is relatively weak and significant dissolution of the deposit may occur. The dissolution process is suppressed at higher current densities.

The current densities used for this study range from 40 to 70 mA/cm^2. A current density of 60 mA/cm^2 was used for the factorial design. Other tests conducted to confirm the effects of the factorial design were conducted at 40 mA/cm^2. This current density was used because conditions are slightly more severe at this level and the effects of the impurities are somewhat magnified. Additional tests conducted to gain an understanding of the effects of acid concentration were conducted at 70 mA/cm^2. This current density was used because plants operating at higher acid concentrations generally use higher current densities (1,2)

Effects of the Design Variables The effects of the single factors chosen for the study were all shown to be significant. Of the factors considered, acid level had the largest effect on reducing the current efficiency, followed in degree of influence by cobalt, temperature, antimony, germanium, and arsenic. The addition of glue to the electrolyte increased the current efficiency and was the only positive single factor. The results indicate that increasing any of the other factors to higher levels causes the zinc current efficiency

to drop.

Acid Effects A more detailed study was conducted for the acid factor because of its significantly detrimental influence on current efficiency. Industrially produced, neutral purified zinc sulfate was used to make an electrolyte containing 60 g/l Zn. The electrolyses were conducted at 40°C and 70 mA/cm^2. The results appear in Figure 2 and show that the current efficiency begins to decline noticeably between 150 and 250 g/l in a non-linear fashion. The slight increase upon adding some acid is due to the increased conductivity and lower viscosity of the solution which reduce dendrite formation (36). Choosing operating ranges at high acid levels may cause large current efficiency fluctuations if the acid level varies significantly about the operating point. For example, if an operating level of 200 g/l H_2SO_4 is chosen and the variability about this point is ±20 g/l, the current efficiency obtained may range from 75 to 86 percent. Such variation would be quite unsatisfactory.

Antimony, Arsenic, and Germanium Effects The factors for antimony, germanium and arsenic will be considered together because these impurities often have been reported to act similarly (3-21). For convenience, the calculated effects are repeated in Table IV. The value for antimony has been adjusted to allow a comparison with germanium and arsenic on an equal concentration basis. The values of the factors indicate that all three impurities cause decreases in current efficiency. Antimony has the largest effect, followed by germanium, and then arsenic. A series of tests using the base electrolyte from the factorial analysis were conducted to confirm

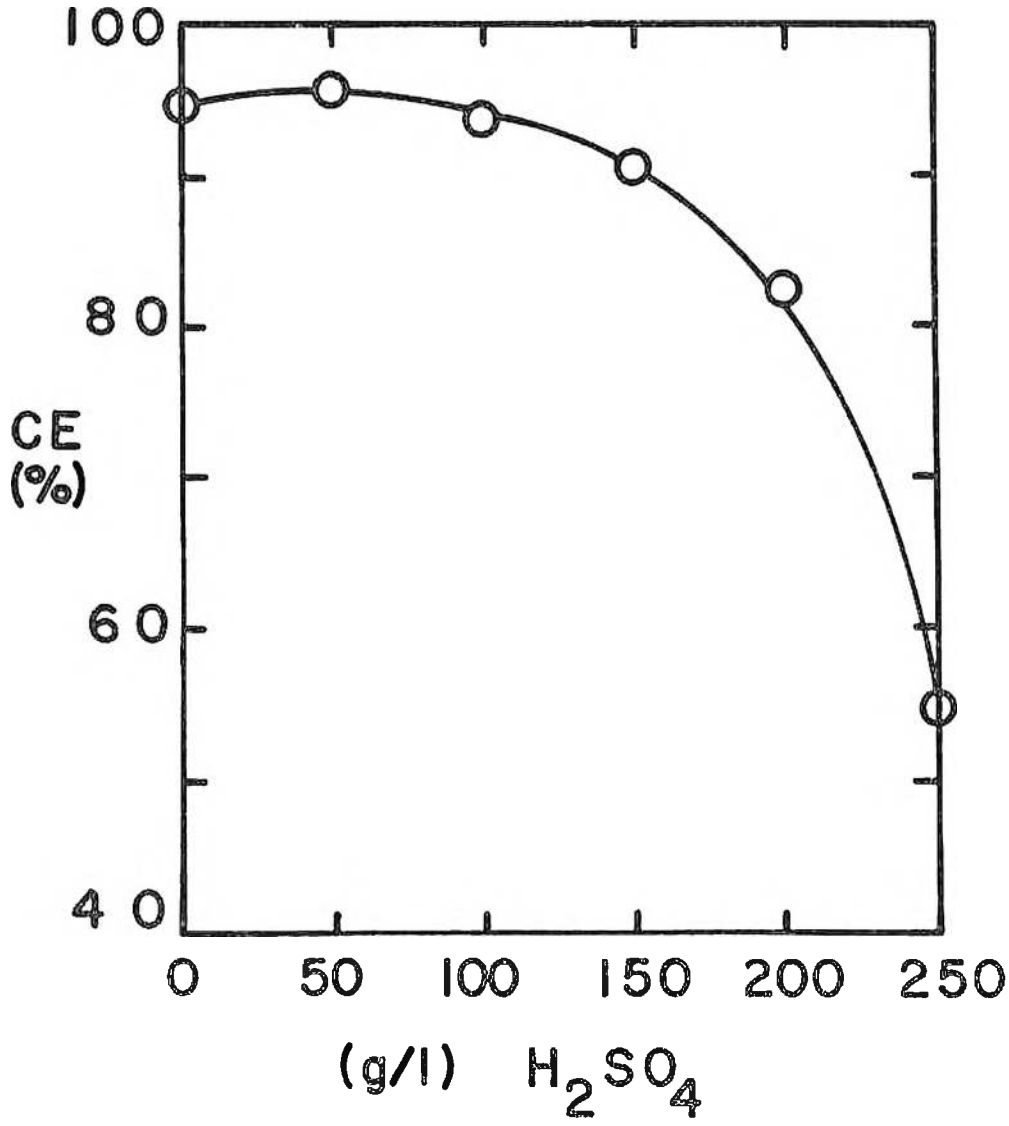

Figure 2. Current Efficiency vs Acid Concentration for Industrial Electrolytes Containing 60 g/ℓ Zn. T = 40°C; Current Density = 40 mA/cm^2.

Table IV. Calculated Factor Effects for Antimony, Germanium, and Arsenic.

Factor	Calculated Factor Effect
Antimony	-14.138*
Germanium	-11.322
Arsenic	-9.631

*Normalized to an equal concentration basis with germanium and arsenic.

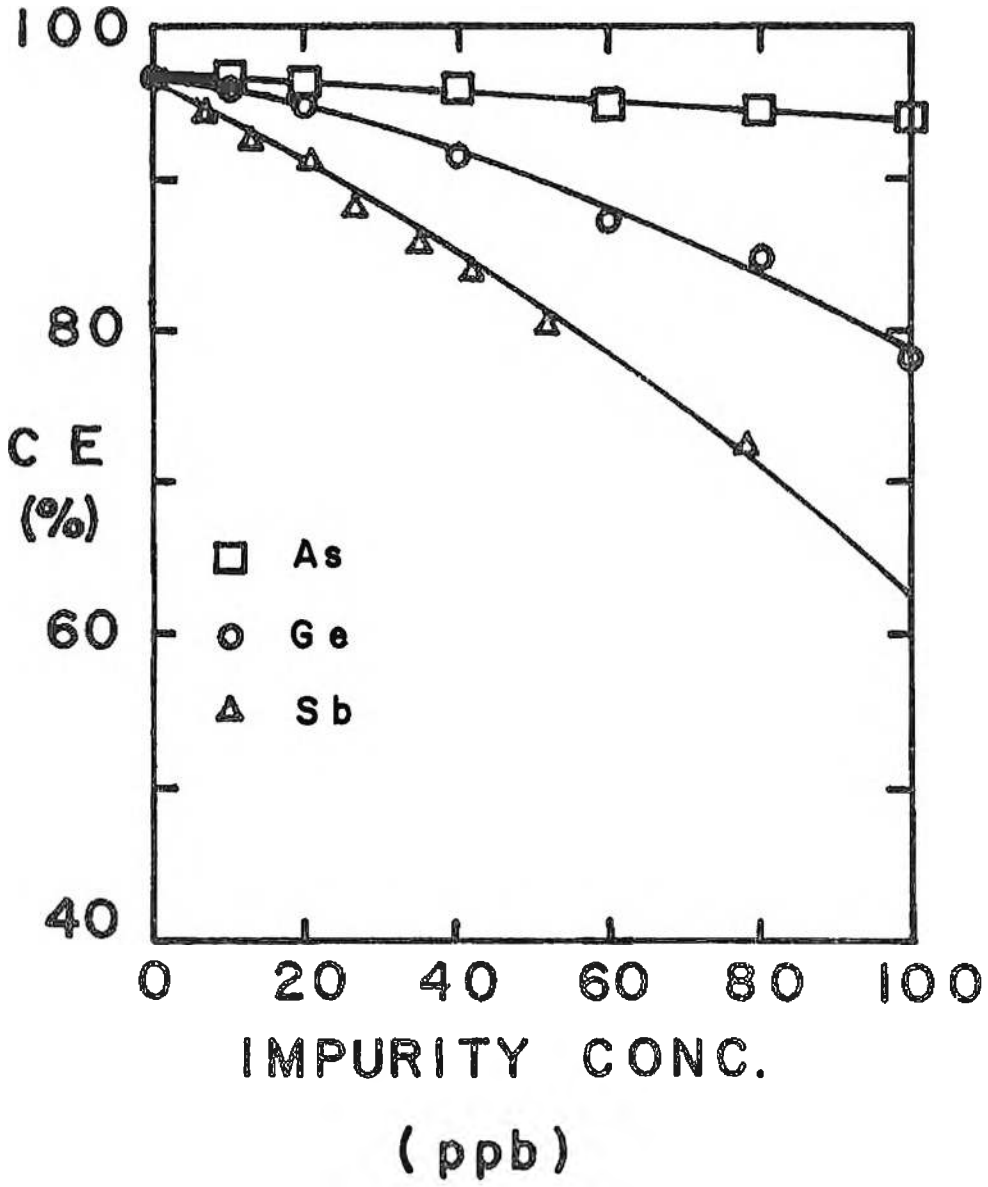

Figure 3. Current Efficiency vs Impurity Concentration for Prepared Electrolytes Containing 65 g/ℓ Zn and 200 g/ℓ H_2SO_4. T = 45°C; Current Density = 40 mA/cm^2.

these trends. A temperature of 45°C, 40 mA/cm^2 current density, and 100 g/l H_2SO_4 concentration were the conditions employed. Results of the tests for each of the three impurities are shown in Figure 3, and these compare favorably with those from the factorial study. At a concentration level of 40 ppb of impurity, the current efficiency for a solution containing antimony was 82%; for germanium, 91%, and for arsenic, close to 95%. Since the current efficiency is sensitive to the nature of the impurity, it is quite important to determine which impurities are present and to adjust the purification process to give levels which can be tolerated in the cell room. Frequently, only the combined amount of antimony and arsenic in solution is reported rather than the individual concentrations.

Cobalt Effects and Interactions with Acid The calculated factor effect for cobalt is very large (-23.603) and is exceeded only by the value obtained for the acid. Since the cobalt concentration was found to be very significant, a separate current efficiency study was done with the same base electrolyte and operating parameters used previously. Two acid levels were considered and the results appear in Figure 4. At the lower acid level (100 g/l), the effect of cobalt is not severe until concentrations greater than 12 mg/l are exceeded. This appeared to contradict the results of the factorial study, but upon increasing the acid content to 150 g/l H_2SO_4, only 6 mg/l was tolerable. At both concentrations of acid, a critical cobalt level appears. Up to this level there is a slight linear decrease of the current efficiency with increasing cobalt content. After this level is exceeded, catastrophic losses in current efficiency result. Increasing the acid content causes this point to shift to decreasing

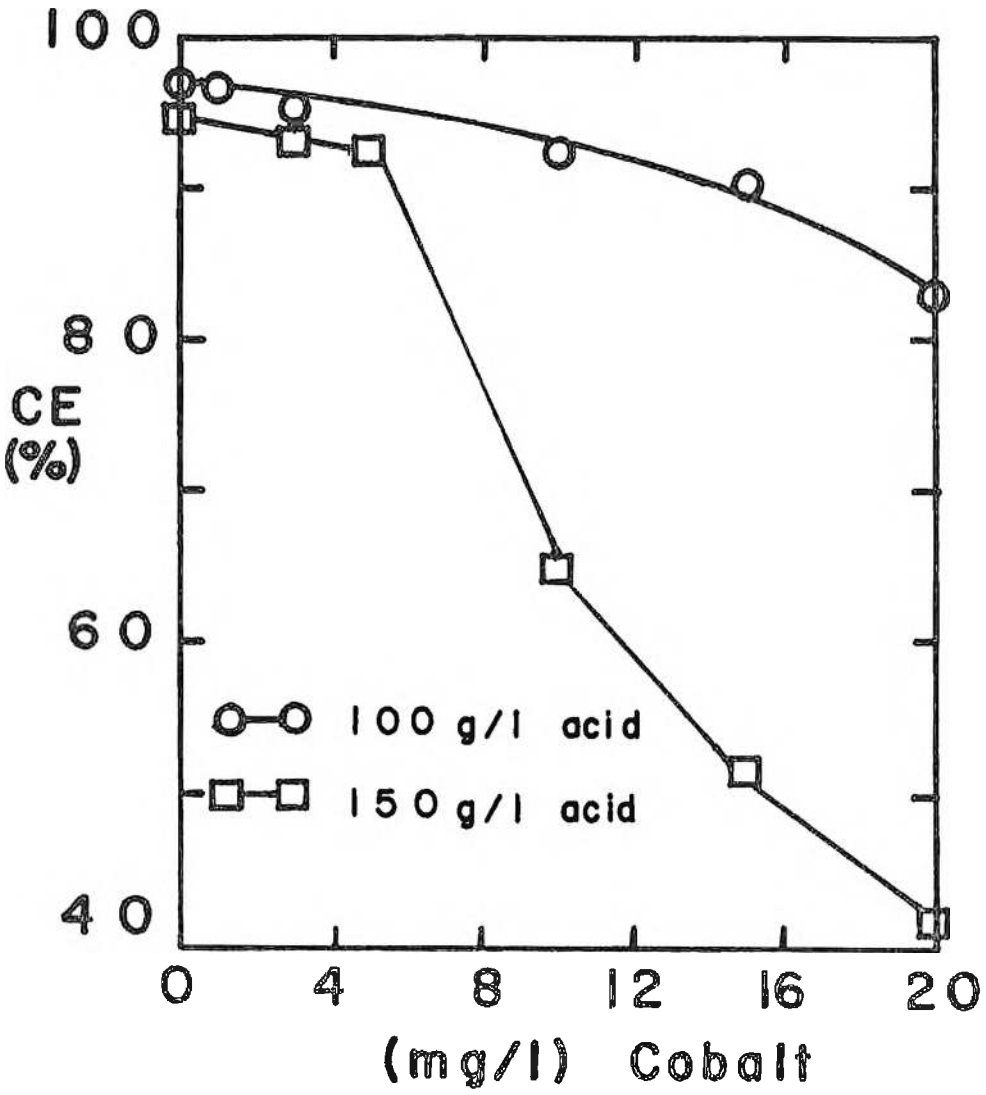

Figure 4. Current Efficiency vs Cobalt Concentration for Prepared Electrolytes Containing 65 g/ℓ Zn and Various Acid Concentrations. T = 45°C; Current Density = 40 mA/cm^2.

cobalt concentrations, which agrees with the results of other investigators (16,27,30,31).

The calculated factor effect for cobalt and acid is -11.287. This is a very large factor and indicates that there is a strong negative interaction between cobalt and acid. Others have attributed the influence of cobalt to local cell action (16,27,30,31). The exchange current value for hydrogen reduction on cobalt is higher than that of zinc and this indicates that hydrogen reduction on cobalt sites is somewhat easier (35). Localized potential differences may arise, caused by changes in surface roughness and this may allow the formation of localized galvanic cells. The cobalt sites then serve as local cathodes and nearby zinc sites as local anodes. Corrosion of the zinc occurs at the anodes with hydrogen reduction at the cathodes. The large acid-cobalt interaction tends to support this mechanism and in addition, the deposits of zinc corresponding to the poor current efficiencies often exhibited severe pitting and other signs of corrosion. Pitting usually accompanies local cell action.

Interaction of Arsenic, Antimony, and Germanium with Acid Arsenic and germanium also exhibit some synergism with acid, but to a smaller degree than cobalt. The factor effects of these impurities are: -3.884 for acid-arsenic and -2.587 for acid-germanium. Antimony shows a beneficial interaction with acid, as indicated by a factor of 5.106. This may be due to the complex interaction of antimony with glue which results in changes in morphology and is discussed later in greater detail. Figures 5, 6, and 7 illustrate the effect of increasing acid concentration for solutions containing the

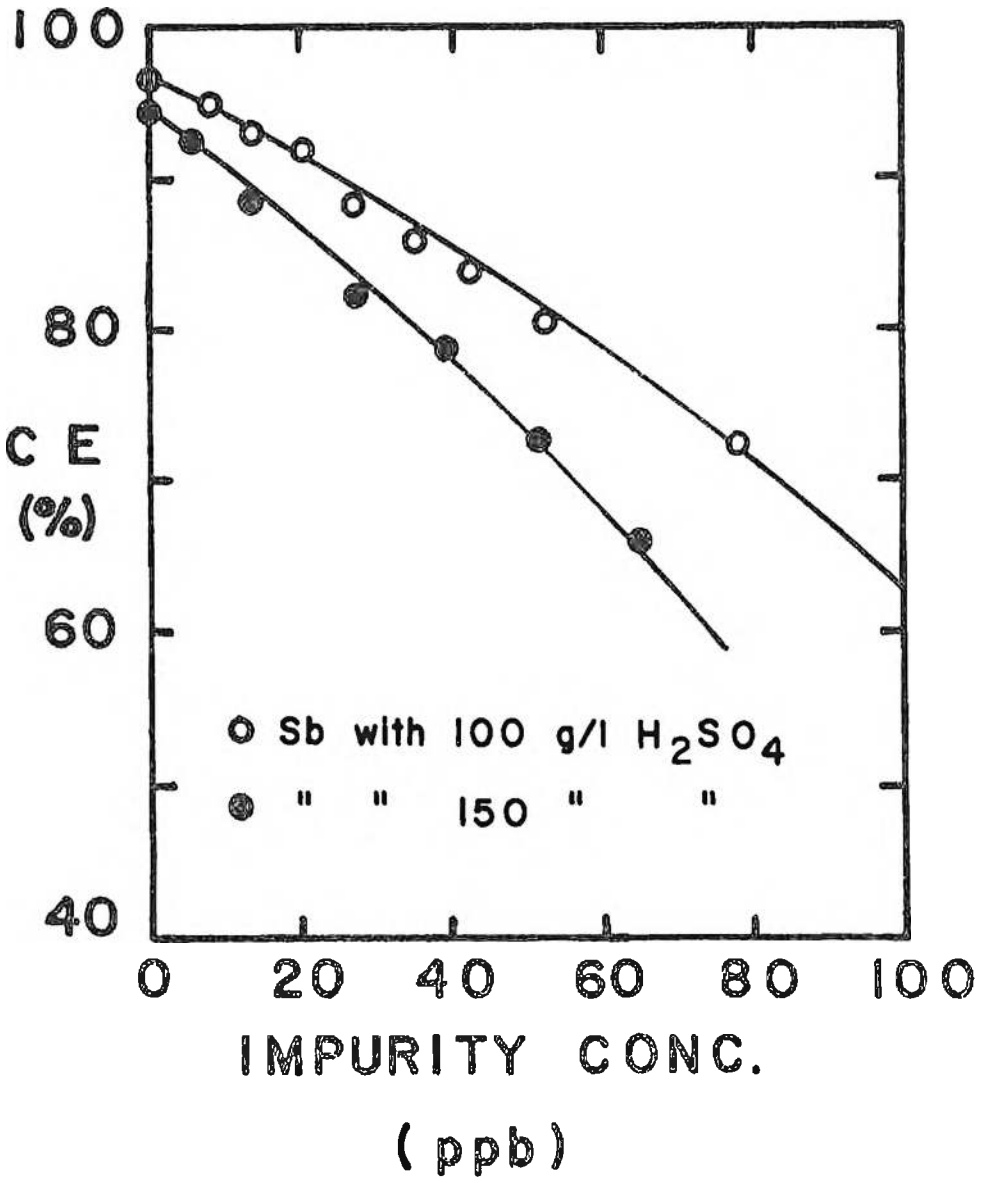

Figure 5. Current Efficiency vs Antimony Concentration for Prepared Electrolytes Containing 65 g/ℓ Zn and Various Acid Concentrations. T = 45°C; Current Density = 40 mA/cm^2.

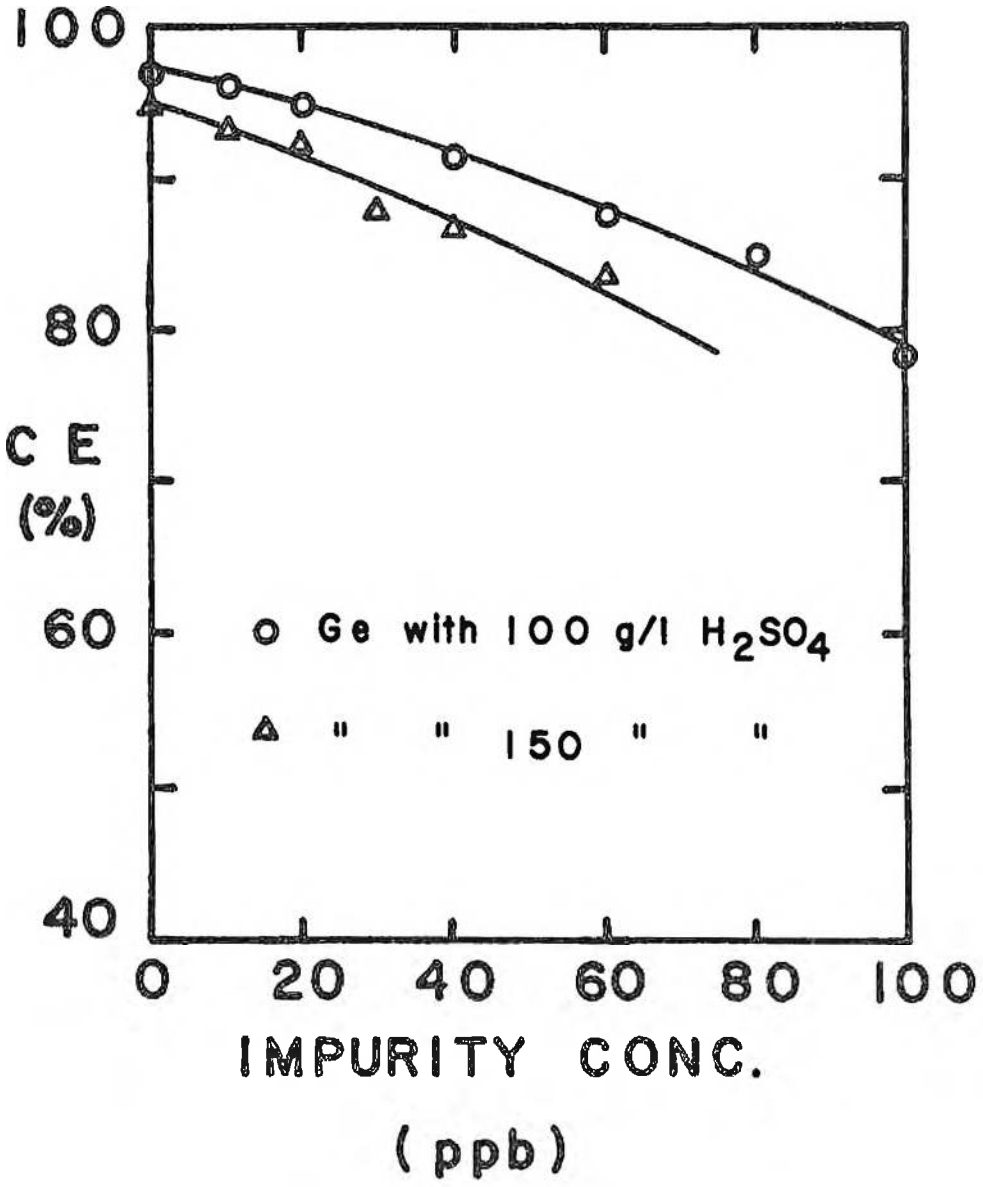

Figure 6. Current Efficiency vs Germanium Concentration for Prepared Electrolytes Containing 65 g/ℓ Zn and Various Acid Concentrations. T = 45°C; Current Density = 40 mA/cm^2.

various impurities. The effect of acid in the presence of either antimony or germanium is less dramatic than that obtained for cobalt. In both cases, the synergism involved is not readily apparent. The conditions employed for testing antimony, germanium, and arsenic were similar to those used for cobalt. Figure 7 indicates that the effect of arsenic is strongly influenced by and a linear function of the acid content. Increasing the level of acid seems to greatly increase the interaction of arsenic at the cathode. Increasing the acid concentration causes a decrease in the current efficiency for all the above cases. The positive synergism exhibited by antimony and acid just indicates that the decrease is somewhat less than would be expected if these two factors acted individually.

Effects of Temperature Temperature was shown to be a critical factor with a calculated factor effect of -16.475. Increasing temperatures caused lower current efficiencies and the magnitude of the change indicated that enhanced activation processes such as zinc dissolution or hydrogen gas evolution were responsible. An interaction between temperature and acid level is indicated by a factor of -3.528. Systems containing high acid levels would be expected to show the greatest loss in current efficiency as the cell temperature is increased. The effect of temperature with the various impurities is only significant for antimony and germanium. For germanium, there is only slight interaction (-2.481), but for antimony the interaction is much greater (-4.844).

The Effects of Glue Addition Organic additives have been used in zinc deposition for a number of years and their addition is reported to increase cathode quality and improve current efficiency for

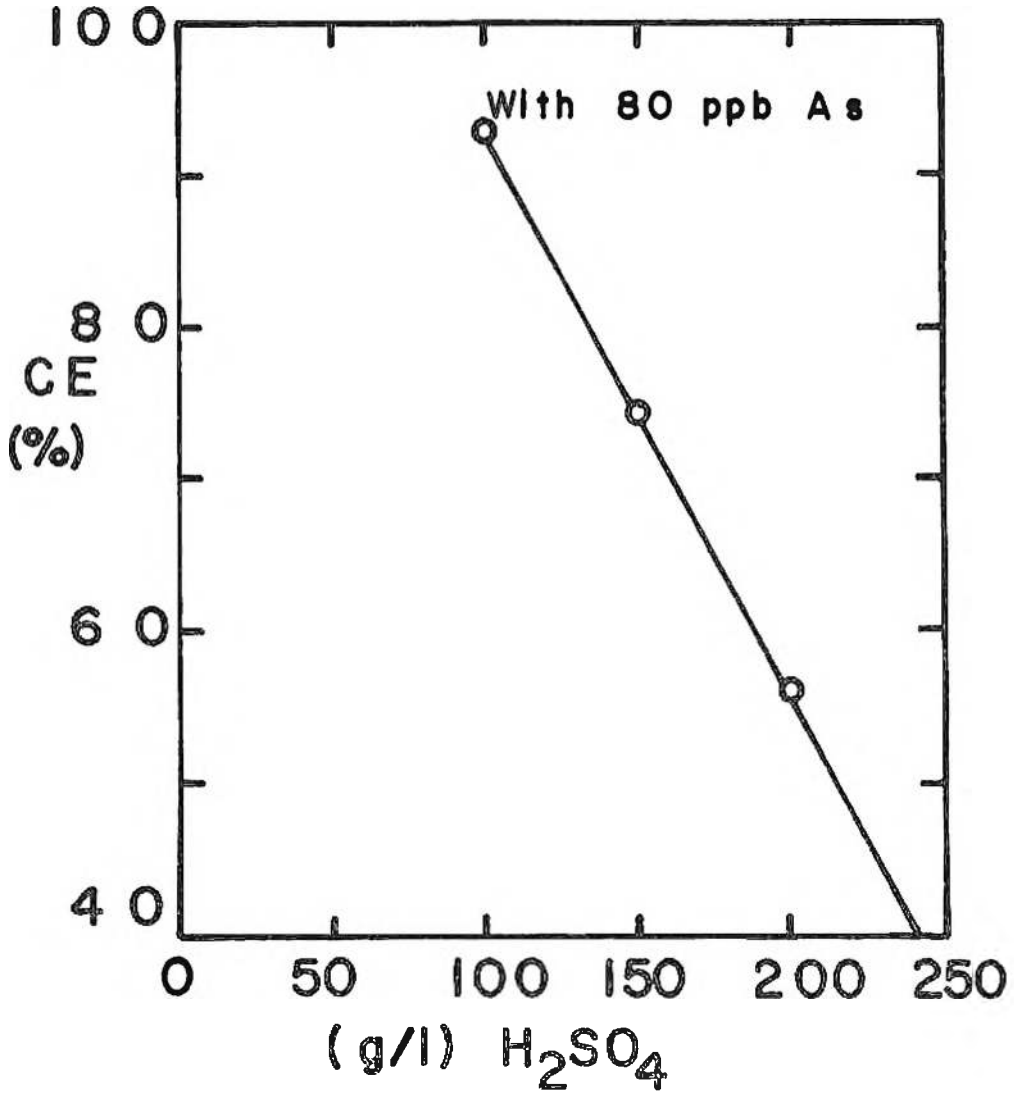

Figure 7. Current Efficiency vs Acid Concentration for Prepared Electrolytes Containing 65 g/ℓ Zn and 80 ppb As. T = 45°C; Current Density = 40 mA/cm^2.

deposits obtained from solutions containing various amounts of impurity (5,6,8,9,15,17-19,37-48). The way in which they interact with the impurities at the cathode or in the solution is not well understood. The calculated factor effect obtained for glue additions is 13.284. This rather large positive factor was the only positive one found for the seven variables of this study.

The results of electrolyzing solutions containing various additions of glue and gum arabic in the absence of impurity addition appear in Figure 8. The electrolyses were conducted at conditions similar to those employed for cobalt and the other impurities. Glue and gum arabic gave similar results. The results show that increasing the concentration of organic agent in the electrolyte only decreases the current efficiency. This contradicts the factorial study. It appears that interaction with other solution constituents is necessary to obtain the beneficial effects of the organic additive. This is also indicated by the interaction parameters calculated for the factorial study.

Antimony and germanium both showed significant interaction with the glue. Cobalt showed some mild interaction with the glue, but no significant interaction was found for arsenic. For antimony, germanium, and cobalt the factor effects are 13.815, 6.678, and 2.591 respectively. Additions of glue to solutions containing antimony and germanium would be expected to show strong gains in current efficiency. Smaller benefits would be obtained for solutions containing cobalt.

Electrolyses were conducted to compare the relative amounts of glue that would be required to counteract the effect of antimony and germanium. A solution of base electrolyte containing a determined

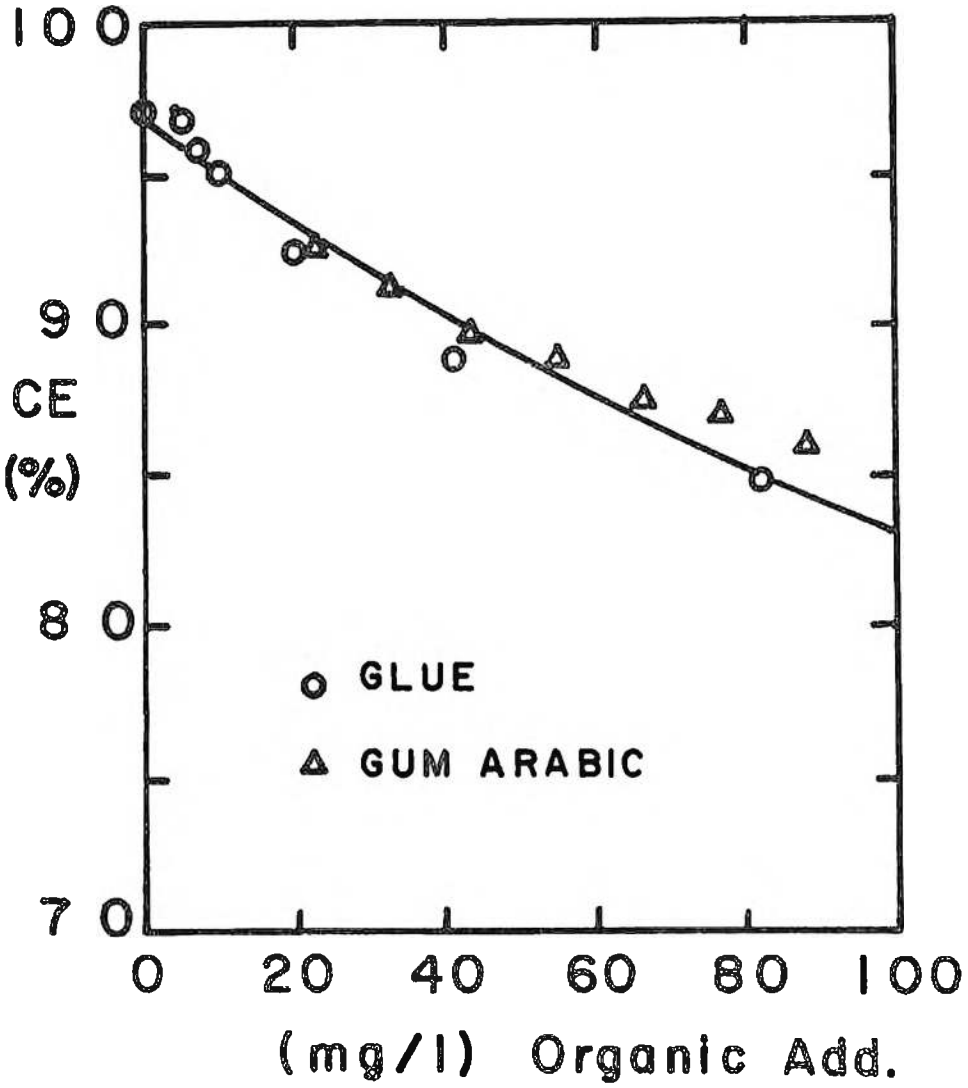

Figure 8. Current Efficiency vs Organic Additive Concentration for Prepared Electrolytes Containing 65 g/ℓ Zn and 100 g/ℓ H_2SO_4. T = 45°C; Current Density = 40 mA/cm^2.

amount of impurity was electrolyzed for 12 hours at 45°C and a current density of 40 mA/cm . The amount of glue added to the solution was varied and the results are shown in Figure 9. The current efficiency is initially increased by adding glue to the solution, but a point is finally reached where further addition of glue causes a decrease in current efficiency to occur. For germanium, this occurred after 13 mg/l (ppm) glue had been added. For antimony of a comparable concentration level, approximately 25 mg/l were required. Since the interaction of cobalt with glue is smaller, even less glue would be required to reach an optimum level of glue addition. The results point out that it is very important to know the composition of the solution if one is to add the proper amount of organic agent to counteract the deleterious effects of the impurities. Recent studies have indicated that balancing impurity content with glue by using cyclic voltammetry is quite feasible (17-19,43). Other investigators have determined the amount of active glue in solution by measuring electrode polarization before and after a solution is brought to a temperature where the glue degrades to inactive hydrolysis products (49,50). Further studies are needed in this area because only an optimum concentration of glue will yield the maximum current efficiency.

The interaction of the glue with the various impurities is lessened when either the temperature or the acid content is increased. This is indicated by the three factor interaction effects calculated from the statistical study. The ternary factors for the interaction of temperature, glue, and impurity are -4.525 for cobalt, -3.100 for germanium, and -2.506 for antimony. The way the factors vary is

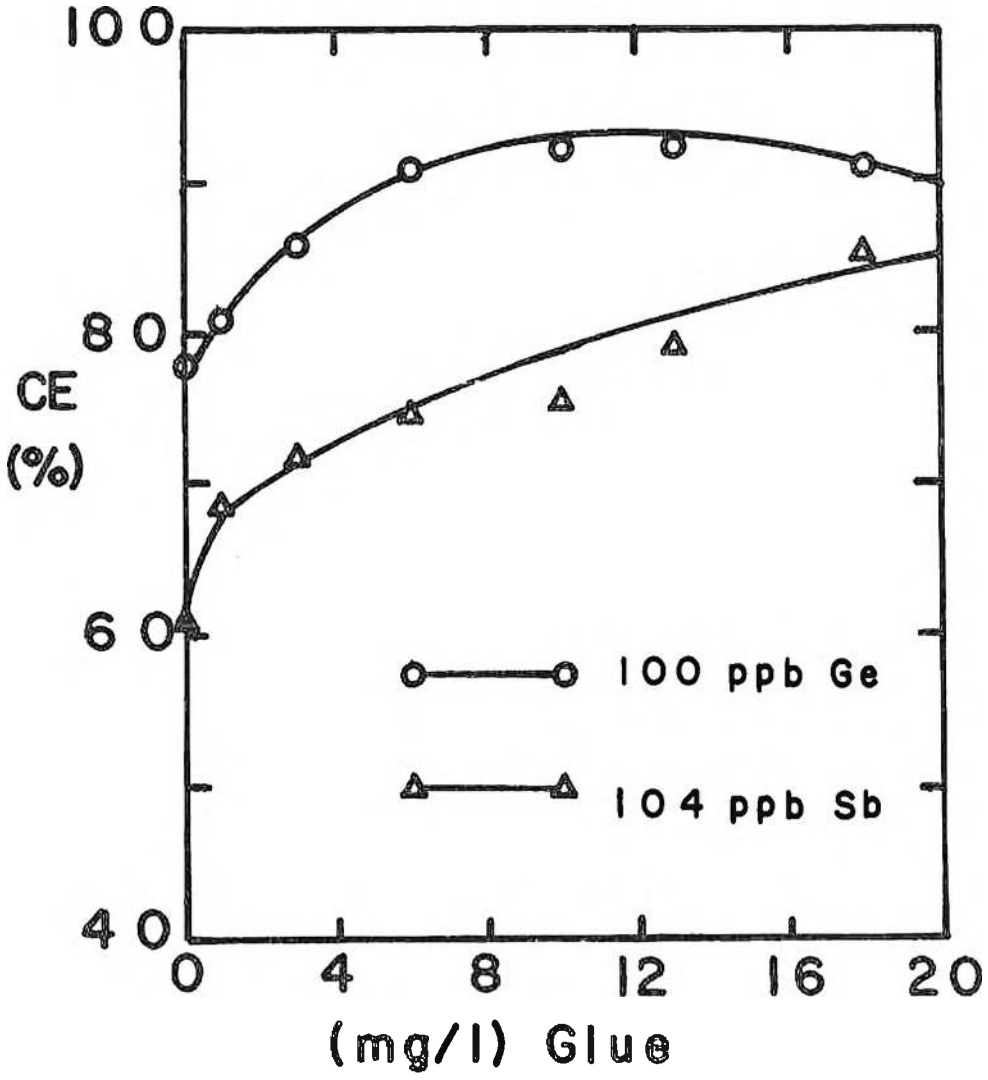

Figure 9. Current Efficiency vs Glue Concentration for Prepared Electrolytes Containing 65 g/ℓ Zn, 100 g/ℓ H_2SO_4 and Constant Amounts of Impurity Addition. T = 45°C; Current Density = 40 mA/cm^2.

entirely consistent with the strength of the simple glue-impurity interactions. Cobalt, which was found to interact only mildly with glue has the biggest ternary factor. Temperature apparently affects the stronger interactions of glue with impurity to a lesser extent. Since the action of glue is lessened by increasing the temperature and acid, more glue may need to be added to the electrolyte to obtain the desired results.

Interactions Among Impurities Interactions among impurities are frequently important from a plant operator's viewpoint. Frequently, levels of impurities which do not exhibit an effect when present alone became intolerable when just small amounts of another impurity are introduced. The factorial design indicated some combinations which exhibit this type of synergism.

Antimony interactions with cobalt and arsenic were found to be insignificant, but this may be misleading because the electrolyte used in the study always had a residual level of glue and the interaction of antimony with glue is extremely important in determining the overall effects of antimony. In a solution containing no glue, a detrimental interaction between cobalt and antimony appears to exist and the combination caused the current efficiency to drop drastically. This is shown in Figure 10. Other investigators report similar results (56). However, in the presence of glue, antimony additions appear to lead to improved current efficiencies when the electrolyte contains other impurities such as cobalt and germanium. Several independent studies have confirmed this behavior (5,8,27,37). The calculated factor effects indicate that the interaction of acid with other impurities is less in the presence of antimony. The

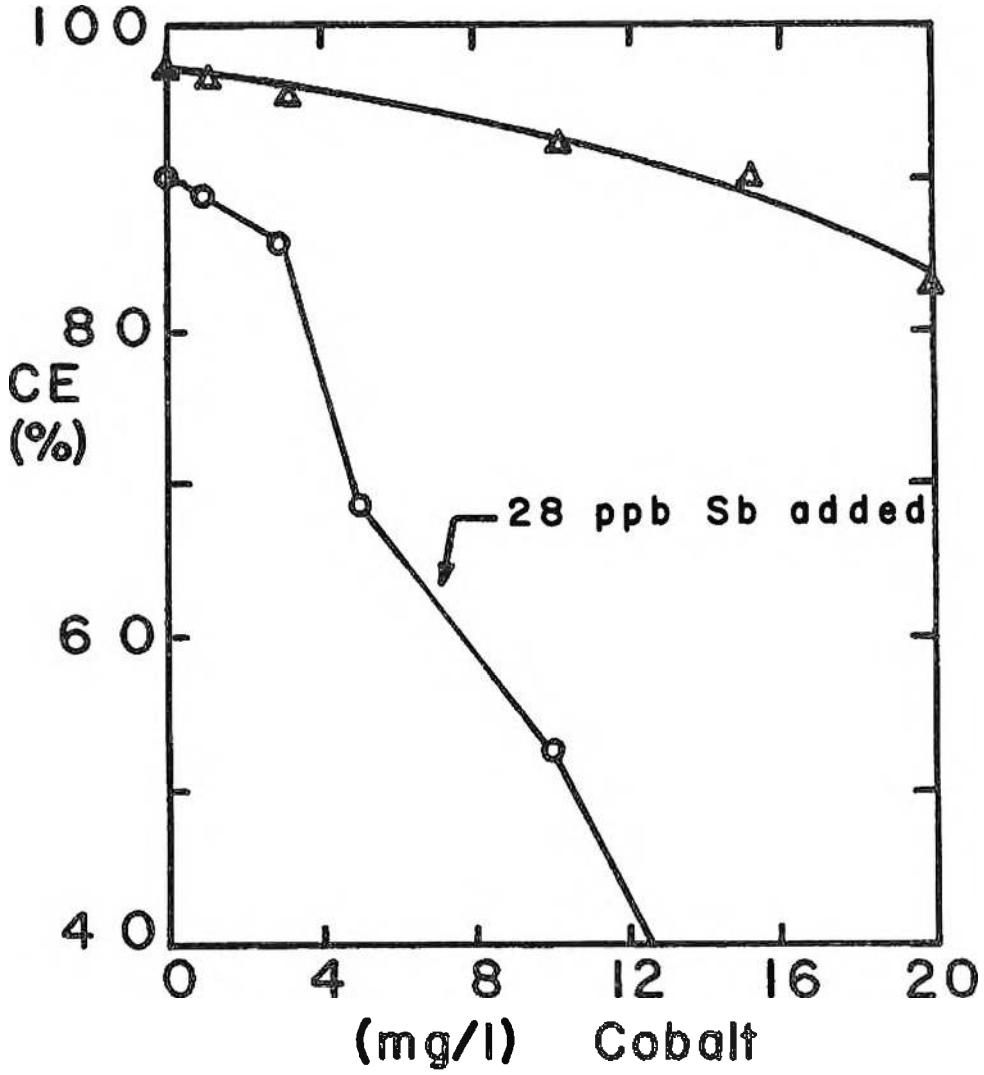

Figure 10. Current Efficiency vs Cobalt Concentration for Prepared Electrolytes Containing 65 g/ℓ Zn and 100 g/ℓ H_2SO_4 With and Without 28 ppb Sb. T = 45°C; Current Density = 40 mA/cm^2.

antimony may interact with glue at the cathode to cause morphological changes which lead to more uniform deposits and to less local cell corrosion of the zinc deposit (17-19).

Germanium shows a small detrimental interaction with antimony (-2.703), but this may be outweighed by the beneficial effects of having some antimony in the solution in the presence of glue. Germanium shows no distinguishable interaction with cobalt and Figure 11 tends to confirm this. Some beneficial interaction may exist between arsenic and germanium as indicated by the calculated factor effect for this combination (3.744).

Cobalt showed a very large interaction with arsenic (-6.331). Processes which have high levels of arsenic in solution will thus be able to tolerate only low levels of cobalt. This was confirmed by electrolyzing a solution containing 4 mg/l Co and 80 ppb As. When either impurity was alone in the electrolyte, current efficiencies greater than 94% were obtained, but for the combination the current efficiency was 41.7%. The H_2SO_4 concentration was 100 g/l for this test (T = 45°C; CD = 40 ma/cm^2). Higher acid levels may increase the effect as both cobalt and arsenic were found to be quite sensitive to the acid content of the solution. In fact, a ternary interaction effect equal to -3.041 was calculated for the combination of acid, cobalt, and arsenic.

The statistical factor for the interaction of glue with acid and arsenic (-3.641) indicates that the presence of arsenic under conditions of increased acid and temperature may lessen the beneficial effects of the addition agent. The presence of arsenic also weakens the interaction of glue with cobalt.

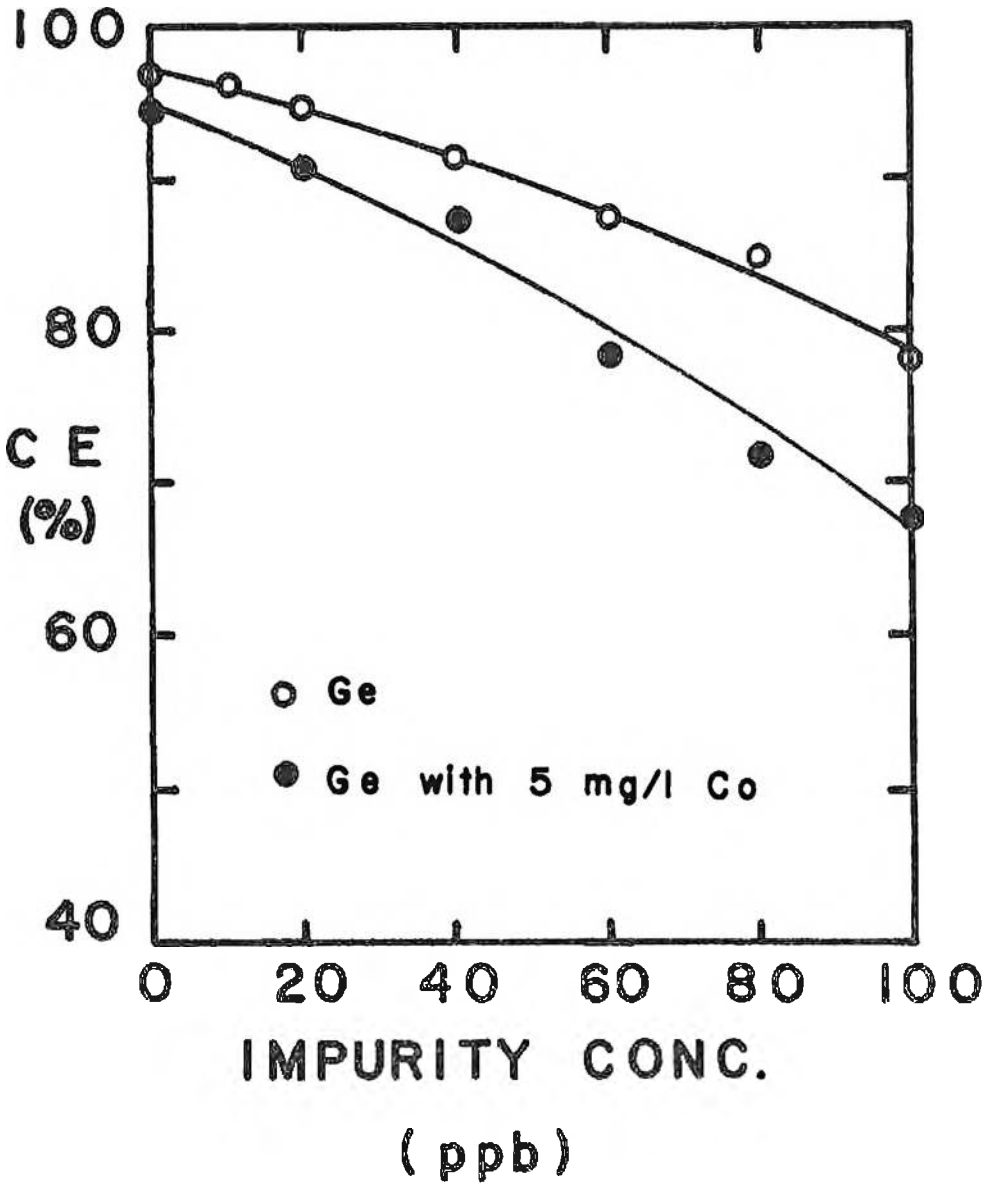

Figure 11. Current Efficiency vs Germanium Concentration for Prepared Electrolytes Containing 65 g/ℓ Zn and 100 g/ℓ H_2SO_4 With and Without 5 mg/ℓ Co. T = 45°C; Current Density = 40 mA/cm^2.

Summary of the Results The statistical analysis shows that the acid level is the most critical of the factors considered. Cobalt level, temperature, antimony concentration, germanium concentration, and arsenic concentration are the next critical factors in decreasing the current efficiency. Glue addition is of some benefit in increasing the current efficiency and this is especially true for solutions containing significant levels of antimony and germanium. Glue interacts less strongly with cobalt and arsenic. Deleterious interaction between cobalt and arsenic appears to exist and increases in severity as the acid concentration is increased. Most of the combined interactions with temperature are detrimental. The method of analysis employed in this study illustrates which combinations to avoid and indicates some of the factors which can be used to control the process. It also indicates which factors warrant closer examination.

Development of the Statistical Model

In addition to illustrating the importance of the various factors, the statistical design permits development of a model which can be used to predict the current efficiency at other levels of the variables. Using the calculated factor effects and coded values of the variables of the factorial design, a model of the form:

$$CE = a_0 + a_1x_1 + a_2x_2 + \ldots + a_px_p + a_{12}x_1x_2 + \ldots$$

$$+ a_{p-1,p}\, x_{p-1}x_p + \text{higher order interactions;}$$

CE = predicted current efficiency

x_j = coded factors for the system

Table V. Coded Factors Used in the Model.

Factor	Symbol	Coded Factor
Temperature	t	$x_t = \frac{t-40}{5}$
H_2SO_4 Concentration	a	$x_a = \frac{a-150}{50}$
Ge Concentration	g	$x_g = \frac{g-20}{20}$
Sb Concentration	s	$x_s = \frac{s-13}{13}$
Co Concentration	c	$x_c = \frac{c-1.2}{1.2}$
As Concentration	r	$x_r = \frac{r-20}{20}$
Glue Concentration	o	$x_o = \frac{o-13}{7}$

Units: t = ^oC

a = g/l

g,s,r = ppb

c,o = ppm

a_j = 0.5 (factor effect for x_j)

$a_{jj'}$ = 0.5 (interaction effect for $x_j x_{j'}$)

a_0 = mean response for the system

was obtained. The values for the coded factors for the present system appear in Table V.

Using the model, calculated current efficiency values were obtained for the values of the factors used in this study. Figure 12 compares the calculated current efficiency and that obtained experimentally. The fit of the model is quite good and an "F" test showed that the variability between the predicted and experimental current efficiencies is within the experimental error of the system.

In order to test the degree of curvature that exists for the experimental system, thirteen center point tests were conducted. The conditions employed for the center point tests were half-way between the high and low levels as listed in Table I. The average of the center points was 79.3. The mean current efficiency for the factorial study was 58.99. A curvature test using these values indicates that significant curvature exists for the system. This means that the model will not fit as well for values of the variables which are different than those employed in the study.

Other tests were conducted at conditions intermediate between those employed in the factorial study. The conditions and calculated and experimental current efficiency values obtained are listed in Table VI. A comparison of the calculated and experimental values indicates that the model does not fit as well as in the case of the experimental design. A better model would need to be considered. This could be done by using a three level design or perhaps using a full

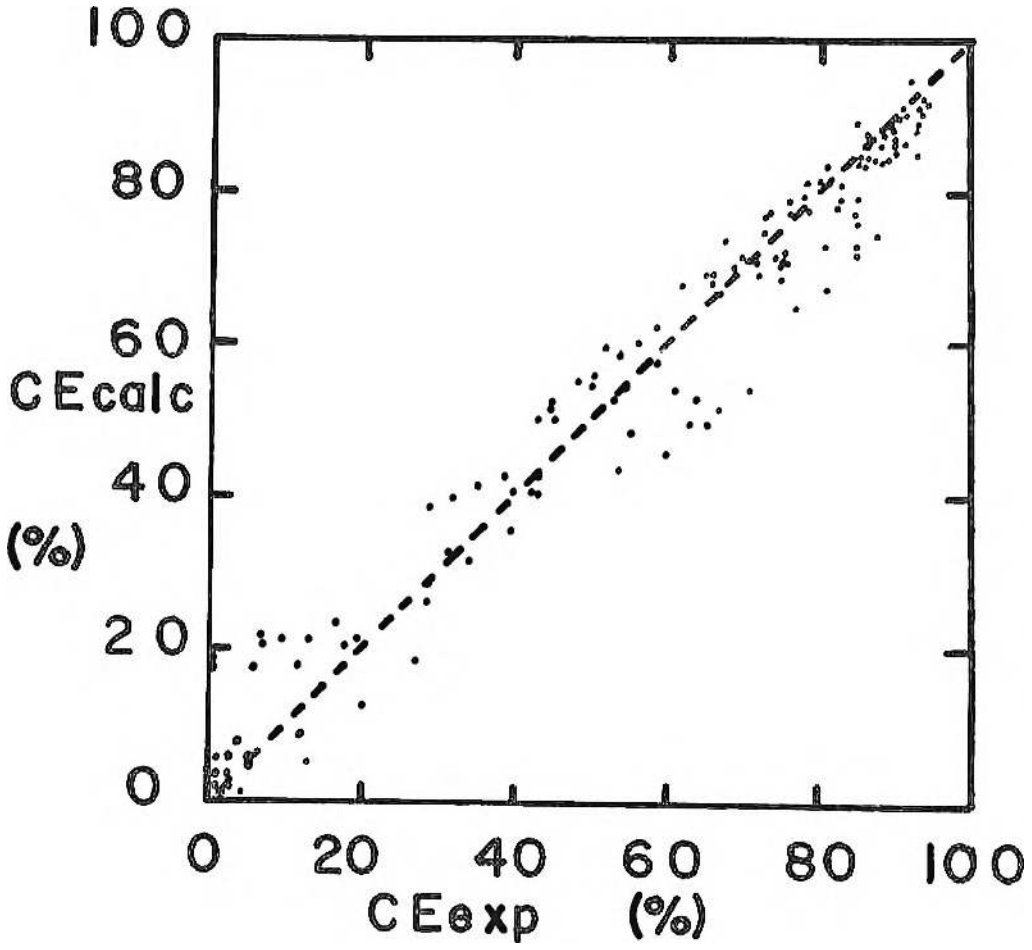

Figure 12. Calculated Current Efficiency vs Experimental Current Efficiency for Results of the Factorial Design.

Table VI. Comparison of Calculated and Experimentally Obtained Current Efficiencies for Other Factor Levels.

Temp. °C	Acid Conc. GPL	Germanium Conc. PPb	Antimony Conc. PPb	Cobalt Conc. PPM	Arsenic Conc. PPb	Glue Conc. PPM	% CE, Exp.	% CE, Calc.
42.2	175	30	13	2.4	50	10	0.5	16.6
42.2	125	60	13	0.8	20	15	85.9	59.2
42.2	150	0	0	4.0	40	0	13.3	19.2
42.2	150	0	0	4.0	0	0	78.0	45.9
42.2	100	0	0	0	0	0	93.2	94.5
42.2	150	0	0	0	0	0	92.8	84.4

response surface such as the Box-Behnken (51) design or the more elaborate Box-Wilson (52) design. The factorial design used in this study indicates what the critical process parameters and interactions are. Once these are known, one can then choose the proper response surface design. The technique can also be used to eliminate factors which are found to be insignificant and to develop further studies which would consider additional variables with those found to be significant.

For the present system, the effects of time and current density were not measured. A future study using this technique and these additional variables may be useful because some impurities such as cobalt often have induction periods associated with their effects (27,30).

Overall, the factorial study and the additional supporting tests were useful in determining the important variables and interactions that exist for the system. The model obtained fits the design values quite well, but unfortunately, does not fit as well at other values. Future tests using three levels would allow other models to be derived which would fit a wider range of factor levels.

Deposit Morphologies

The morphologies and crystallographic orientations of the zinc deposits were determined by the use of scanning electron microscopy and x-ray diffraction. Deposits were obtained from solutions containing the base electrolyte (65 g/l Zn and 100 g/l H_2SO_4) and various addition agents. The current density and temperature were maintained at 40 mA/cm^2 and 45°C, respectively. Distinct changes in crystallographic orientation and deposit morphology were observed for even low levels of addition agent. The various types of morphologies obtained

Table VII. Zinc Deposit Crystallographic Orientations.

Electrolyte Additions	Surface Orientation (ratio to ASTM Standard)*						
	(00·2)	(10·1)	(10·2)	(10·3)	(10·4)	(10·2)	(10·4)
No Addition	0.43	0.91	0.89	1.43	0.94	0.52	1.44
(20 - 100) ppb Arsenic	0.22	1.0	1.76	1.32	1.17	1.45	1.93
(2 - 80) ppm Glue	0	1.0	0.68	0.83	0	0.46	0
(7 - 65) ppb Antimony	1.89	0.23	0.32	1.14	1.67	0.22	0.89
(1 - 10) ppm Cobalt	1.23	0.72	0.96	1.66	1.70	0.62	1.98
(10 - 100) ppb Germanium	1.89	0.21	0.45	0.84	1.51	0.32	1.05
100 ppb Ge & 6 ppm Glue	0.21	0.58	3.57	2.28	1.33	0.39	1.27
100 ppb Ge & 10 ppm Glue	0.06	0.32	3.57	1.12	0.33	0.43	0.64
100 ppb Ge & 13 ppm Glue	0	1.0	0.79	0.28	0	1.0	1.0
100 ppb Ge & 18 ppm Glue	0	1.0	2.04	0.48	0	3.30	1.18
100 ppb Ge & 21 ppm Glue	0	1.0	1.64	0.12	0	1.52	0.46

Electrolytic Conditions: 65 g/ℓ Zn; 100 g/ℓ H_2SO_4; 45°C; 40 mA/cm^2

*(00·2) 53; (10·1) 100; (10·2) 28; (10·3) 25; (10·4) 3; (11·2) 23; (11·4) 11.

are illustrated in Figures 13-21. The characteristic orientations appear in Table VII.

Addition-free Electrolyte Figure 13 shows the typical morphology of the zinc deposits obtained from addition-free electrolytes. The morphology is quite similar to that obtained by other investigators using purified electrolytes (19). The characteristic orientation of these deposits were generally (10·3), (11·4), but other orientations have some significance. The platelets are growing at various angles to the substrate and the growth mode is generally mixed.

Arsenic-Containing Solutions For solutions containing up to 0.1 mg/l arsenic, the morphology of the deposit was quite similar to that obtained for the no-addition deposit. The crystallographic orientations and platelet size are also quite similar. Figure 14 shows a typical deposit. It would appear that the arsenic had little influence under the conditions employed. The current efficiencies for the low acid solutions containing arsenic were consistently quite high. At higher acid levels, the interactions of arsenic were found to be more severe and changes in the morphology may result.

Solutions Containing Glue Marked changes in platelet size, morphology and crystallographic orientation were found for deposits obtained from glue-containing electrolytes. Gum arabic gave similar results. The crystallite size was markedly decreased and the platelets became smaller as more glue was added to the solution. At high glue levels, the zinc seemed to grow in colonies and the high glue deposits were often quite brittle. The dominant feature for the glue type of deposits is the appearance of zinc platelet edges, with the basal planes lying perpendicular to the electrode surface.

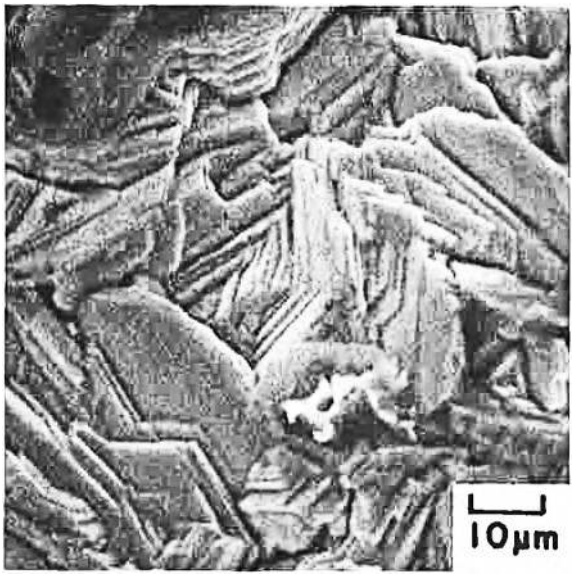

Figure 13. Deposit Obtained for a No-addition Electrolyte. T = 45°C, Current Density = 40 mA/cm^2. (1000x)

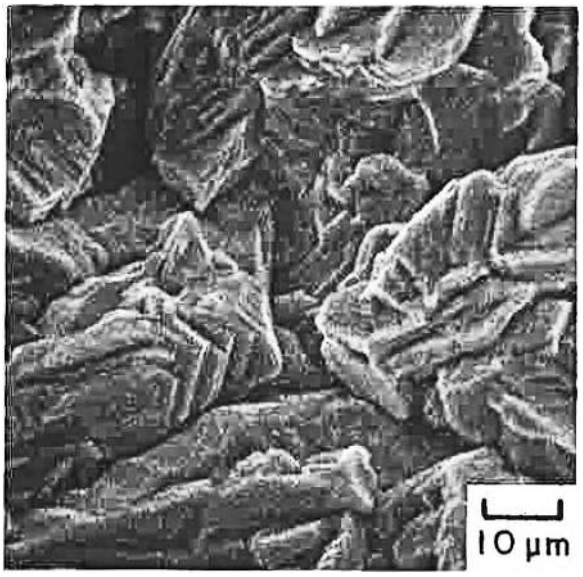

Figure 14. Deposit Obtained for Electrolyte Containing 0.1 mg/ℓ As. T = 45°C; Current Density = 40 mA/cm^2. (1000x)

Outward growth of the deposits seems to be predominant and the crystallographic orientation obtained is highly preferred (10·1). At very high levels of glue some (11·0) begins to appear. The results are quite consistent with those obtained by other investigators (17-19).

The addition of glue to the addition-free electrolyte also decreases the current efficiency. Investigators attribute this to the inhibition of both zinc and hydrogen discharge by glue adsorption with the former being inhibited to a higher degree (53,54). The adsorption of glue also causes more nucleation and hinders crystalline growth resulting in a finer-grained, more uniform deposit. The overvoltage of zinc deposition from electrolytes containing organic additives has been found to be higher than that obtained from addition-free electrolytes (17-19). Increased polarization favors increased nucleation, which results in a finer crystallite size. Figure 15 shows the characteristic morphology for the organic addition agents.

In general, uniform deposits were obtained for solutions containing glue. This unformity may hinder the formation of local corrosion cells when impurities are present in the electrolyte.

Solutions Containing Antimony, Germanium, or Cobalt The deposits obtained from solutions containing these impurities showed marked signs of corrosion at the higher impurity concentrations. Noticeable pitting of the deposit occurred in all three cases. Dendrite and nodular growth were also quite evident for solutions containing antimony. Figures 16-18 show the types of morphology obtained for the zinc deposits. The platelet size was generally larger than that obtained for the deposit from the addition-free electrolyte and the

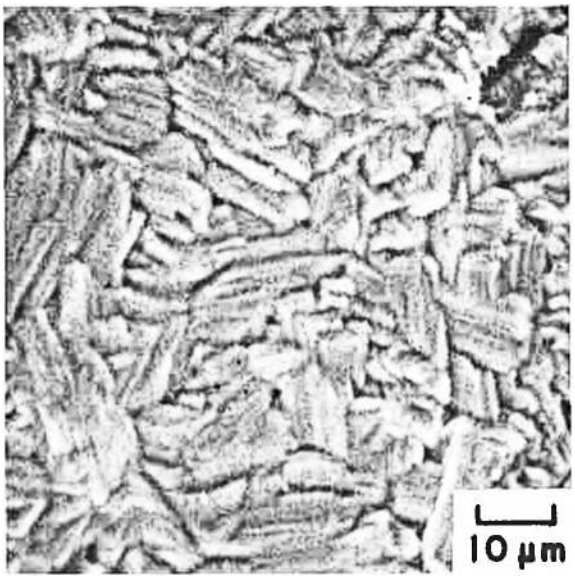

Figure 15. Deposit Obtained for an Electrolyte Containing 21 mg/ℓ Glue. T = 45°C; Current Density = 40 mA/cm^2. (1000x)

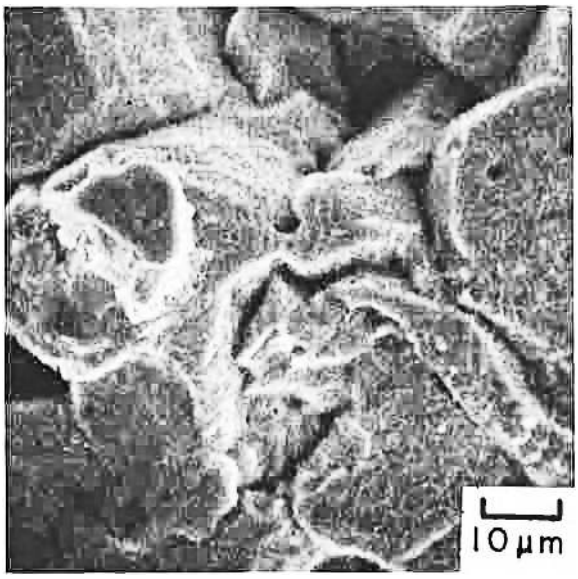

Figure 16. Deposit Obtained for an Electrolyte Containing 0.026 mg/ℓ Sb. T = 45°C; Current Density = 40 mA/cm^2. (1000x)

basal planes of the platelets appear to lie parallel to the substrate surface and exhibit lateral growth. The deposits obtained from the antimony and germanium and to a lesser extent cobalt-bearing electrolytes exhibit highly preferred (00·2), (10·4), (10·3) orientations. This is in general agreement with the results of other investigators (19,55). The deposits are not very uniform and differences in crystallite height are readily apparent. The platelets generally show rounded edges and give indications of some corrosion. The increase in crystallite size indicates a degree of depolarization. Other investigators have found a correspondence between the degree of depolarization and the crystallite size (17-19). The formation of hydrides or local cell action may cause depolarization by providing an alternative path for hydrogen discharge. Surface roughness increases the possibility of local cell action and the morphological characteristics of the deposits are quite consistent with this mechanism of impurity interaction. Whether the local cell action is caused by hydride formation or by hydrogen deposition on impurity sites needs further investigation.

Solutions Containing Germanium and Glue Combinations The deposits obtained for solutions containing 0.1 mg/l germanium and increasing glue contents exhibited considerable variation in orientation and morphology as the glue content in the electrolyte was increased. Figures 18-21 show this variation. As more glue is added to the solution, the mode of platelet growth becomes outward. Initially, the basal planes of the platelets are parallel to the substrate, but upon increasing the glue content, significant angularity appears and at high glue concentrations the basal planes appear to be oriented perpendicularly to the substrate. The crystallite size is somewhat reduced and the faceting

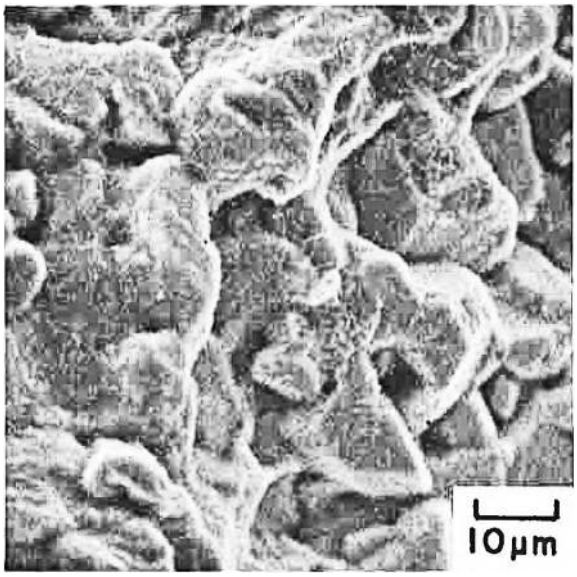

Figure 17. Deposit Obtained for an Electrolyte Containing 5 mg/ℓ Co. T = 45°C; Current Density = 40 mA/cm^2. (1000x)

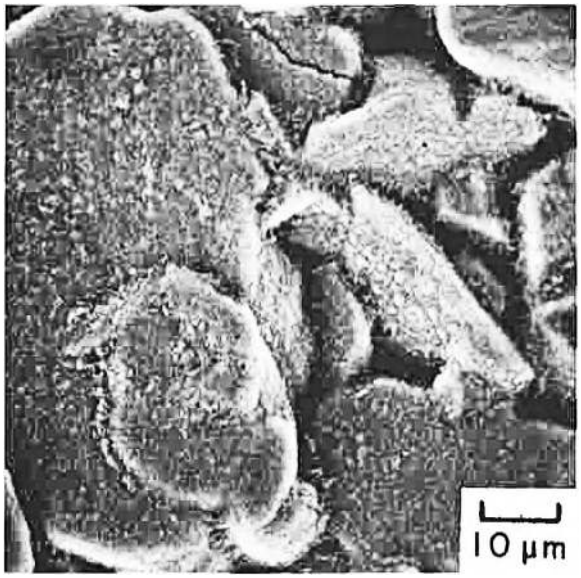

Figure 18. Deposit Obtained for an Electrolyte Containing 0.1 mg/ℓ Ge. T = 45°C; Current Density = 40 mA/cm^2. (1000x)

is more distinct with increased glue concentration. This is an indication of less corrosion of the zinc deposit. At low glue addition, (00·2), (10·4) preferred orientations predominate, but at high glue levels the morphology and crystallographic orientations are very similar to that obtained for the glue only solution ((10·1), (10·2), (11·2)).

The combination 0.1 mg/l Ge and 13 mg/l glue was found to have the best current efficiency. This balanced combination of glue and germanium resulted in a deposit morphology quite like that obtained for the no-addition solution. Increasing the glue content still further caused some decrease in the current efficiency and a deposit morphology and orientation approaching those obtained for solutions containing glue alone. Examination of Figures 15 and 21 confirms this trend.

A practical implication of these phenomena may be the determination of the optimum level of glue for solutions containing various impurity contents by monitoring the deposit morphology and crystallographic orientations. More research is necessary to determine if this is practical. The same trends were observed for antimony and glue combinations. Other investigators have obtained similar results (17-19). In general, the crystallographic orientations appear to go through the sequence (00·2), (10·4), (10·3), (11·4), (11·2), (10·2), (10·1), (11·0) upon increasing the glue content. Nearly the same trend has been reported by other investigators for studies on antimony-glue combinations (19). These investigators also conducted polarization studies and found that significant depolarization was associated with the (00·2) orientations and significant polarization

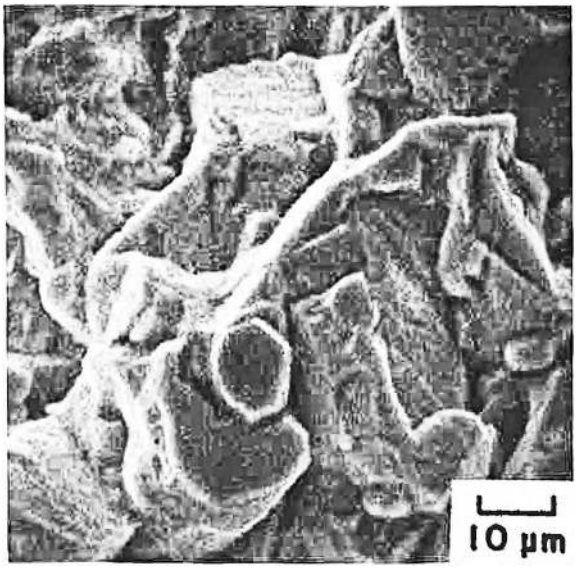

Figure 19. Deposit Obtained for an Electrolyte Containing 0.1 mg/ℓ Ge and 6 mg/ℓ Glue. T = 45°C; Current Density = 40 mA/cm^2. (1000x).

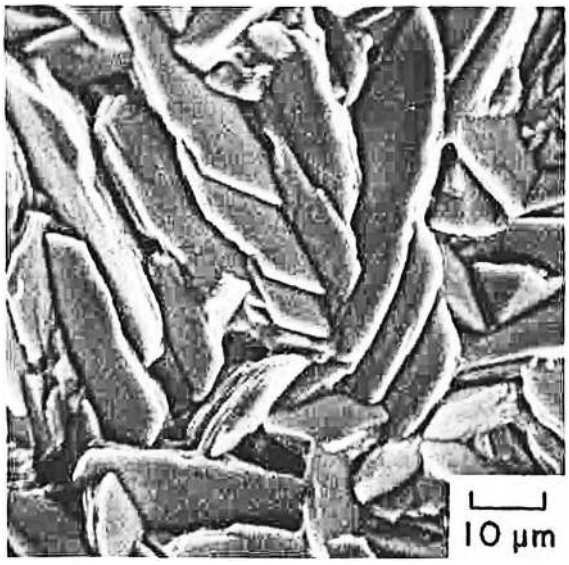

Figure 20. Deposit Obtained for an Electrolyte Containing 0.1 mg/ℓ Ge and 13 mg/ℓ Glue. T = 45°C; Current Density = 40 ma/cm^2. (1000x)

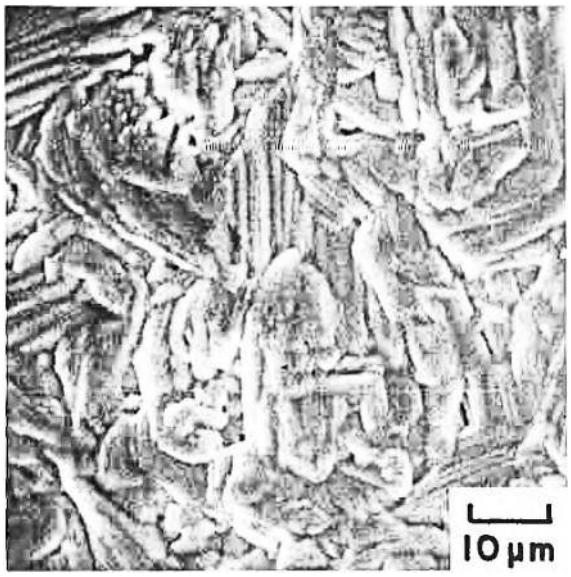

Figure 21. Deposit Obtained for an Electrolyte Containing 0.1 mg/ℓ Ge and 21 mg/ℓ Glue. T = 45°C; Current Density = 40 mA/cm^2. (1000x)

for the (10·1) orientations. Thus, the orientation may also indicate the degree of polarization of the cathode.

In summary, changes in morphology and crystallographic orientation were found for deposits from electrolytes containing various additions. The concentration levels which cause these changes are quite low and the differences between the various types of deposits are often quite profound. Solutions containing significant quantities of antimony, germanium, and cobalt often lead to deposits which exhibit noticeable surface roughness and this may enhance local cell corrosion. The platelets of zinc are generally aligned parallel to the substrate for deposits obtained from these solutions. For glue-containing electrolytes, the deposits are uniform and outward growth occurs. The uniformity of the deposit may aid in suppressing local cell formation. Combinations of glue and germanium lead to a series of deposit morphologies which depend on the amount of each additive. Apparent optimum levels lead to deposit morphologies that correspond quite closely to those obtained for a no-addition electrolyte.

Conclusions

1. Factorially designed experiments are quite useful in determining which factors are the most critical in affecting the current efficiency and the synergistic interactions existing among the various factors.
2. Acid level was found to be the most critical of the factors tested. Cobalt level, followed by temperature, antimony, germanium, and arsenic levels, were the next critical factors.
3. Significant detrimental synergism occurs for acid-cobalt combinations and care must be exercised with these two factors. Arsenic also appears to have a detrimental synergistic interaction with acid.
4. Cobalt and arsenic act synergistically and cause larger current efficiency losses than expected.
5. The combination of glue and antimony appears to lessen the deleterious effects of the other impurities. In the absence of glue, antimony appears to have a detrimental synergistic interaction with cobalt.
6. There is a definite correlation between cathode morphology and the additives in the electrolyte.
7. Proper combinations of glue and impurity appear to optimize the current efficiency.
8. A model can be derived using the calculated factor effects which allows some predictability for the system. A better model may be obtained by going to a more sophisticated design.

Acknowledgements

The authors wish to acknowledge the financial assistance provided by the AMAX Foundation, New York, NY, and the technical assistance provided by Cominco, Ltd., Trail, British Columbia, Canada, and AMAX Zinc Company, Sauget, IL. We would also like to thank ASARCO, Inc., Hillsboro, IL, for providing the French process zinc oxide used in this study. Without the continued interest and help of the above this work would not have been possible.

References

1. D. I. J. Evans and R. S. Shoemaker: International Symposium on Hydrometallurgy, 770-805, A.I.M.E., New York, 1973.
2. C. H. Cotterill and J. M. Cigan: World Symposium on Mining and Metallurgy of Lead and Zinc, Vol. II, 177-328, A.I.M.E., New York, 1970.
3. Giovanni Scacciati: Industria mineraria, 1953, 4, 511-16.
4. A. G. Pecherskaya and V. V. Stender: J. Appl. Chem. U.S.S.R., 1950, 23, 975-989.
5. V. S. Kolevatova and A. I. Levin: J. Appl. Chem. U.S.S.R., 1954, 27, 423-426.
6. Kurt Peukert and Willy Schreiter: Metallurgie u. Gressereitech, 1954, 4, 397-401.
7. G. N. Pakhomova and S. I. Orlova: Sbornik. Nauch. Trudov Gosudarst. Nauch. - Issledovatel. Inst. Tsvetn. Metal., 1955, No. 10, 183-99.
8. A. I. Levin, et al.: J. Appl. Chem. U.S.S.R., 1958, 31, 569-576.
9. N. T. Kudryavtsev and A. G. Atanasyants: Trudy Moskov. Khim. - Teknol. Inst. im. D. I. Mendeleeva, 1956, No. 22, 143-57.
10. A. V. Pomosov, et al.: J. Appl. Chem. U.S.S.R., 1958, 31, 727-734.
11. K. N. Kovalenko, et al.: Uchenye Zapiski Rostov.-na-Donu Univ., 1958, No. 41, 27-38.
12. N. T. Kudryavtsev: Trudy Soveshchaniyapo Voproson Vliyaniga Poverkhn. Aktiv. Veshchestv na Elektroosazhdenie Metal, 1958, 113-21.

13. Miroslav Kett: Hutnicke Listy, 1951, 16, 660-71.

14. Isao Kushima, et al.: Suiyokaishi, 1956, 13, 67-79.

15. A. A. Salin and V. S. Volkova: Sb. Nauchn.-Tekhn. Tr. Nauchn.-Issled. Inst. Met. Chelyab. Sovnarkhova, 1961, No. 4, 139-143.

16. Reiner Liebscher: Neue Heutte, 1969, 14, No. 11, 651-3.

17. D. J. Robinson and T. J. O'Keefe: J. Appl. Electrochem., 1976, 6, 1-7.

18. B. A. Lamping and T. J. O'Keefe: Met. Trans. B, 1976, 7B, No. 12, 551-558.

19. D. J. MacKinnon and J. M. Brannen: J. Appl. Electrochem., 1977, 7, No. 5, 451-459.

20. Peyu Bechev, et al.: Rudodobiv Met., 1966, 21, No. 8, 28-30.

21. S. T. Ross and J. L. Bray: J. Metals, 1951, 3, 465-7.

22. G. Z. Kir'yakov: Zhur. Fiz. Khim., 1958, 32, 2561-4.

23. A. F. Nikiforov and V. V. Stender: Ukrain. Khim. Zhur., 1959, 25, 18-24.

24. G. Z. Kir'yakov and F. K. Bainietova: Trudy Inst. Khim., Nauk Akad. Nauk Kazakh. S.S.R., 1958, 3, 64-71.

25. G. Z. Kir'yakov and Yu. D. Dunaev: Tr. Inst. Khim. Nauk., Akad. Nauk. Kaz. S.S.R., 1969, 24, 32-40.

26. A. F. Nikiforov: J. Appl. Chem. U.S.S.R., 1964, 37, No. 2, 360-363.

27. I. W. Wark: Proc. Australian Conf. Electrochem., 1st., Sydney, Hobart, Australia, 1963, 889-900.

28. M. Maja: Electrochim. Metal., 1967, 2, No. 4, 469-72.

29. Mario Maja and S. Pozzoli: Chim. Ind., 1969, 51, No. 2, 133-8.

30. Ignazio R. Bellobono: Ind. Chem. Belge, 1967, 32, 305-8.

31. D. R. Fosnacht: Masters Thesis, Columbia University, New York, 1975.

32. Strategy of Experimentation, E. I. du Pont de Nemours & Co., Wilmington, Delaware, 1975.

33. Sylvain Ehrenfeld and Sebastian Littauer: Introduction to Statistical Method, pp. 519-523, McGraw-Hill Book Company, New York, 1964.

34. U. F. Turomshina and V. V. Stender: J. Appl. Chem. U.S.S.R., 1954, 27, 1019-1025.

35. G. C. Bratt: Electrochem. Technol., 1964, 2, No. 11-12, 323-6.

36. A. R. Ault, et al.: paper presented at Aus. I.M.M. Conference, South Australia, July, 1975.

37. A. I. Levin, et al.: Ural Politekh. Inst. im. Kirova, Korroziya i Metallopokrytiya, Sbornik Statei, 1953, No. 43, 24-55.

38. Z. A. Sheka: Ukrain. Khim. Zhur., 1956, 22, 387-93.

39. Z. A. Sheka: Ukrain. Khim. Zhur., 1956, 22, 691-6.

40. A. I. Zhurin and S. P. Pyunnen: Trudy Leningrad. Politekhn. Inst. im. M. I. Kalinina, Elektromet. Tsvetnykh Metal, 1957, No. 188, 204-11.

41. P. Guareschi: Industria chimica, 1933, 8, 704-8.

42. V. G. Bundzhe and G. Z. Kir'yakov: Tr. Inst. Khim. Nauk. Akad. Nauk. Kaz. S.S.R., 1962, 9, 3-17.

43. R. C. Kerby, H. E. Jackson, T. J. O'Keefe, and Y. Wang: Met. Trans. B, 1977, 8B, No. 4, 661-668.

44. L. Cambi and G. G. Monselise: Rend. ist. lombardo sci., 1936, 69, 392-6.

45. G. N. Pakhomova: Tsvetnye. Metal., 1965, 38, No. 9, 33-6.

46. A. A. Salin, et al.: Tsvetnye. Metal., 1962, 35, No. 12, 13-18.

47. G. N. Kir'yakov, et al.: Tr. Inst. Khim. Nauk., Akad. Nauk. Kaz. S.S.R., 1969, 24, 50-6.

48. Pietro Guareschi: Industria chimica, 1934, 9, 1466-76.

49. T. N. Andersen, R. D. Budd, and R. W. Strachan: Met. Trans. B, 1976, 7B, No. 9, 333-338.

50. C. J. Krauss: J. Metals, 1976, 28, No. 11, 5-9.

51. G. E. P. Box and D. W. Behnken: Technometrics, 1960, 2, 455-475.

52. G. E. P. Box and K. B. Wilson: J. Royal Statistical Society, Series B, 1951, 1-45.

53. G. Z. Kir'yakov: Izv. Akad. Nauk Kaz. S.S.R., Ser. Khim., 1962, No. 2, 41-6.

54. F. O. El Kashif, J. Gerlach, and J. Osterwald: Metall., 1968, 22, No. 8, 792-5.

55. H. H. Fukubayashi, T. J. O'Keefe, and W. C. Clinton: R. I. 7966, U. S. Bureau of Mines, 1974.

56. Georg Steintveit and Hans Holtan: J. Electrochem Soc., 1960, 107, 247-8.

57. G. T. Weaver: J. Metals, 1959, 11, No. 2, 130.

58. G. M. Meisel: J. Metals, 1974, 26, No. 8, 25-32.

List of Figures

Figure 1. Current Efficiency vs Current Density for Industrial Electrolytes Containing 60 g/ℓ Zn and 200 g/ℓ H_2SO_4. T = 40°C.

Figure 2. Current Efficiency vs Acid Concentration for Industrial Electrolytes Containing 60 g/ℓ Zn. T = 40°C; Current Density = 40 mA/cm^2.

Figure 3. Current Efficiency vs Impurity Concentration for Prepared Electrolytes Containing 65 g/ℓ Zn and 200 g/ℓ H_2SO_4. T = 45°C; Current Density = 40 mA/cm^2.

Figure 4. Current Efficiency vs Cobalt Concentration for Prepared Electrolytes Containing 65 g/ℓ Zn and Various Acid Concentrations. T = 45°C; Current Density = 40 mA/cm^2.

Figure 5. Current Efficiency vs Antimony Concentration for Prepared Electrolytes Containing 65/ℓ Zn and Various Acid Concentrations. T = 45°C; Current Density = 40 mA/cm^2.

Figure 6. Current Efficiency vs Germanium Concentration for Prepared Electrolytes Containing 65 g/ℓ Zn and Various Acid Concentrations. T = 45°C; Current Density = 40 mA/cm^2.

Figure 7. Current Efficiency vs Acid Concentration for Prepared Electrolytes Containing 65 g/ℓ Zn and 80 ppb As. T = 45°C; Current Density = 40 mA/cm^2.

Figure 8. Current Efficiency vs Organic Additive Concentration for Prepared Electrolytes Containing 65 g/ℓ Zn and 100 g/ℓ H_2SO_4. T = 45°C; Current Density = 40 mA/cm^2.

List of Figures (Continued)

Figure 9. Current Efficiency vs Glue Concentration for Prepared Electrolytes Containing 65/ℓ Zn, 100 g/ℓ H_2SO_4 and Constant Amounts of Impurity Addition. T = 45°C; Current Density = 40 mA/cm^2.

Figure 10. Current Efficiency vs Cobalt Concentration for Prepared Electrolytes Containing 65 g/ℓ Zn and 100 g/ℓ H_2SO_4 With and Without 28 ppb Sb. T = 45°C; Current Density = 40 mA/cm^2.

Figure 11. Current Efficiency vs Germanium Concentration for Prepared Electrolytes Containing 65 g/ℓ Zn and 100 g/ℓ H_2SO_4 With and Without 5 mg/ℓ Co. T = 45°C; Current Density = 40 mA/cm^2.

Figure 12. Calculated Current Efficiency vs Experimental Current Efficiency for Results of the Factorial Design.

Figure 13. Deposit Obtained for a No-addition Electrolyte. T = 45°C; Current Density = 40 mA/cm^2. (1000x)

Figure 14. Deposit Obtained for an Electrolyte Containing 0.1 mg/ℓ As. T = 45°C; Current Density = 40 mA/cm^2. (1000x)

Figure 15. Deposit Obtained for an Electrolyte Containing 21 mg/ℓ Glue. T = 45°C; Current Density = 40 mA/cm^2. (1000x)

Figure 16. Deposit Obtained for an Electrolyte Containing 0.026 mg/ℓ Sb. T = 45°C; Current Density = 40 mA/cm^2. (1000x)

Figure 17. Deposit Obtained for an Electrolyte Containing 5 mg/ℓ Co. T = 45°C; Current Density = 40 mA/cm^2. (1000x)

Figure 18. Deposit Obtained for an Electrolyte Containing 0.1 mg/ℓ Ge. T = 45°C; Current Density = 40 mA/cm^2. (1000x)

List of Figures (Continued)

Figure 19. Deposit Obtained for an Electrolyte Containing 0.1 mg/ℓ Ge and 6 mg/ℓ Glue. T = 45°C; Current Density = 40 mA/cm^2. (1000x)

Figure 20. Deposit Obtained for an Electrolyte Containing 0.1 mg/ℓ Ge and 13 mg/ℓ Glue. T = 45°C; Current Density = 40 mA/cm^2. (1000x)

Figure 21. Deposit Obtained for an Electrolyte Containing 0.1 mg/ℓ Ge and 21 mg/ℓ Glue. T = 45°C; Current Density = 40 mA/cm^2. (1000x)

Evaluation of Zinc Sulfate Electrolytes Containing Certain Impurities and Additives by Cyclic Voltammetry and Electron Microscopy

Donald R. Fosnacht and Thomas J. O'Keefe

Abstract

The polarization characteristics of acid zinc sulfate electrolytes containing various amounts of germanium, antimony, cobalt, and glue were examined by cyclic voltammetry. The effects of zinc concentration, acid concentration, temperature, and surface preparation were also investigated. Small concentrations of impurities cause measureable changes in polarization behavior. Levels as low as 0.02 mg/l Ge or Sb and 0.1 mg/l Co can be detected using this technique. Polarization characteristics caused by the presence of impurities can be used to optimize the amount of glue needed to counteract the effects of the impurities. The actual mechanism of impurity interaction is more clearly delineated using this technique. Germanium and cobalt appear to form local galvanic cells, however, antimony does not. The results of these short term tests have proven to be correlatable with classical long term efficiency tests. The deposit morphologies obtained for short-time cathodic cycles were also studied using scanning electron microscopy.

Introduction

The presence of impurities in the electrolyte is a major problem for the zinc electrowinning industry. Decreases in zinc current efficiency and changes in deposit morphology and cathodic polarization occur for electrolytes containing small concentrations of impurities. Levels as low as parts per billion for antimony, germanium, and arsenic and parts per million for cobalt are reported to greatly influence the cathodic deposition of zinc (1-19).

Impurity behavior is not well understood and many questions remain regarding the acceptable limits of impurities for efficient operation of a zinc electrolysis circuit. Characterization of the electrolyte is very important and extensive analytical analyses are conducted to determine the levels of impurities in the electrolyte. Chemical analyses have always served as the primary means of evaluating the quality of the electrolyte. Unfortunately, not only the absolute magnitude of the various impurities, but also the synergistic interactions among them ultimately determine the electrolyzability of the solution. Thus, a rapid electrochemical evaluation test to complement existing analyses would be desirable. A promising development in this area is the application of cyclic voltammetry to evaluate zinc-bearing electrolytes. Recent investigations have shown that glue additions to antimony-containing zinc electrolytes can be optimized using this technique (2,4,6). Low levels of antimony and glue were found to cause measurable changes in cathodic polarization. The application of this technique to electrolytes containing nickel impurities indicated that nickel levels as low as 0.05 mg/l could be

detected (20). The mechanism of nickel interaction was also evaluated using this technique.

In the present study, scanning electron microscopy and cyclic voltammetry were used in an attempt to characterize the effects of cobalt, germanium, antimony, and glue on cathodic polarization and zinc deposition. The techniques were used to gain some insight into the mechanism of impurity interaction at the cathode and to develop a practical test procedure which could be applied to cathodic zinc processes.

Experimental

Solution Preparation

A stock solution of neutral (pH = 4.0 - 4.5) purified zinc sulfate solution was prepared by using high purity, French process zinc oxide powder and reagent grade sulfuric acid. The zinc sulfate was purified by adding 0.1 to 0.2 ml/l of 0.1 N $KMnO_4$; heating to near the boiling point with vigorous stirring; settling of the precipitates for 30 minutes at 80-85°C and then filtering. The filtrate was purified by adding 2 g/l of zinc dust; heating to the boiling point with stirring for 30 to 45 minutes and then filtering to remove excess zinc dust. An analysis of the neutral purified solution appears in Table I. Base electrolytes of varying zinc contents were prepared using this solution.

A stock solution containing 13 mg/l of antimony was prepared by dissolving antimony potassium tartrate in distilled water. Cobalt solution was prepared by dissolving cobaltous sulfate in distilled water to a concentration of 800 mg/l. A stock solution of germanium (10 mg/l) was prepared by dissolving the germanium in dilute sulfuric acid after GeO_2 was fused with Na_2CO_3 and K_2CO_3. All the stock solutions were analyzed by atomic absorption analysis. The solutions were stored in plastic bottles and analyzed periodically.

A stock solution of (1 g/l) glue (Swift -- EZ TPC # 3) was prepared by dissolving the organic in distilled water. The glue solution was stored under refrigeration to minimize degradation.

Test solutions were prepared by taking the required amount of neutral purified solution, reagent grade sulfuric acid, impurity

Table I. Analyses of Neutral Purified Solutions (mg/ℓ).

	Prepared
Zn	130,000
Mn	<0.1
Cd	1.3
Sb	0.01
As	<0.04
Sb + As	--
Ge	0.002
Co	<0.1
Ni	<0.05
Fe	0.4
Cu	0.08
F^-	0.1
Cl^-	1.0

solution, and glue and placing them in a 500 ml volumetric flask. The volume was adjusted to 500 ml by adding distilled water.

Cyclic Voltammetry

The cyclic voltammetry experiments were conducted in a Pyrex "H" cell employing an Al working electrode (1 cm^2 = area), a Pt counter electrode, and a mercurous sulfate reference electrode. A constant temperature water bath was used to maintain the desired temperature. A Petrolite Potentiodyne Analyzer (Model M-4100) was used to generate the cyclic voltammograms. The polarization behavior was recorded as a log current density versus potential plot. Figure 1 is a schematic of the experimental set-up.

The working electrodes were prepared by wet polishing on 600 grit paper. The electrodes were washed in an ultrasonic cleaner after polishing and then rinsed with distilled water and dried with hot air. The electrodes were then placed in the "H" cell and allowed to come to the test temperature. Tests were also conducted on electrodes which were wheel polished using 0.05μ γ-alumina. The cleaning and drying procedures were the same as described previously.

After reaching the test temperature, a voltammogram was obtained by driving the potential from -0.600 V vs S.H.E. to a more cathodic potential capable of producing a total current of 50 mA/cm^2. At this point the process was reversed and driven anodically to the original starting potential. Various scan rates were tried, but 0.5 mV/sec gave the most consistent results and was employed for the bulk of the studies. The factors studied were additive concentration, temperature, acid concentration, surface preparation, and zinc concentration.

In addition to the transient studies, tests were performed using

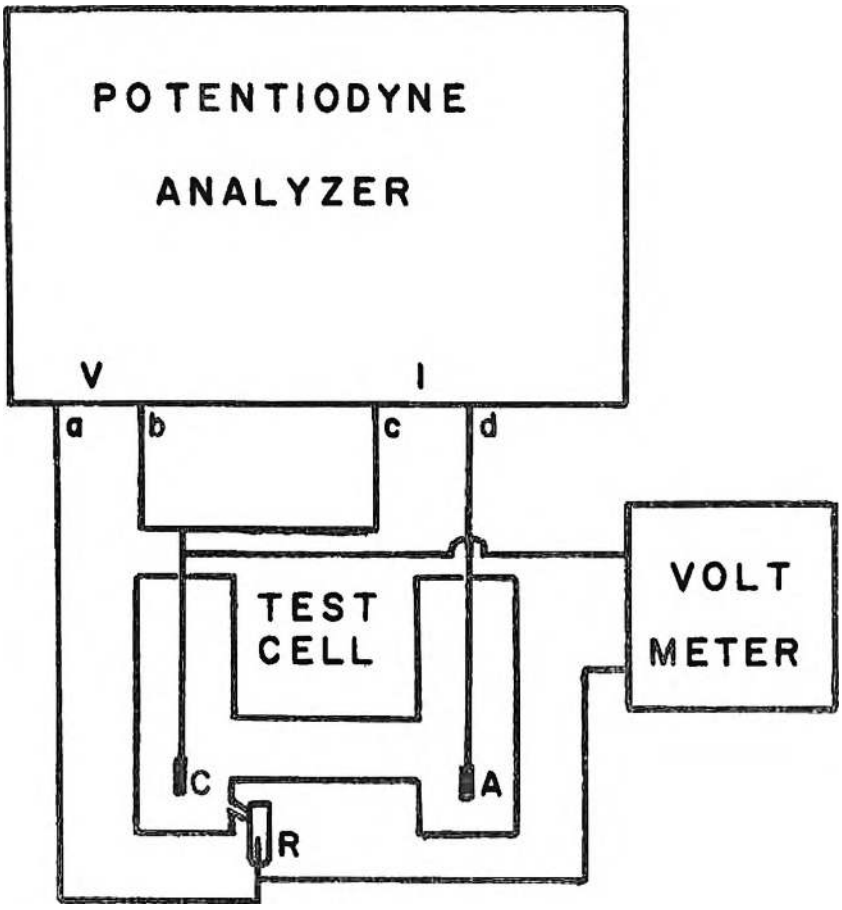

Figure 1. Schematic of Equipment Used for the Cyclic Voltammetry Experiments. [C = Working Electrode (Al); R = Mercurous Sulfate Reference Electrode; A = Auxiliary Electrode (Pt); V = Voltage Monitoring Terminals; and I = Current Supply Terminals].

constant potentials to determine the stability of the deposited zinc under various conditions. The morphologies of the zinc deposits were obtained using scanning electron microscopy.

Results and Discussion

In order to gain a better understanding of the voltammograms and other results that follow, reactions that are useful in describing the processes occurring at the working electrode are listed in Table II. These reactions will be discussed in light of the results throughout this section.

Voltammograms for No-Addition Electrolytes

For an electrolyte containing 65 g/l Zn and 200 g/l H_2SO_4 and a 45°C temperature, a voltammogram of the type shown in Figure 2 is obtained. From point A to point C (-0.782 V vs S.H.E.), only hydrogen evolution on the aluminum substrate occurs. At potentials more negative than point C (the zinc deposition potential), both hydrogen evolution and zinc deposition occur on the aluminum substrate. At point D, the scan direction is reversed and the potential is driven in an anodic direction.

Zinc stability tests were conducted to determine where the zinc becomes unstable. It was found that the zinc becomes unstable at a potential (-0.781 V vs S.H.E.) roughly 20 mV more electronegative than point E. When the potential was held at this value, the zinc completely dissolved after 20 minutes. At potentials more electronegative than this point, the current reaches a steady state value and zinc can be detected on the electrode surface. At point E (-0.761 V vs S.H.E.), the net current becomes anodic and stays anodic until point F is reached. The elimination of the zinc from the electrode causes the anodic current to drop and after point F the current again becomes cathodic and only hydrogen discharge occurs. From E to F,

Table II. Possible Reactions Occurring at the Working Electrode

Cathodic Reactions

1.	$H^+(aq) + e = \frac{1}{2}H_2(g)$	(Aluminum Substrate)
2.	$M^{n+}(aq) + ne = M(s)$*	(Aluminum Substrate)
3.	$Zn^{2+}(aq) + 2e = Zn(s)$	(Aluminum Substrate)
4.	$M^{n+}(aq) + ne = M(s)$*	(Zinc Substrate)
5.	$Zn^{2+}(aq) + 2e = Zn(s)$	(Zinc Substrate)
6.	$H^+(aq) + e = \frac{1}{2}H_2(g)$	(Zinc Substrate)
7.	$H^+(aq) + e = \frac{1}{2}H_2(g)$	(M(s) Substrate)
8.	$xM^{n+}(aq) + yH^+(aq) + (xn+y)e = MxHy$	(Aluminum or Zinc Substrates)

Anodic Reaction

9.	$Zn(s) = Zn^{2+}(aq) + 2e$	(Aluminum or Zinc Substrates)

*where M = Co, Ge, Sb.

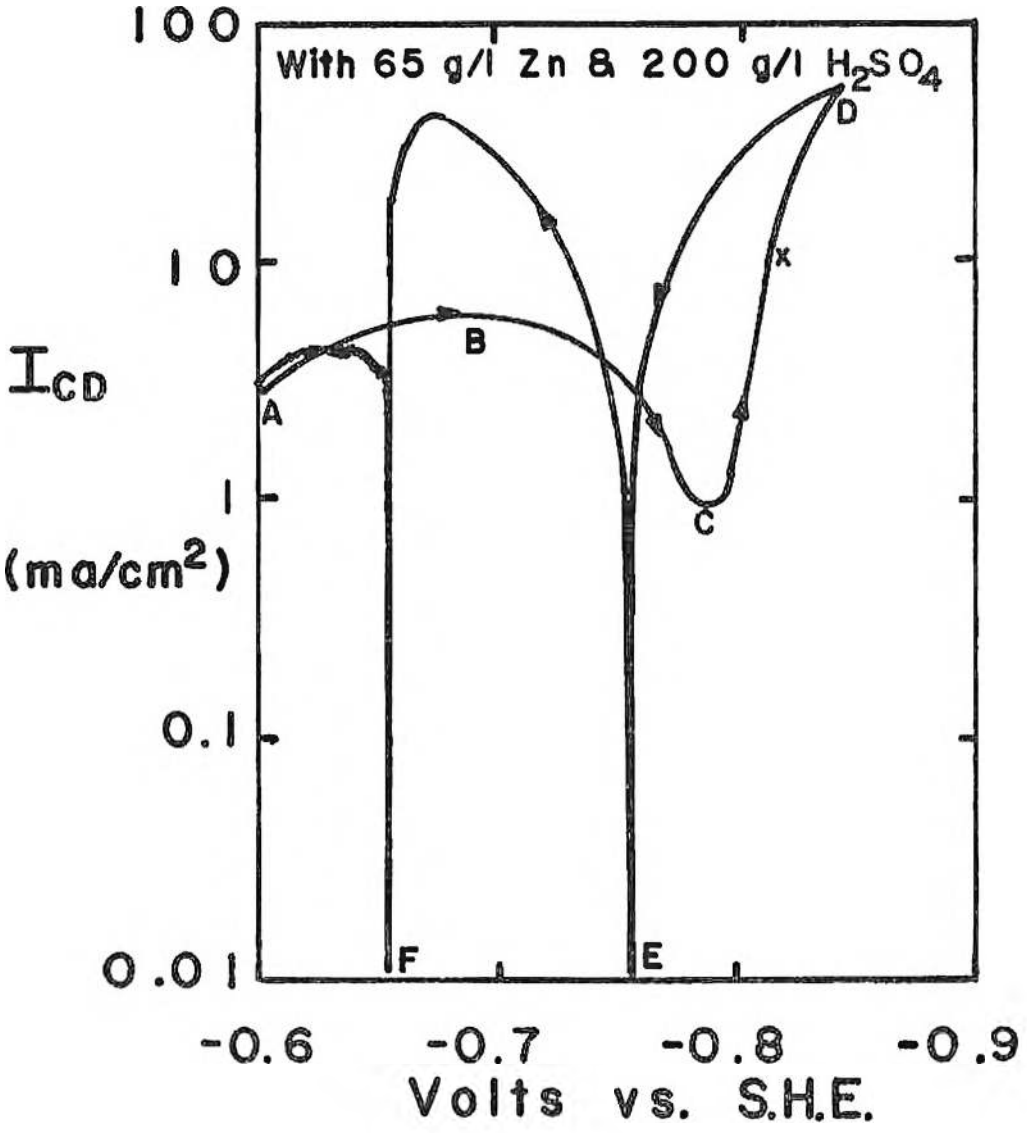

Figure 2. Voltammogram for No-Addition Electrolyte.

T = 45°C; Scan Rate = 0.5 mV/sec.

the zinc dissolution current is higher than the hydrogen reduction current and the net current is therefore anodic. Hysteresis of the curve from D to E exists because zinc and hydrogen ions discharge on both zinc and aluminum substrates. Zinc deposition on zinc requires less activation overpotential, so the current is higher than that measured on the front sweep when compared at the same potential.

A separate test was conducted to determine the reasons for the decrease in hydrogen discharge from B to C. The results, shown in Figure 3, indicate that the hydrogen current continually increases for solutions containing only sulfuric acid. When 1 M $MgSO_4$ is added, some polarization occurs. The general shape of the curves in both cases is, however, quite similar. The decreased current is probably due to physical adsorption of the Mg^{++} ions in the double layer.

The addition of zinc ions to the acid solution causes considerably greater polarization and a change in the shape of the curve as well. Initially, the hydrogen current increases slightly when the potential becomes more electronegative, but a current maximum is reached. Up to this point the zinc ions may act similarly to the magnesium ions, but beyond this point they dramatically suppress hydrogen current. The large decrease in hydrogen current appears to be due to the specific adsorption of zinc ions or other species formed on the aluminum substrate (21-23). The film thus formed may alter the hydrogen discharge reaction. Zinc ion adsorption is reported to hinder the discharge of cobalt, nickel, and iron in a similar fashion (22-23), and appears to be one of the dominating factors in zinc electrowinning.

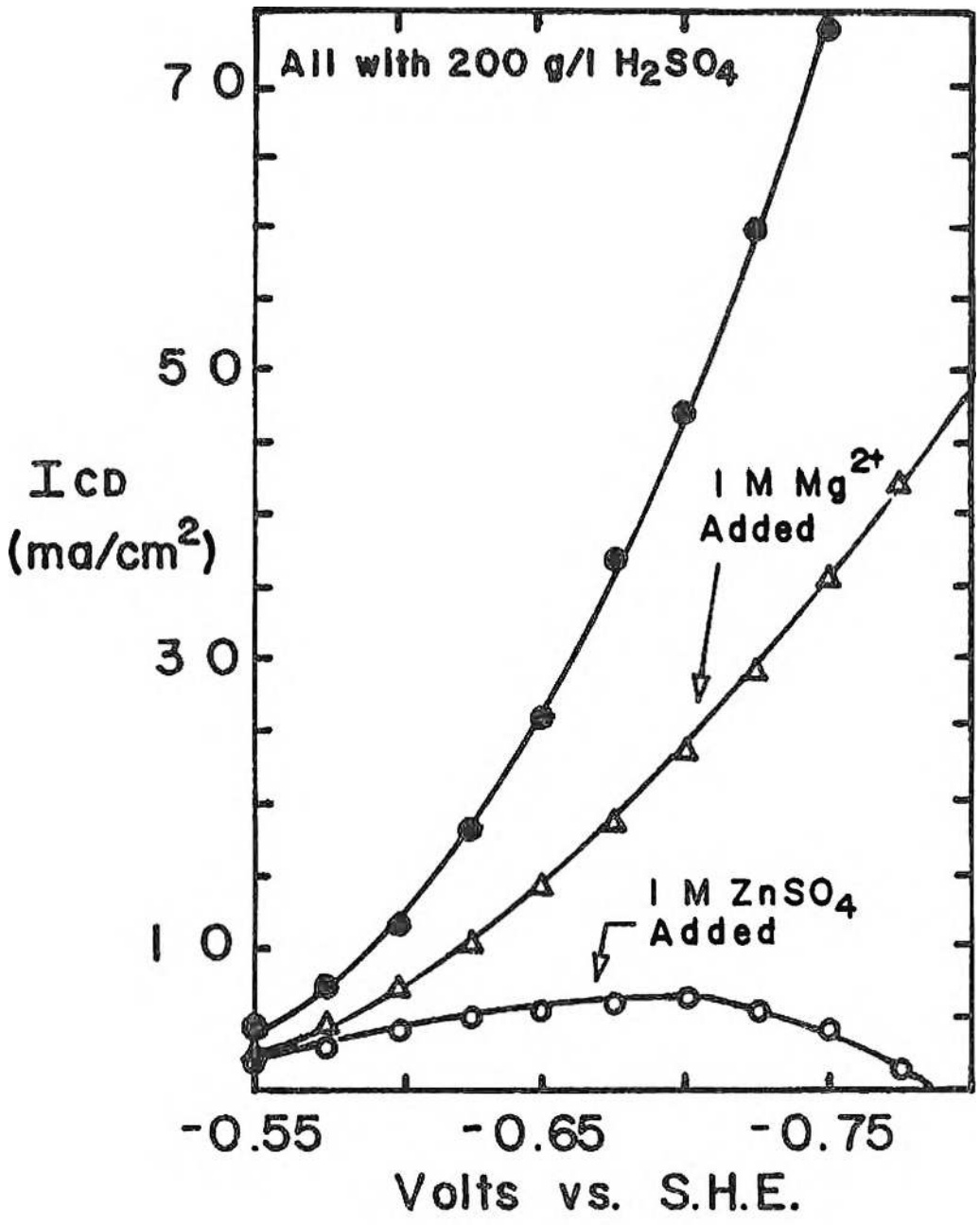

Figure 3. Hydrogen Current Density vs Electrode Potential for Electrolytes Containing 200 g/ℓ H_2SO_4 and the Indicated Additions. T = 45°C; Scan Rate = 0.5 mV/sec.

Voltammograms for Electrolytes Containing Germanium or Cobalt Additions

The presence of low levels of Co and Ge impurities causes changes in the zinc polarization curve as illustrated in Figures 4 and 5. Levels as low as 0.08 mg/l germanium and 1 mg/l cobalt cause measureable changes in polarization for electrolytes containing 65 g/l Zn and 200 g/l H_2SO_4.

At low levels of these impurities a small inflection appears in the basic curve at point i. Upon increasing the impurity content this changes to a flat plateau and finally to a hump or peak at point ai. The sequence of changes which occur are shown in Figure 5. The value of the current density at point ai (subsequently called the peak current density) is found to be proportional to the amount of impurities in the electrolyte. Figure 6 illustrates the trend of this peak current density with increasing cobalt content at 45°C and 55°C. Increasing the temperature causes the peak height to increase at a given impurity concentration.

This peak appears only after some zinc has deposited. The peak does not appear when the cathodic sweep direction is reversed prior to reaching the zinc deposition potential. At this peak vigorous hydrogen evolution occurs and the deposited zinc completely dissolves from the electrode surface even though the net current is cathodic. Stability tests conducted on electrolytes containing these impurities indicate that the zinc becomes completely unstable after the potential is made more electropositive than point i. At potential values more electronegative than point i, another phenomenon occurs for solutions containing moderate levels of impurity. Instead of reaching a steady state current at a given potential, cycles of deposition and

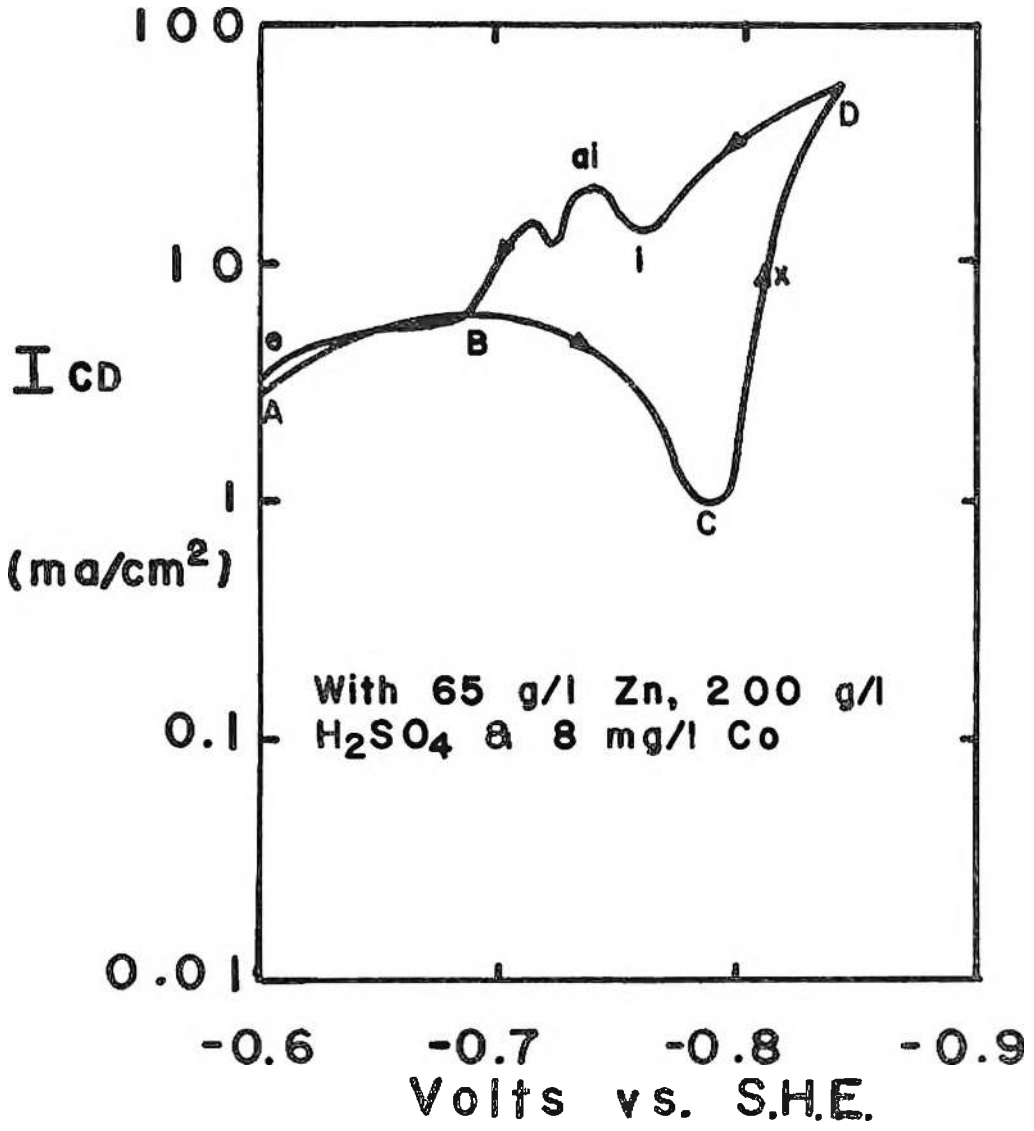

Figure 4. Voltammogram Obtained for Electrolytes Containing Germanium or Cobalt Additions. T = 45°C; Scan Rate = 0.5 mV/sec.

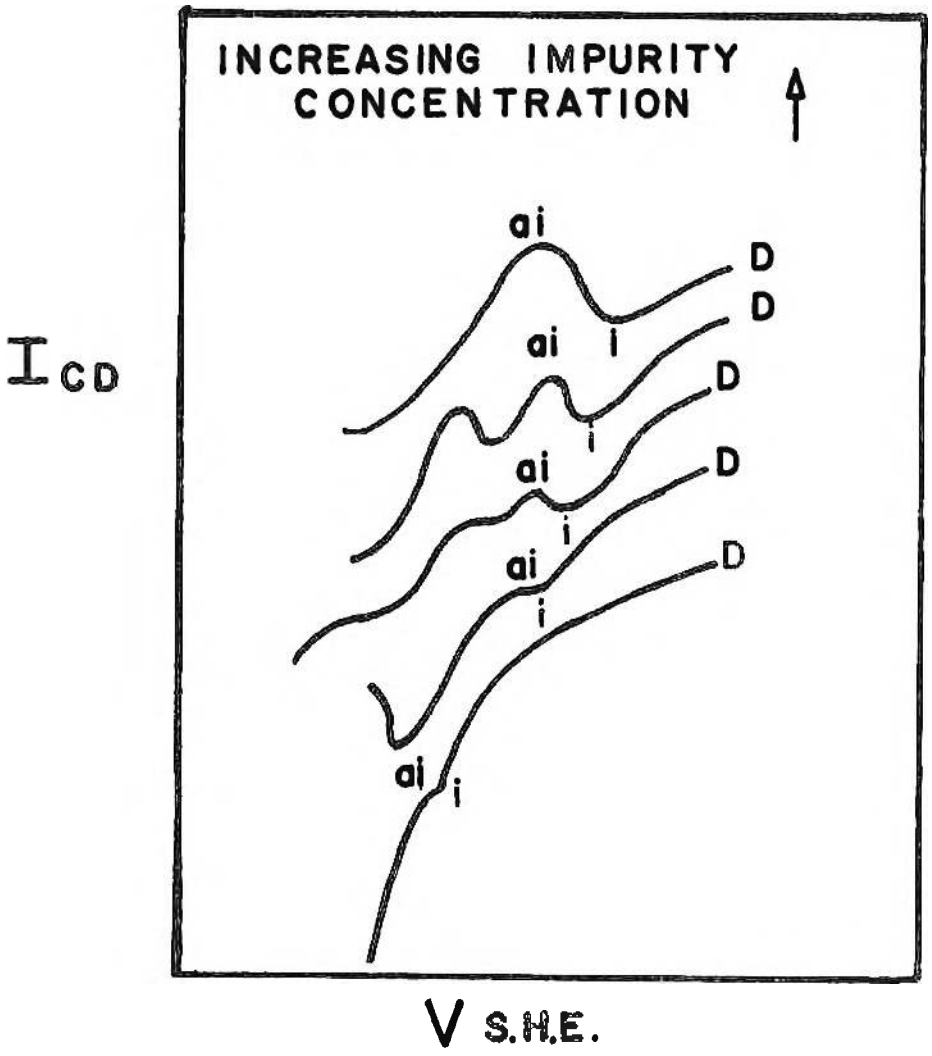

Figure 5. Sequence of Changes that Occur at Points i and ai as the Impurity Concentration Increases for Electrolytes Containing Germanium or Cobalt Additions.

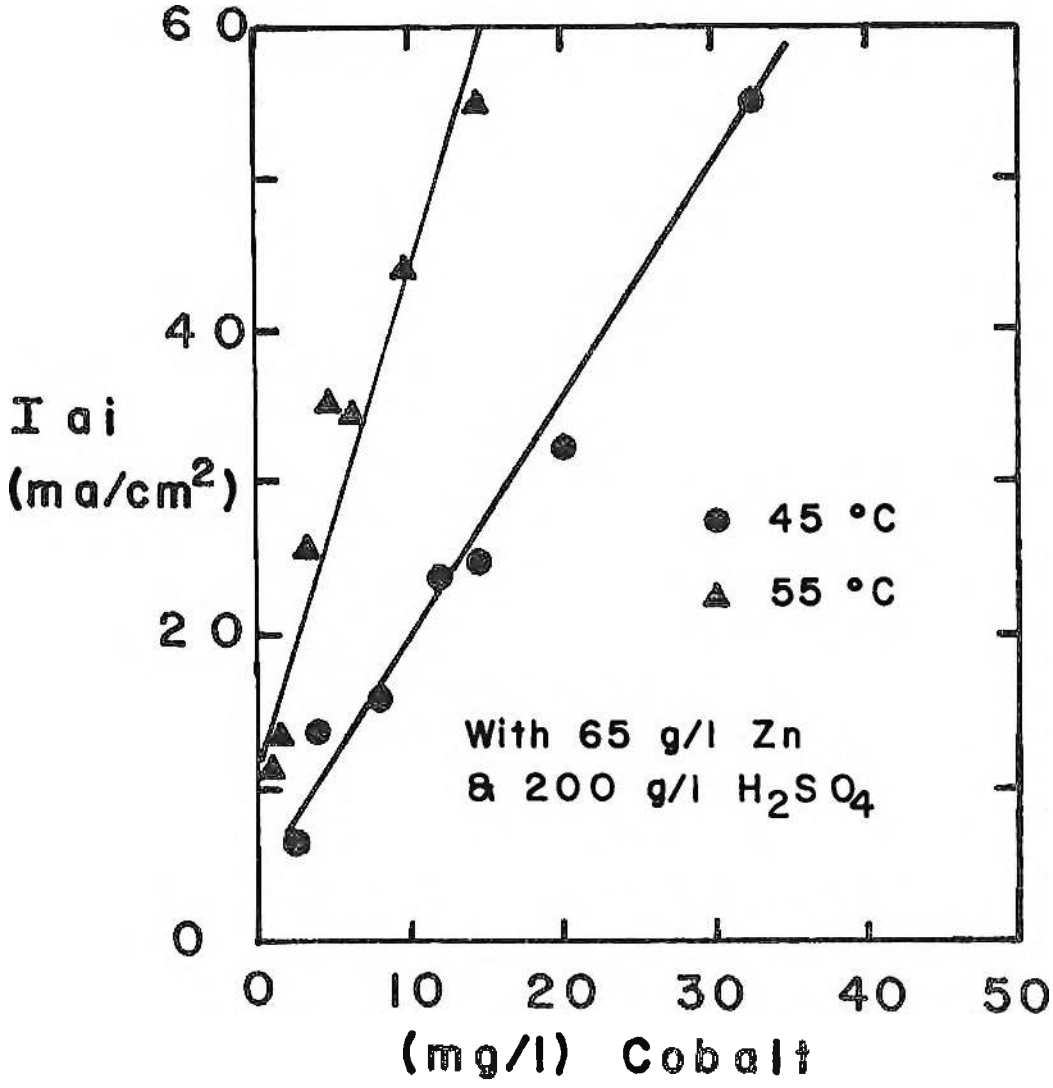

Figure 6. Peak Current Density vs Cobalt Content. Scan Rate = 0.5 mV/sec.

dissolution occur. Zinc deposits initially; but, with time, vigorous hydrogen evolution begins and very high current densities are obtained (200 mA/cm^2). The current peaks and then falls to relatively low values (less than 10 mA/cm^2). The electrodes were checked for zinc on the SEM at this point, but neither zinc nor impurity metal were detected. Zinc redeposition begins after a certain time interval, and the sequence is repeated. The cycle time depends on the impurity concentration. Electrolysis studies done by other investigators confirm similar cyclic behavior for solutions containing cobalt, nickel, and germanium impurities (9,10).

The impurities do not seem to accumulate on the working electrode. Continuous cycling yields relatively similar scans, which indicates little impurity accumulation. The impurities may become unstable when the zinc dissolves because of the loss in cathodic protection afforded by the presence of the deposited zinc or they may not adhere well to the aluminum substrate and are physically flushed from the electrode surface by the vigorous hydrogen evolution. If the impurities did accumulate on the electrode surface, higher hydrogen currents would be expected even after the zinc had completely dissolved because the exchange currents for hydrogen discharge on cobalt and germanium are significantly higher than that of aluminum or zinc and hydrogen discharge on these metals should be easier.

The point at which the zinc becomes completely unstable (point i) is found to occur at a potential value similar to that of the no-addition electrolyte (approximately -0.783 V vs S.H.E.) and this point appears to depend only on the zinc and acid concentrations and not on the impurity concentration. Point i will be called the zinc

instability potential in subsequent discussions.

Germanium and cobalt cause significant changes in the back scan, as demonstrated above, but do not affect the front scan. The zinc deposition potential and the potential at point x (potential which gives a current density of 10 mA/cm^2) are nearly identical, as shown by values given in Table III. This similarity is illustrated by Figures 7-9. The deposits were obtained by scanning to point D and holding the potential constant at this point for 1 minute. The coverage was evenly distributed for all these deposits and each crystallite appears to be growing independently of its neighbors. There appears to be little tendency for the particles to clump together. The crystallite size is quite similar for the deposits obtained from no-addition electrolytes and for those containing 0.1 mg/l germanium. The crystallite size is slightly smaller for the deposit obtained from the electrolyte containing 8 mg/l cobalt.

Since there is virtually no change in the front scan portion of the voltammogram, the amount of impurity deposition prior to zinc deposition appears to be insignificant or at least insufficient to cause any notable increase in the cathodic hydrogen current. This is most likely due to the inhibiting effect of specifically adsorbed zinc ions which greatly reduce the rate of discharge of the impurity ions. Other investigators have found that the presence of as little as 6 g/l Zn in a 1 M $CoSO_4$ electrolyte can prevent virtually any cobalt deposition at potentials less than the zinc discharge potential (21-23,25, 26). The retarding effect of the zinc ion is less when the zinc ions begin to deposit and significant amounts of impurity co-deposit with the zinc (23).

Table III. Comparison of Zinc Deposition Potential and Potential at Point x for Electrolytes With and Without Impurity Addition.

	Zn Deposition Potential V vs S.H.E.	Potential at Point x V vs S.H.E.
No Addition	-0.782	-0.806
4-32 mg/l Co	-0.783	-0.809
0.1 mg/l Ge	-0.788	-0.811

Experimental Error ± 7 mv.

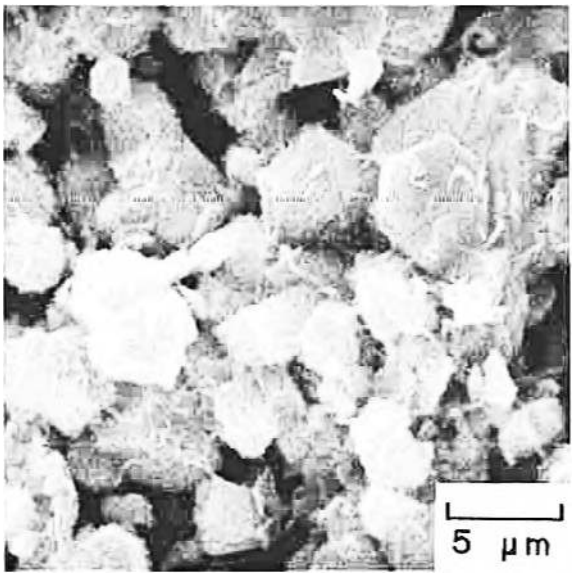

Figure 7. Zinc Deposit Obtained for Electrolyte Containing 65 g/ℓ Zn and 200 g/ℓ H_2SO_4. Potential Held at Point D for 1 Minute. (3000x)

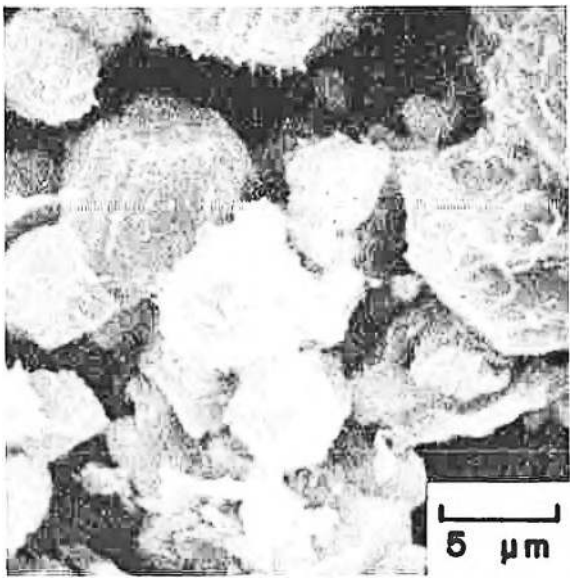

Figure 8. Zinc Deposit Obtained for Electrolyte Containing 65 g/ℓ Zn, 200 g/ℓ H_2SO_4, and 100 ppb Ge. Potential Held at Point D for 1 Minute. (3000x)

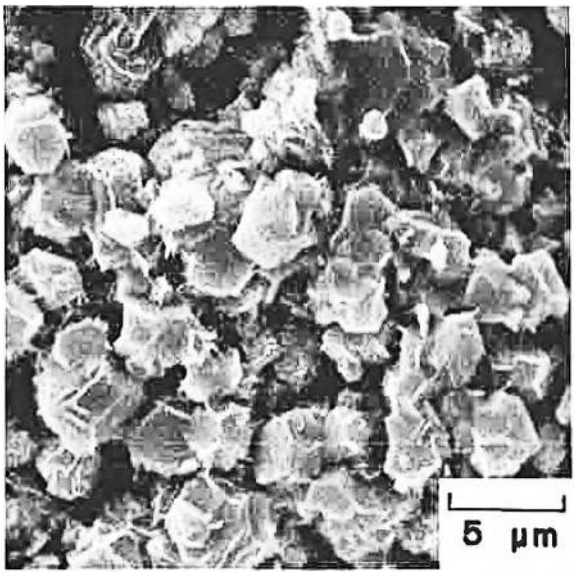

Figure 9. Zinc Deposit Obtained for Electrolyte Containing 65 g/ℓ Zn, 200 g/ℓ H_2SO_4, and 8 mg/ℓ Co. Potential Held at Point D for 1 Minute. (3000x)

Factors Affecting the Co and Ge Voltammograms

It was found that increased temperature, surface roughness, acid concentration and decreased zinc concentration increase the peak current density.

Zinc Concentration The effect of varying zinc concentration is shown in Figure 10. Increasing the zinc concentration suppressed the effect of the impurity and also caused a shifting of the zinc deposition potential and zinc instability point to less electronegative potentials. Concentrations of 0.1 mg/l Co and 0.02 mg/l Ge could be detected by diluting the base electrolyte to 6.5 g/l Zn with 200 g/l sulfuric acid.

Acid Concentration The interaction of the impurities was significantly enhanced by increasing the sulfuric acid concentration. The cyclic voltammetry experiments indicate that significantly less impurity can be tolerated at higher acid concentrations as might be expected. This is illustrated by the results shown in Figure 11. Increasing acid concentration also increases the initial hydrogen ion reduction (see Figure 12). Increasing acid concentrations lead to increased impurity effects and greater amounts of cathodically produced hydrogen. Both factors lead to a decrease in zinc current efficiency.

Surface Roughness The effect of increased surface roughness is illustrated by Figure 13. The 600 grit polished electrodes were more sensitive to increasing impurity content than the wheel-polished electrodes. Increasing surface roughness increases the detrimental interaction of the impurities at the electrode. The increased sensitivity of the rougher 600 grit polished electrodes was utilized by

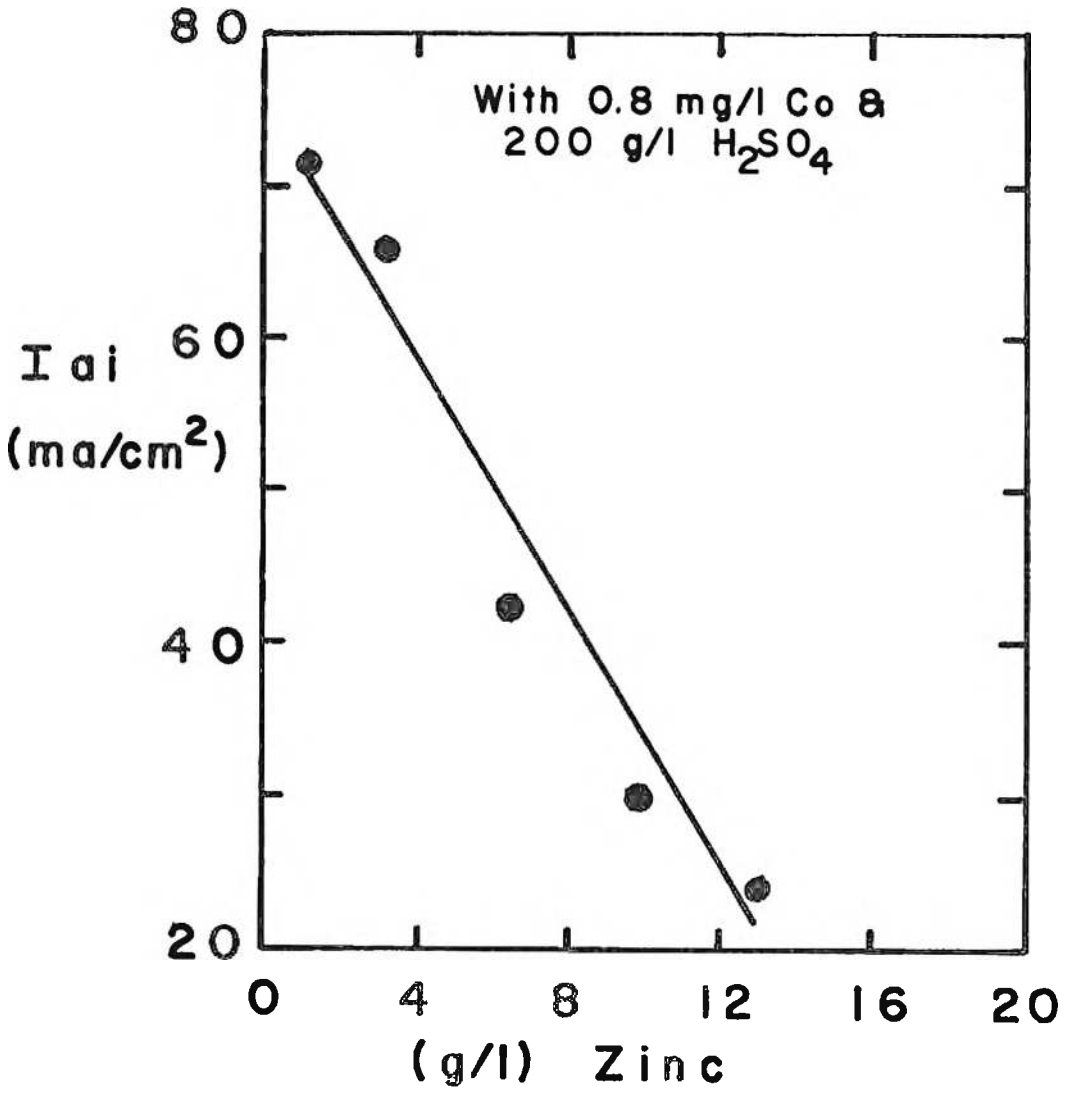

Figure 10. Peak Current Density vs Zinc Concentration.

Scan Rate = 0.5 mV/sec; T = 45°C.

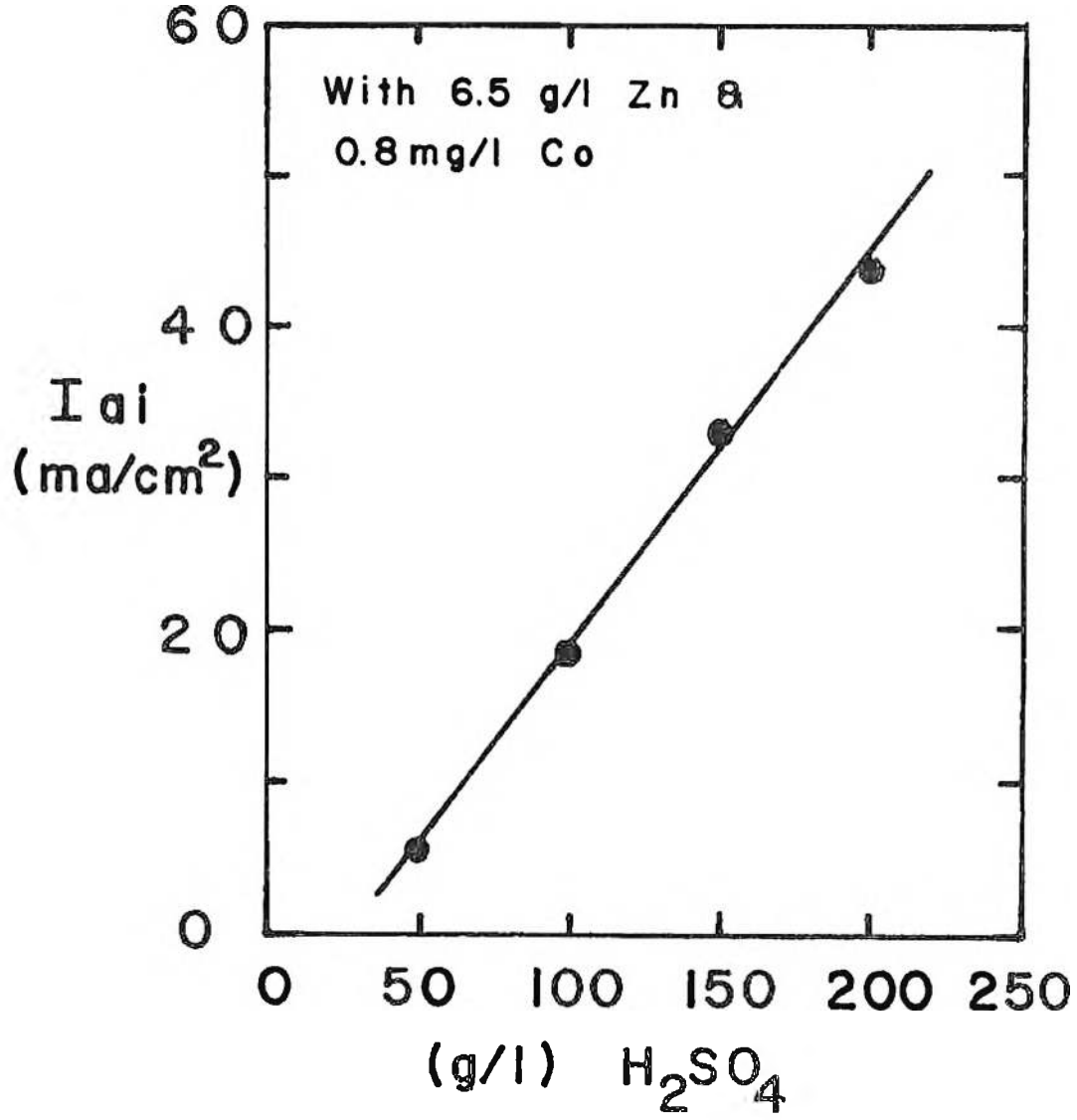

Figure 11. Peak Current Density vs Acid Concentration.

Scan Rate = 0.5 mV/sec; T = 45°C.

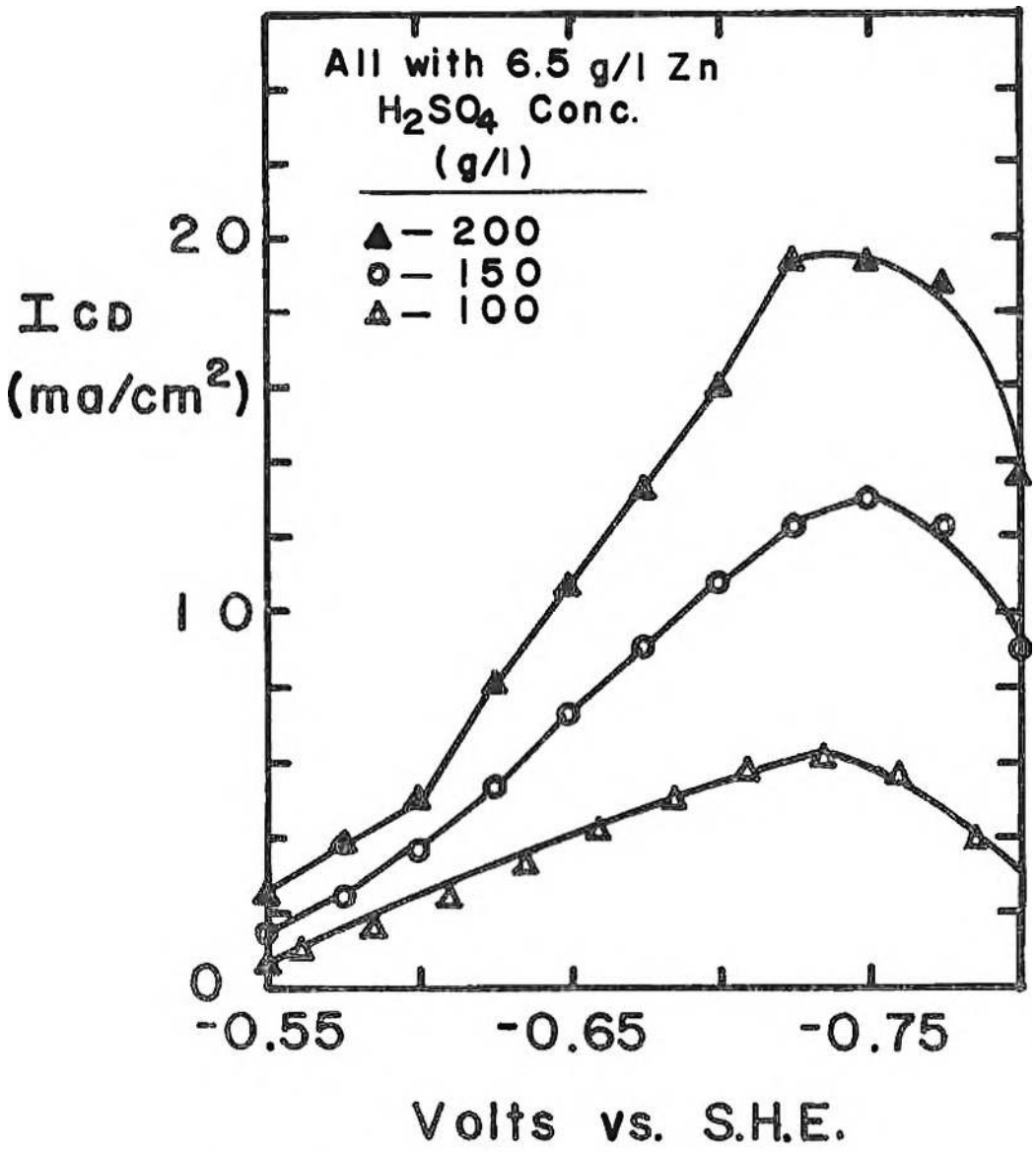

Figure 12. Hydrogen Current Density vs Electrode Potential for Electrolytes Containing 6.5 g/ℓ Zn and Various H_2SO_4 Concentrations. Scan Rate = 0.5 mV/sec; T = 45°C.

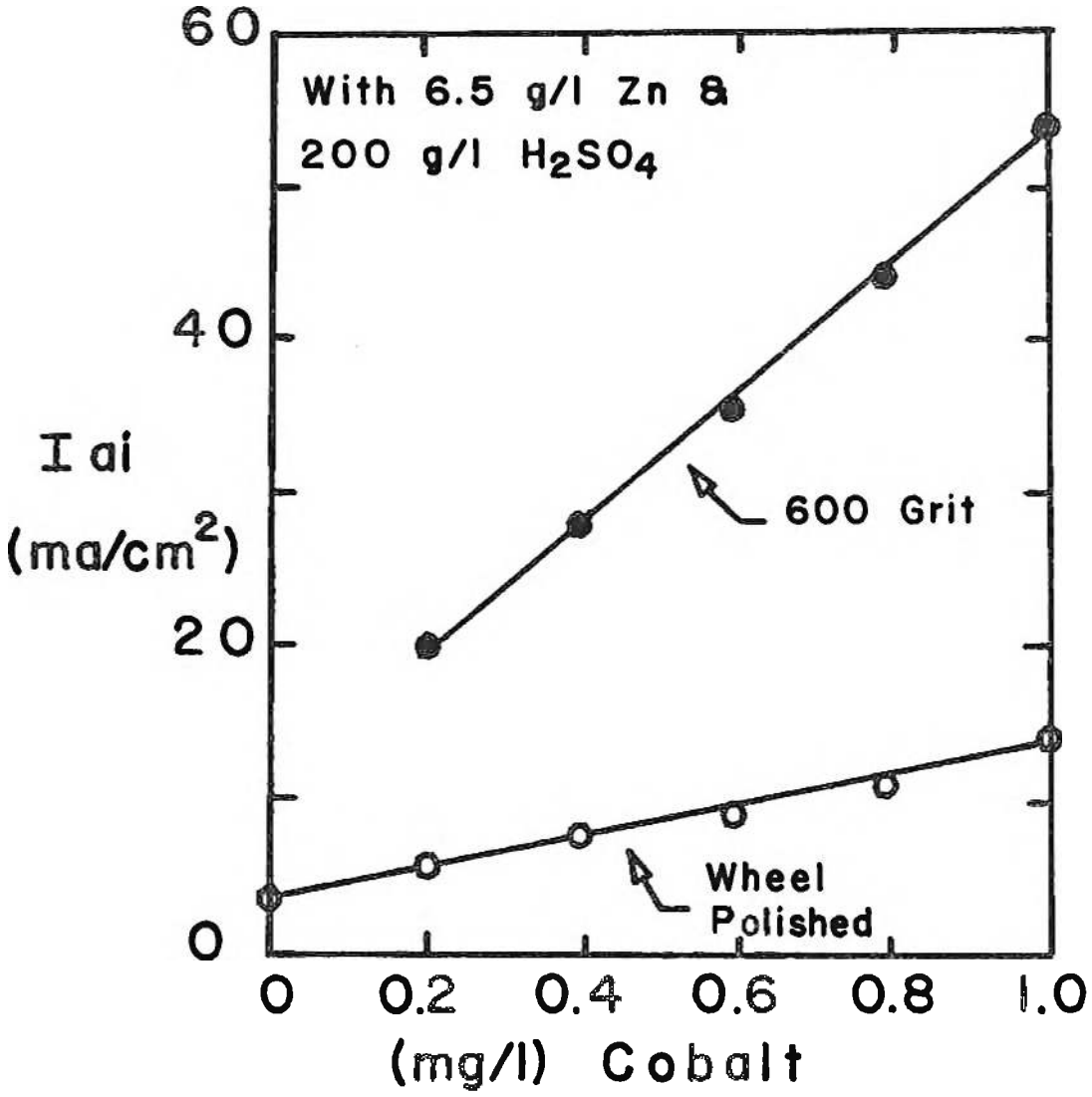

Figure 13. Peak Current Density vs Cobalt Concentration for Working Electrodes Having Different Surface Preparation. Scan Rate = 0.5 mV/sec; T = 45°C.

conducting most of the tests with these electrodes. The variability was somewhat higher than that of the wheel-polished samples (± 3 mA/cm^2 to ± 1 mA/cm^2), but the increased sensitivity compensated for this increased variability.

Impurity Concentration and Temperature The linearity of the peak current density with impurity concentration is illustrated by Figures 14 and 15. Figure 14 shows the results obtained for germanium and Figure 15 for cobalt. The linear variation of peak current density with impurity concentration indicates indirectly that the rate of impurity deposition is diffusion controlled. Other investigators using different techniques have also found this to be the case for comparable impurity levels (11,24,27-29). Figure 15 also illustrates the effect of temperature on the peak current density. A temperature change from 35 to 55°C results in increased peak current densities for the same level of impurity concentration. The temperature increase causes an enhanced impurity effect at the electrode and zinc stability is reduced. Higher temperatures increase the sensitivity of the cylic voltammetry technique allowing lower levels of impurity detectability. For cobalt, the detectable limit is 0.4 mg/l at 35°C and 0.1 mg/l at 55°C for an electrolyte containing 6.5 g/l Zn and 200 g/l H_2SO_4.

Test Time The total test time of the voltammograms discussed thus far is approximately 25 minutes. This test time can be greatly reduced by using a fast scan speed for the front scan (5 mV/sec) and a slow scan from point D on (0.5 mV/sec). The resulting voltammogram is similar in shape to that obtained using the slow scan throughout. The peak current densities again show the same type of relationship

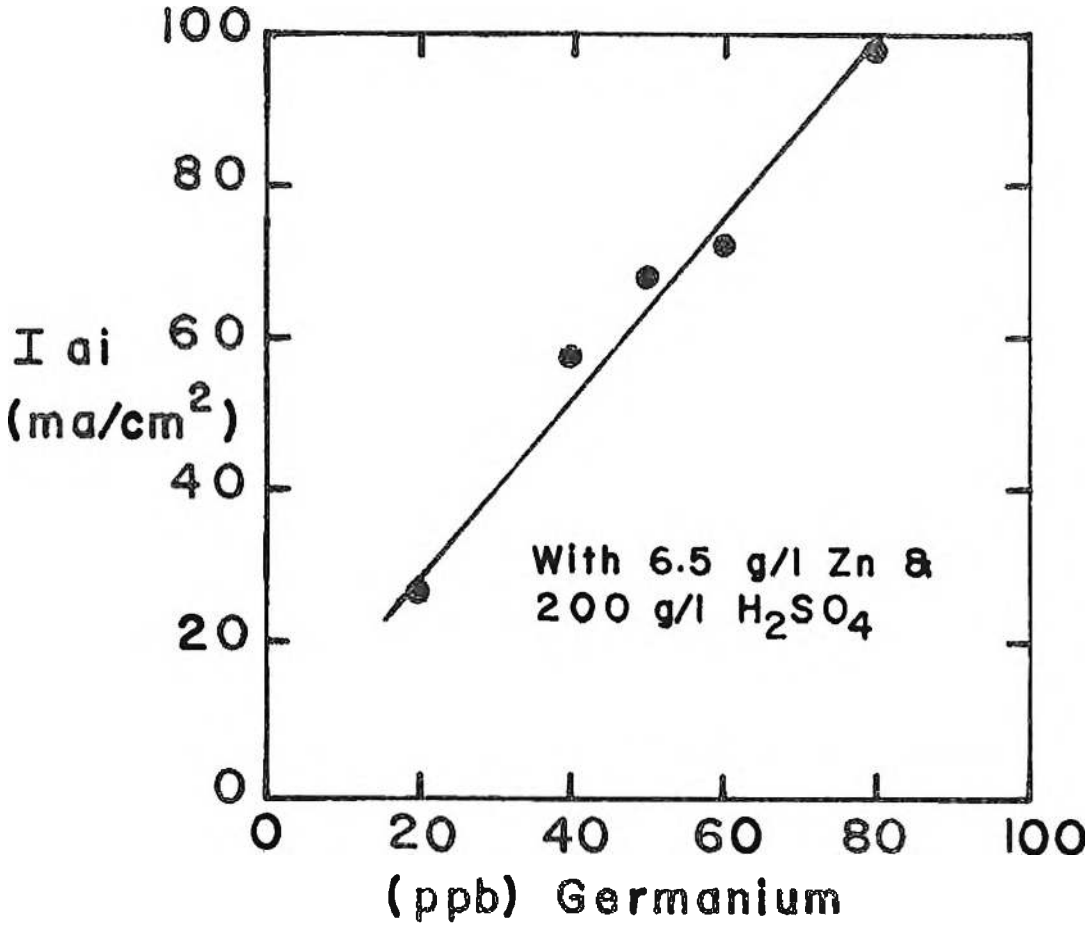

Figure 14. Peak Current Density vs Germanium Concentration.

Scan Rate = 0.5 mV/sec; T = 45°C.

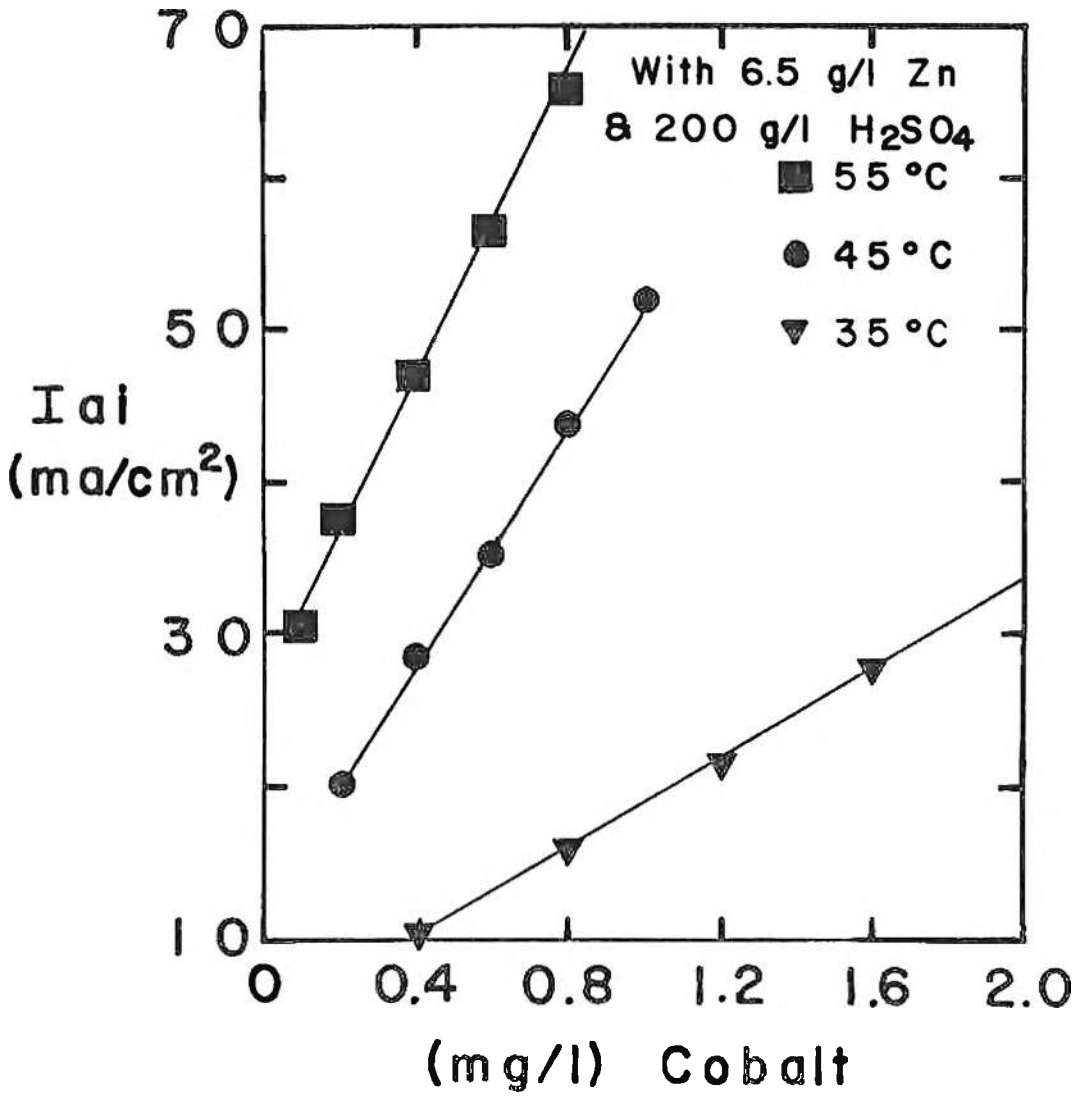

Figure 15. Peak Current Density vs Cobalt Concentration for Various Temperatures. Scan Rate = 0.5 mV/sec.

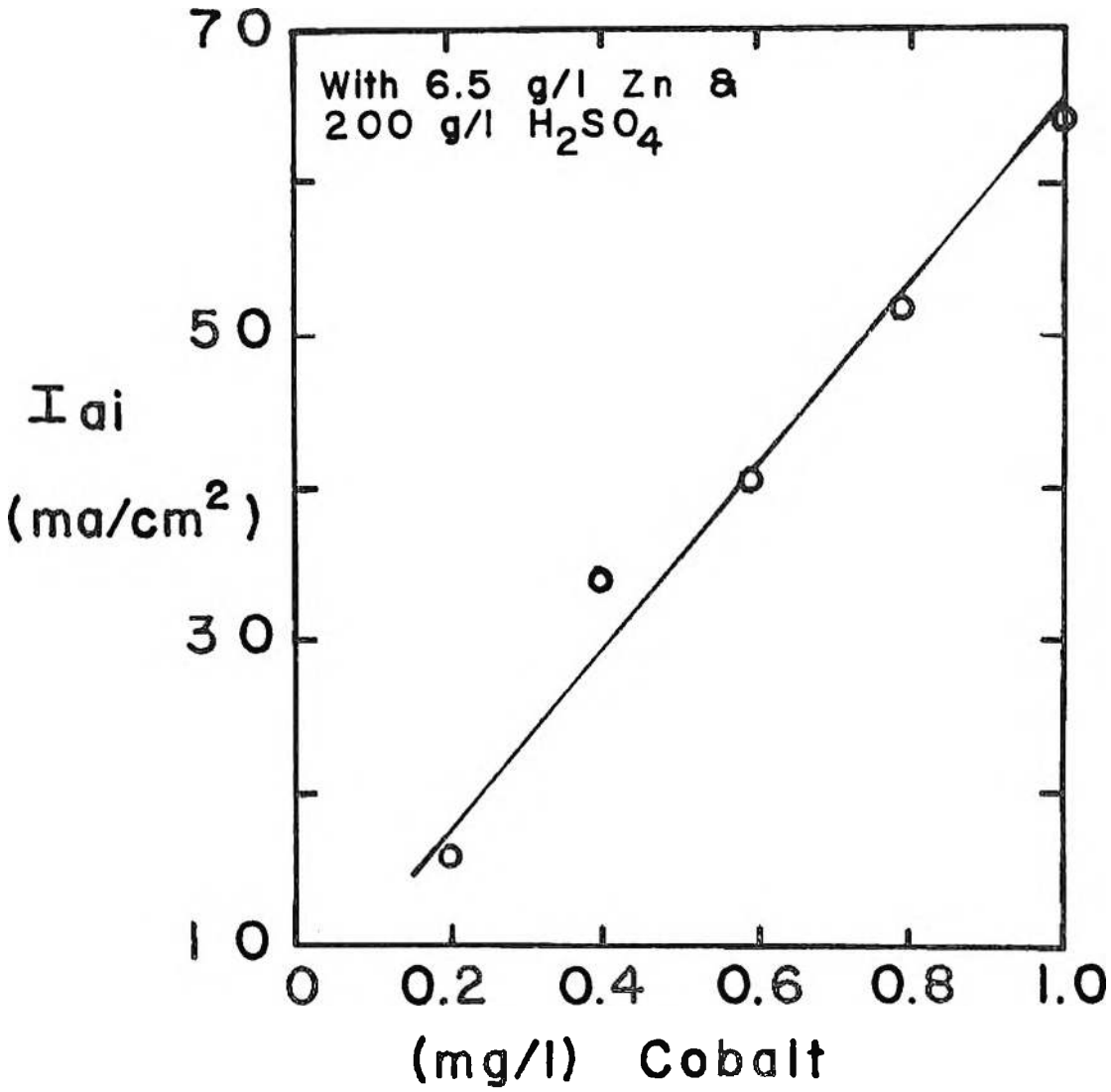

Figure 16. Peak Current Density vs Cobalt Concentration. Fast Scan (5 mV/sec) to Point D then Slow Scan (0.5 mV/sec) back to Starting Potential.

with impurity concentration (see Figure 16). The reproducibility is not as good (±4 mA/cm^2), but the total test time is reduced to 8 to 10 minutes.

Further work in this area is necessary to properly delineate the influence of the processing conditions on the voltammograms. However, the sensitivity and reproducibility of this technique are quite comparable to atomic absorption analysis.

Apparent Mechanism of Germanium and Cobalt Interaction at the Working Electrode

The data obtained using the cyclic voltammetry technique indicate that germanium and cobalt behave similarly at the working electrode. The polarization behavior in both cases is nearly the same. The main difference is that germanium interaction becomes apparent at lower concentration levels than for cobalt. For a solution containing 6.5 g/l Zn and 200 g/l H_2SO_4, a cobalt concentration of 0.4 mg/l was required to produce a peak current density of 28 mA/cm^2. A germanium concentration of 0.02 mg/l produced this same peak current density. This indicates that roughly 20 times the amount of cobalt as germanium is necessary to produce similar polarization behavior.

The exchange current densities for hydrogen discharge on germanium, cobalt, and zinc are reported to be 1×10^{-5}, 4.5×10^{-7}, and 1.26×10^{-8} A/cm^2, respectively (24). The higher exchange current densities for germanium and cobalt in comparison to zinc indicate that hydrogen discharge on these metals should be easier than on the zinc. It is interesting that the ratio of the exchange current values for germanium and cobalt is equal to 21. This ratio is nearly the same as that obtained for the ratio of cobalt to germanium needed to produce

equivalent peak current densities. It appears that the interaction of the impurity is dependent on its ability to act as a site of hydrogen discharge. The degree of zinc corrosion and consequent loss in zinc current efficiency depend on the concentration of impurity in the solution. The instability of the zinc, as shown by the cyclic behavior of the zinc deposit in the presence of these impurities and the massive amounts of hydrogen that are liberated at the electrode as the zinc dissolves, seem to confirm a local cell type of impurity interaction. The cobalt and germanium sites act as local cathodes and the adjacent zinc sites as local anodes.

As the deposition process starts, both the impurities and the zinc are deposited over the whole electrode surface. The deposition rate of the impurity is proportional to its concentration in the electrolyte since the rate is diffusion-controlled. The surface remains generally smooth during the initial deposition period, and a uniform cathode potential exists without the presence of any extensive mixed potential regions. After a certain time, activation of the co-deposited impurities begins due to changes in the morphology or surface roughness. When the surface becomes rough, the specific cathode current density decreases at the recessed areas. A local potential difference is created, and zinc corrosion is initiated. As the zinc corrodes, more impurity is exposed, and it tends to agglomerate since it is cathodically protected. Hydrogen evolution increases because more sites favorable to hydrogen discharge are uncovered. The re-solution of the zinc proceeds at an ever increasing rate. The pH at the corrosion site can also be higher due to a deficiency in H^+ ions which are reduced to hydrogen. Thus, the

potential differences between the corroding and non-corroding areas are accentuated, thereby increasing the driving force of the reaction. Once the process is initiated, it can sometimes become auto-catalytic.

The results of the cyclic tests support the above mechanism. Cycling of the zinc in the presence of the impurities; the formation of a peak current density; the massive amounts of hydrogen evolution that accompany zinc dissolution; and the favorable exchange current characteristics of germanium and cobalt all tend to confirm the proposed mechanism of impurity interaction.

Voltammogram for Electrolytes Containing Antimony

The polarization behavior obtained for solutions containing antimony is significantly different than that of either the no-addition electrolyte or that for electrolytes containing cobalt or germanium. Several changes in the voltammogram are found (see Figure 17). First, the initial hydrogen reduction current densities from points A to C are lower for the antimony-containing electrolytes and this effect becomes greater as the zinc concentration is reduced. For an electrolyte containing 6.5 g/l Zn and 200 g/l H_2SO_4 and no antimony the current density at point B (the maximum hydrogen reduction current density for the front sweep) is greater than 15 mA/cm^2, but for a solution containing 104 ppb Sb, it is less than 8 mA/cm^2. Voltammograms obtained for non-zinc acid electrolytes with and without antimony addition also show this behavior. This is illustrated by the results shown in Table IV. As can be seen, the current density obtained for the antimony-containing electrolyte is greatly reduced at all the potential values listed.

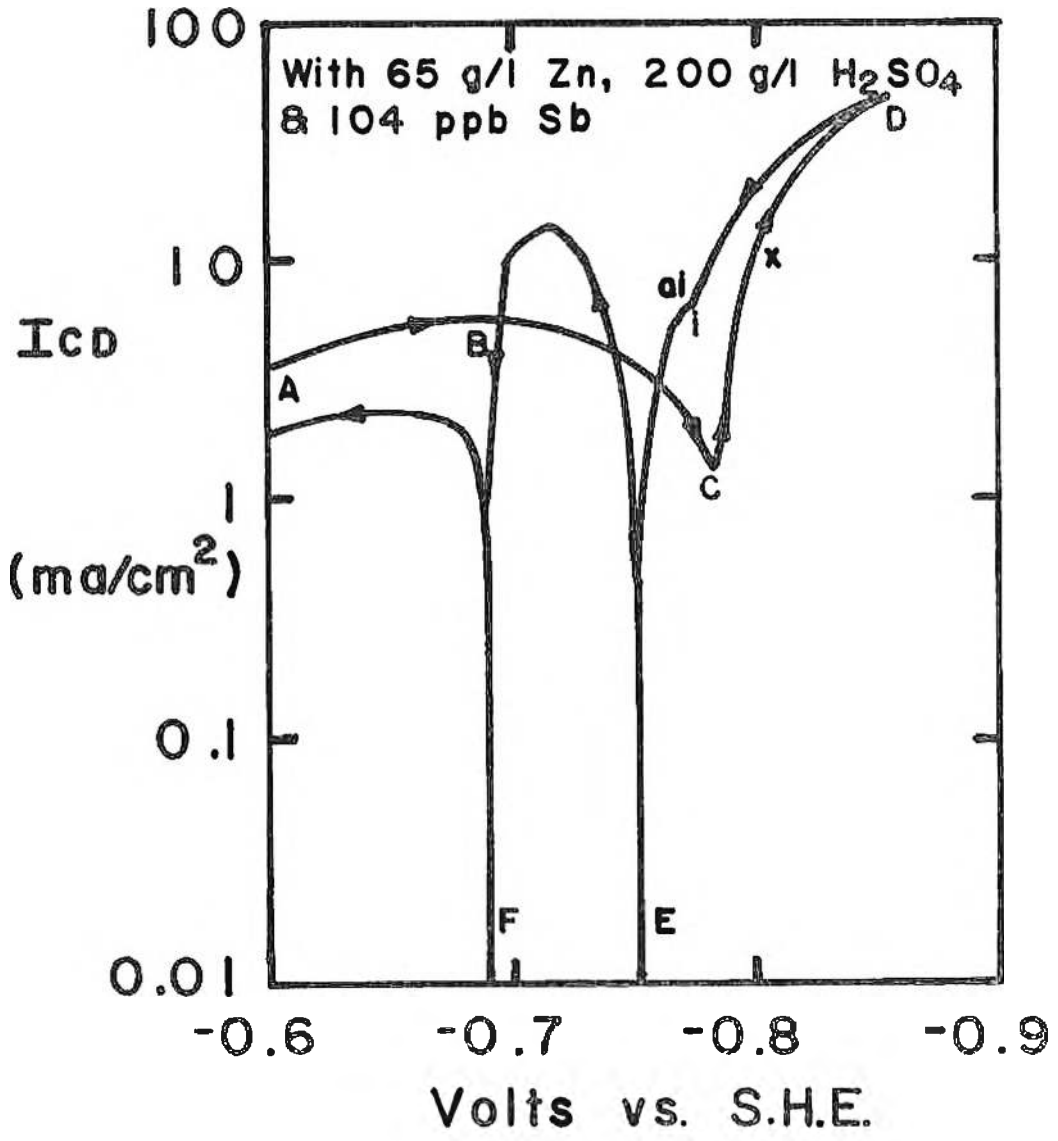

Figure 17. Voltammogram Obtained for Electrolytes Containing Antimony Additions. T = 45°C; Scan Rate = 0.5 mV/sec.

Table IV. Comparison of Current Densities Obtained for 200 g/ℓ H_2SO_4 Electrolytes With and Without 104 ppb Sb.

Potential V vs S.H.E.	Current Density (mA/cm^2) No Antimony	104 ppb Antimony
-0.60	11.0	2.7
-0.65	25.0	4.7
-0.70	46.0	7.0
-0.75	72.0	11.5
-0.80	100.0	17.5
-0.85	135.0	29.0

The second difference in the voltammogram occurs at point x. The zinc deposition potential (point C) is the same as that obtained for the other electrolytes, but the potential necessary to produce a current density of 10 mA/cm (point x) is less electronegative for solutions containing antimony. The potential at this point for a solution containing 104 ppb Sb is -0.797 V vs S.H.E. compared to -0.806 V vs S.H.E. for a no-addition electrolyte.

This depolarization effect is also reflected in the morphology of the deposited zinc. The deposit was obtained by scanning to point D and then holding the potential constant at this point for 1 minute. The zinc crystallites are significantly larger than those obtained for the non-antimony containing electrolytes and large sections of the aluminum substrate are not covered by the zinc (see Figure 18).

The back scan is quite similar to that obtained for the no-addition electrolyte. There is a slight inflection at point i, but this is much less pronounced than that obtained for germanium-containing electrolytes of comparable concentration level. The zinc stability potential is also quite similar. A large anodic dissolution area is also found for the antimony-containing electrolytes. There is, however, one final difference on the voltammogram. After all the zinc has dissolved (approx. at point F), the current again becomes cathodic, but instead of approaching that obtained on the front scan, it is actually somewhat lower.

The differences in the polarization behavior and morphology for the antimony-containing electrolytes suggest that the mechanism of antimony interaction at the electrode is different than that of cobalt or germanium. Other investigators believe that antimony interacts at

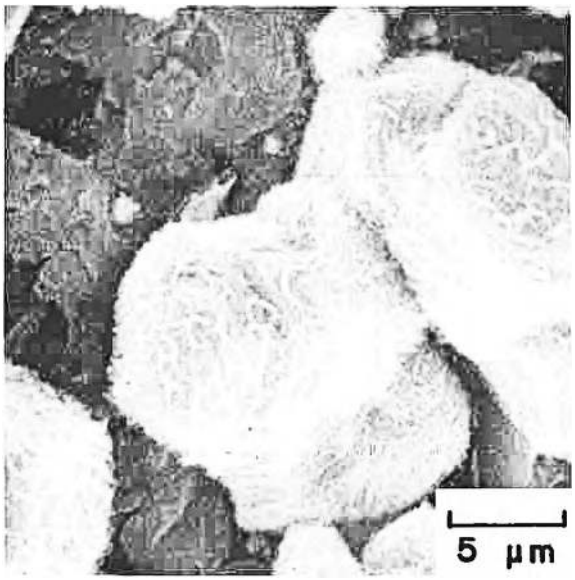

Figure 18. Zinc Deposit Obtained for Electrolyte Containing 65 g/ℓ Zn, 200 g/ℓ H_2SO_4, and 104 ppb Sb. Potential Held at Point D for 1 Minute. (3000x)

the electrode by forming volatile hydrides (see reaction 8, Table II) (2,12). The formation of these hydrides can provide an alternative path for hydrogen evolution and may aid in removal of adsorbed atomic hydrogen from the electrode surface. Either action would result in decreased polarization at the electrode. This decreased polarization leads to a reduction in zinc nucleation and an increase in the size of the observed zinc platelets. The results of this investigation support this mechanism of antimony interaction.

Voltammograms for Electrolytes Containing Glue

The polarization characteristics for electrolytes containing glue are illustrated by the voltammogram in Figure 19. The initial part of the scan from A to C is almost identical to that obtained for the no-addition electrolytes and zinc deposition begins at potentials very close to that for the non-glue electrolytes. After zinc deposition begins, however, a change in the polarization behavior is found. A characteristic hump in the polarization curve (point C to point z) is found and this becomes more pronounced as the glue concentration is increased. In addition, the potential necessary to obtain a current density of 10 mA/cm^2 (point x) is more electronegative than that for the electrolytes containing no glue addition. The potential at point x for an electrolyte containing 65 g/l Zn, 200 g/l H_2SO_4, and 10 mg/l glue is -0.845 V vs S.H.E. compared to -0.806 V vs S.H.E. for the electrolyte without glue addition. This increased polarization is most likely due to the adsorption of glue onto the growing zinc deposit at the electrode which makes further zinc deposition more difficult (2-4,30-33). The morphology of the zinc deposit is also affected by the presence of glue in the electrolyte (see Figure 20).

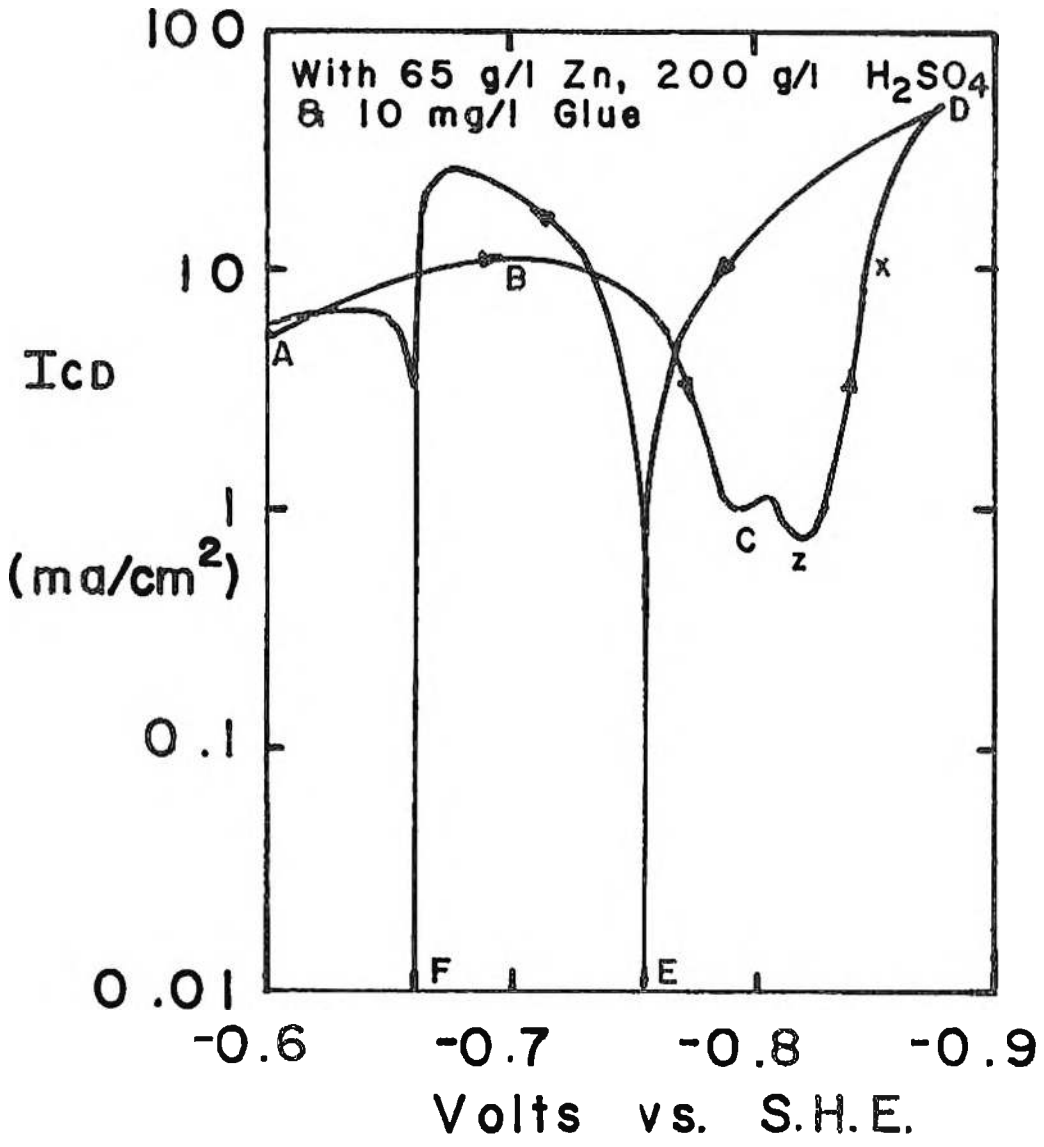

Figure 19. Votlammogram Obtained for Electrolytes Containing Glue Additions. T = 45°C; Scan Rate = 0.5 mV/sec.

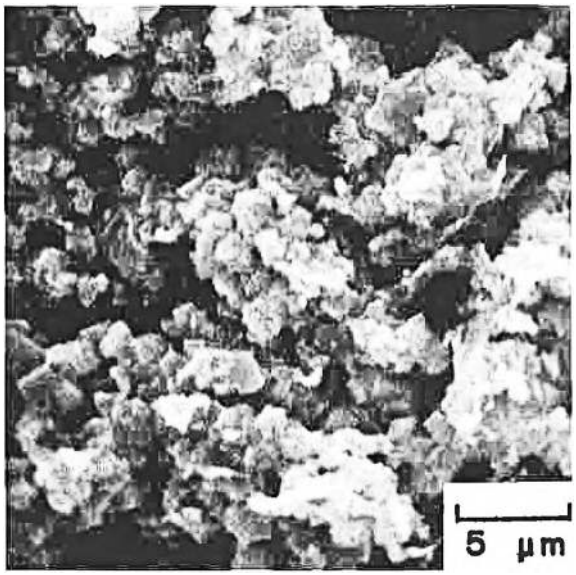

Figure 20. Zinc Deposit Obtained for Electrolyte Containing 65 g/ℓ Zn, 200 g/ℓ H_2SO_4, and 10 mg/ℓ Glue. Potential Held at Point D for 1 Minute. (3000x)

The deposit was obtained in the same fashion as before. The size of the zinc platelets is markedly smaller than that for the non-glue electrolytes and significant clumping of the crystallite occurs. The increased polarization caused by glue adsorption causes more nucleation and hinders crystalline growth resulting in a finer grained deposit because more energy is available to cause nucleation at the more electronegative potential.

The voltammogram from point D back to the starting potential is similar to that obtained for the no-addition electrolyte. The effects of glue addition mostly influence the polarization characteristics of the front scan.

Effects of Glue-Impurity Combinations on Zinc Polarization Behavior

Antimony-Glue Combinations Antimony and glue interactions at the electrode cause measurable changes in polarization that mainly affect the front scan portion of the voltammogram. Antimony causes depolarization to occur and glue addition causes significant polarization. Current efficiency studies conducted prior to the cyclic voltammetry studies show that antimony and glue tend to counteract each other and the proper combination of the two result in optimum current efficiencies (1). This effect is reflected in the polarization behavior found for a combination of 104 ppb Sb and 10 mg/l glue. The voltammogram obtained is quite similar to that of the no-addition electrolyte. The potential required to produce a current of 10 mA/cm^2 (point x) is -0.820 V vs S.H.E. for the antimony-glue combination. This value is between that of the electrolyte containing only antimony (-0.797 V vs S.H.E.) and that of the electrolyte containing glue alone (-0.845 V vs S.H.E.). The potential at point x depends on the levels of glue

and antimony in the electrolyte. Other investigators using similar reference points have attempted to optimize the level of glue addition for antimony-containing electrolytes by matching the potential for the antimony-glue combination with that of the no-addition electrolyte (2,4). The technique appears to be quite promising. More research should be conducted in this area and the results should be correlated with current efficiency studies for long-time deposits.

Combinations of Glue with Germanium or Cobalt Combinations of glue with germanium or cobalt result in voltammograms of the form shown in Figure 21. Both glue and impurity behavior are apparent for this type of voltammogram. The potential at point x becomes more electronegative with increasing glue concentration and the peak current density (ai) is reduced. The variation in potential at point x for solutions containing 100 ppb Ge and 8 mg/l Co with glue concentration is shown by Figures 22 and 23, respectively. The initial addition of glue causes the potential to become more electronegative quite rapidly, but the relative change decreases with further glue additions. The change in potential is much larger for germanium-containing electrolytes than for cobalt. Glue also causes the peak current density to drop, but the effect is limited and an optimum glue level seems to exist. This is illustrated by the results shown in Figures 24 and 25. For an electrolyte containing 100 ppb Ge, the peak current density is 28 mA/cm^2 when no glue is present in the solution. As glue is added, the peak current density drops to a low value of 5.4 mA/cm^2 and then begins to increase. The minimum peak current density was obtained for a glue concentration of approximately 13 mg/l. The change in peak current density with glue addition

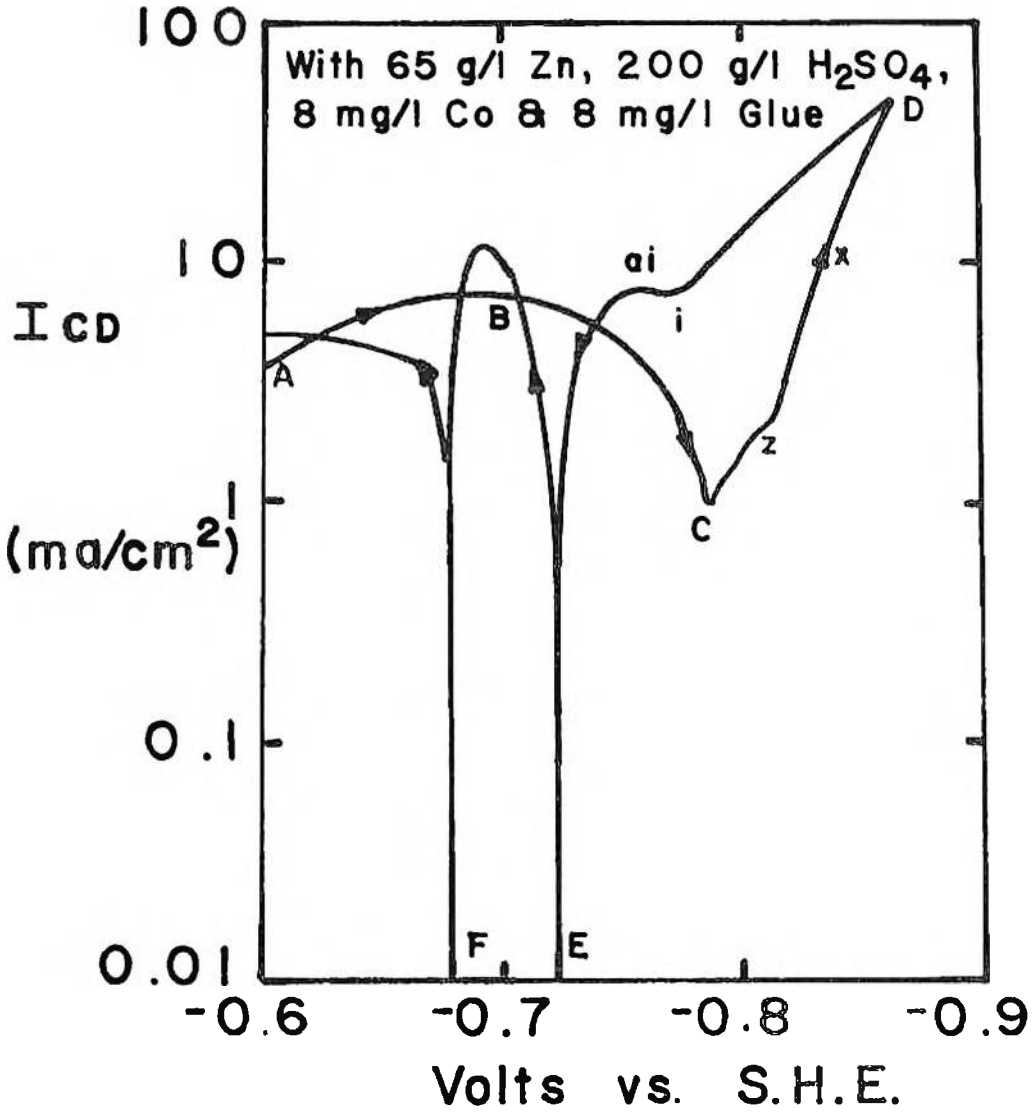

Figure 21. Voltammogram Obtained for Electrolytes Containing Glue and Cobalt or Germanium Additions. T = 45°C; Scan Rate = 0.5 mV/sec.

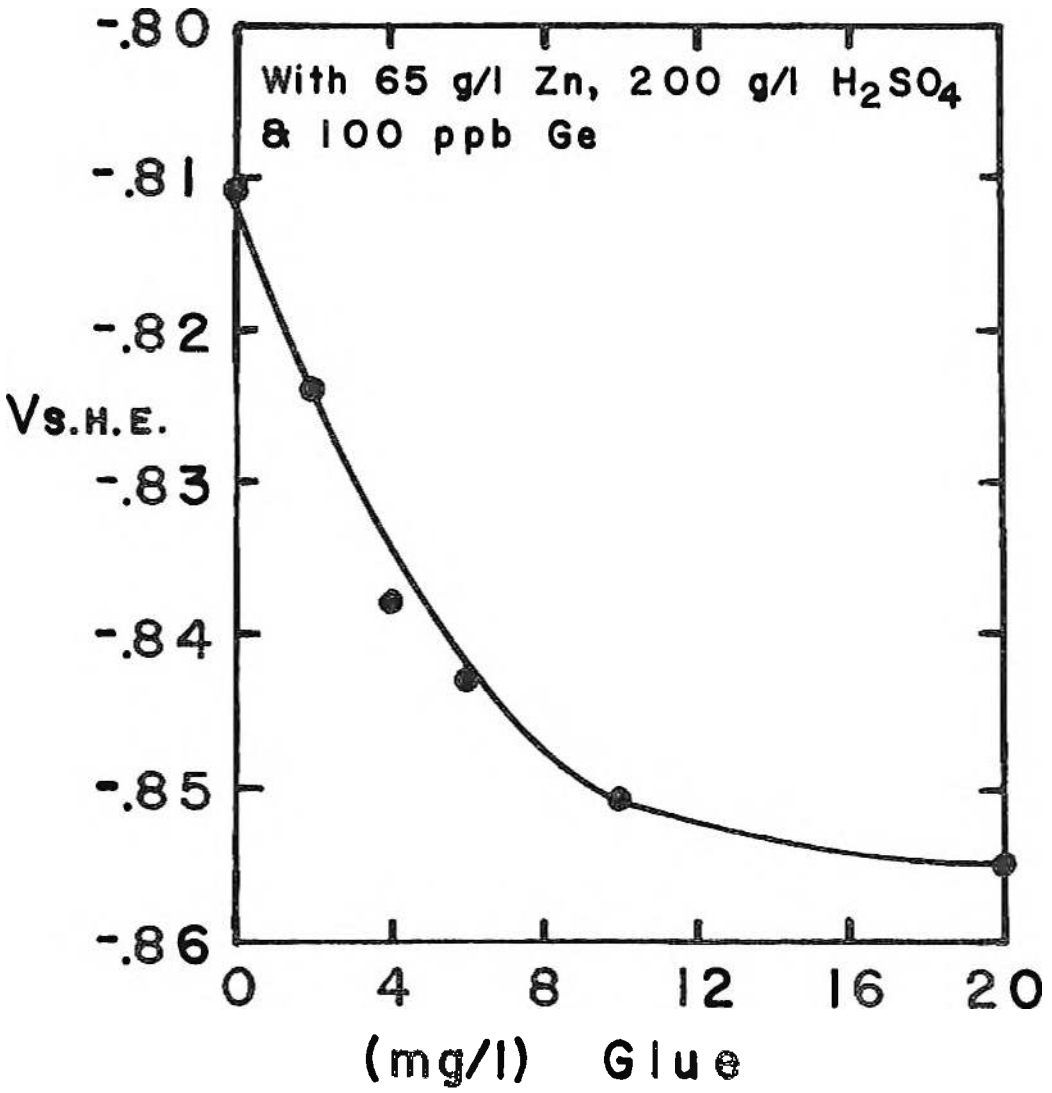

Figure 22. Potential at Point X vs Glue Concentration for Electrolytes Containing Germanium Additions. T = 45°C; Scan Rate = 0.5 mV/sec.

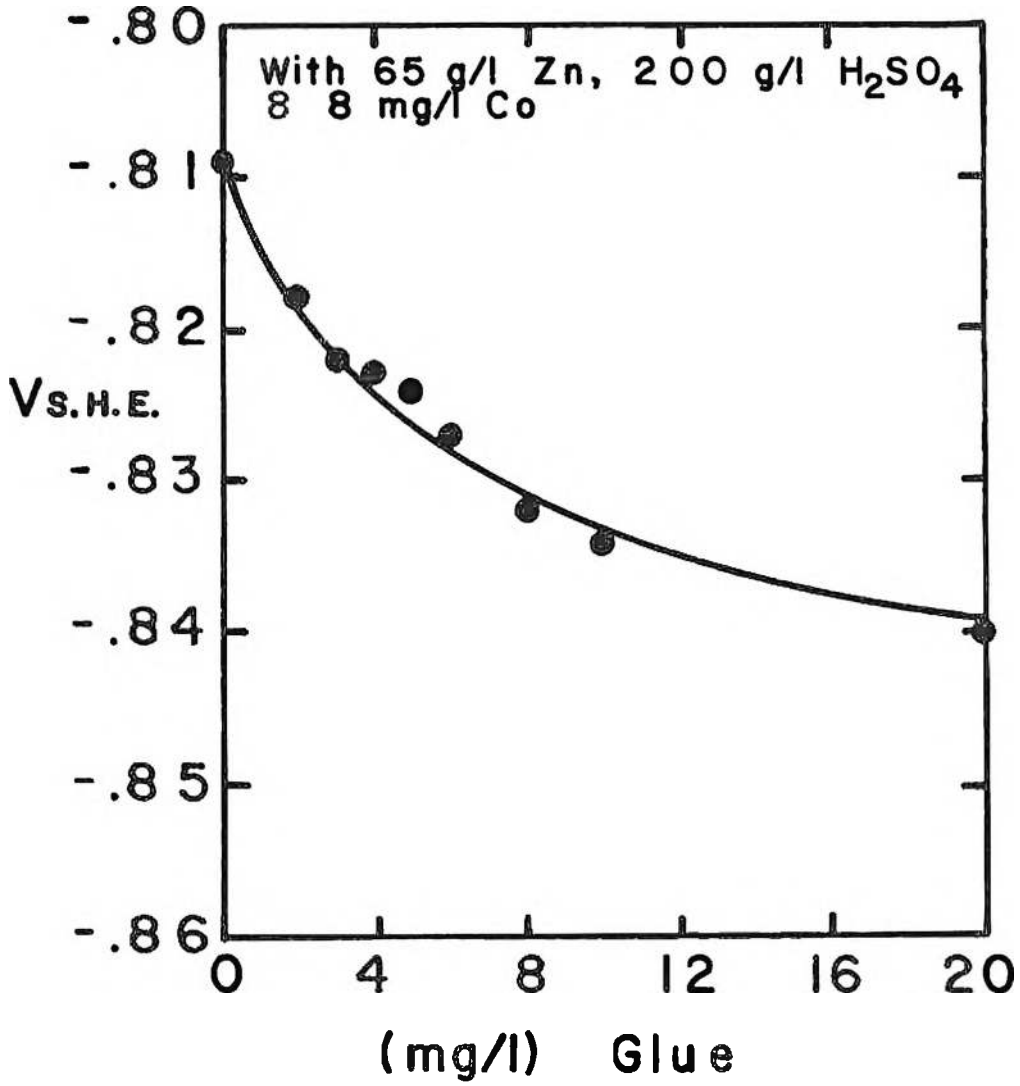

Figure 23. Potential at Point X vs Glue Concentration for Electrolytes Containing Cobalt Additions. T = 45°C; Scan Rate = 0.5 mV/sec.

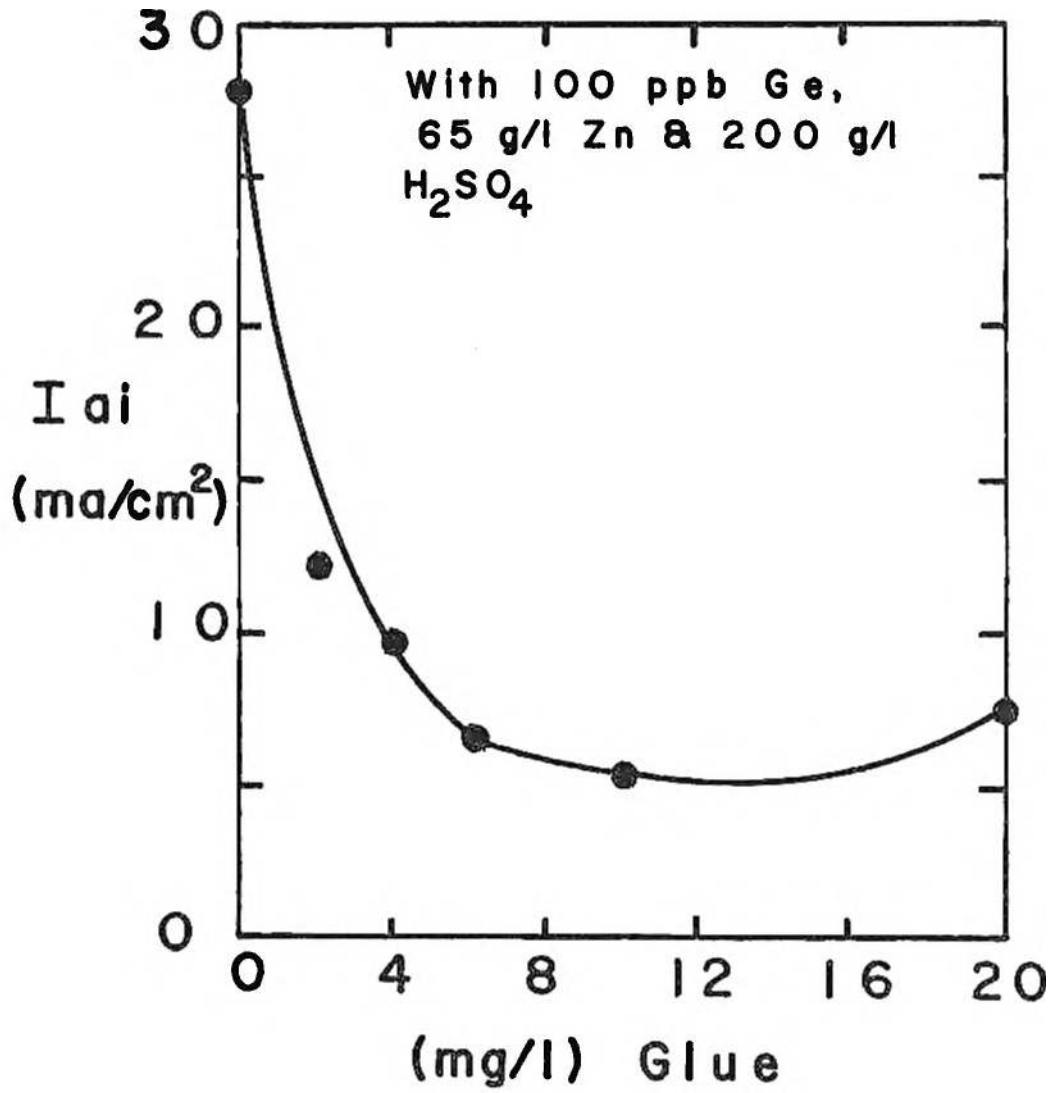

Figure 24. Peak Current Density vs Glue Concentration for Electrolytes Containing Germanium Additions. T = 45°C; Scan Rate = 0.5 mV/sec.

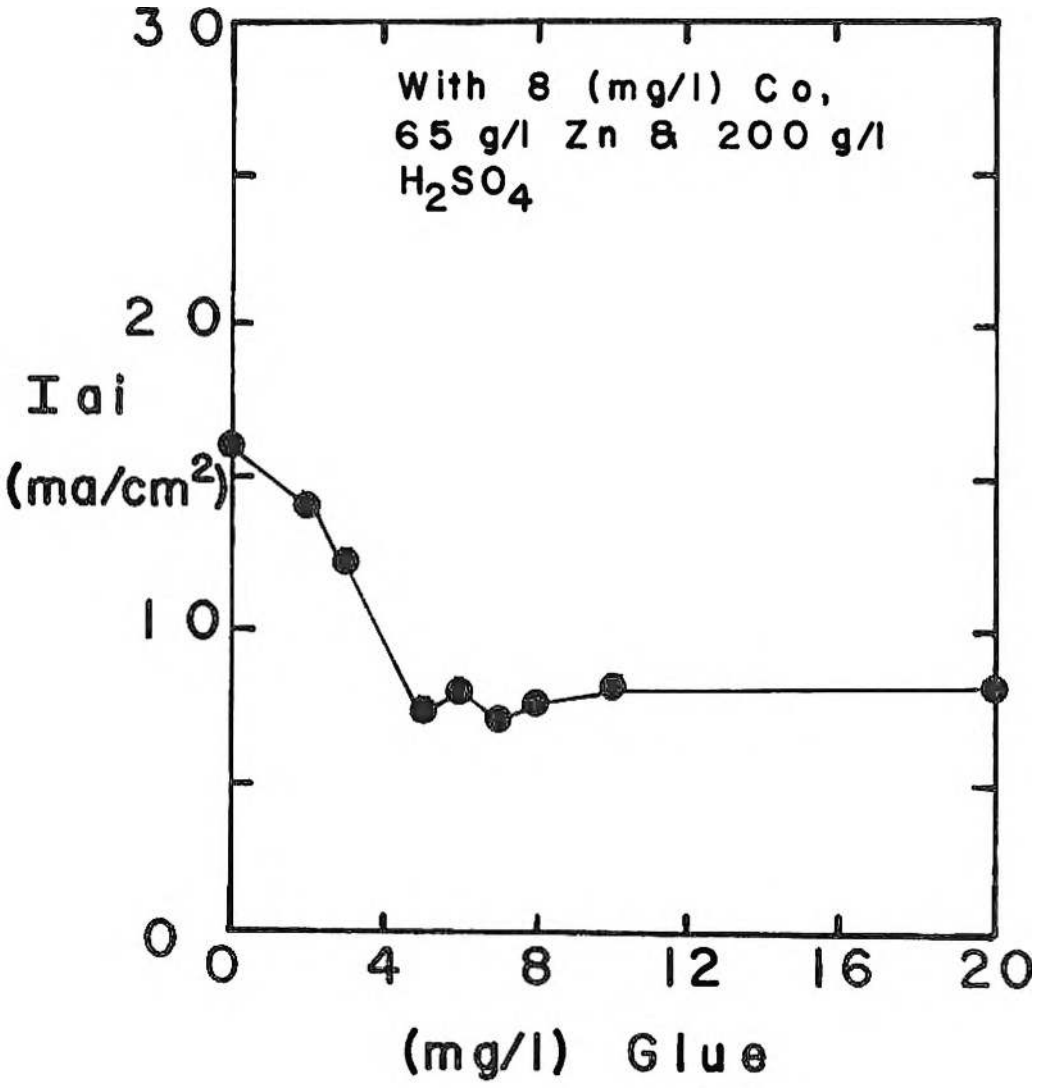

Figure 25. Peak Current Density vs Glue Concentration for Electrolytes Containing Cobalt Additions. T = 45°C; Scan Rate = 0.5 mV/sec.

is not as large for the cobalt-containing electrolytes. This can be seen in Figure 25. For an electrolyte containing 8 mg/l Co and no glue addition, the peak current density is 16.5 mA/cm^2. As glue is added to the electrolyte, the peak current is reduced and reaches a minimum at a glue concentration of 7 mg/l. The peak current density at this minimum is 7.1 mA/cm^2. After this point the peak current density gradually rises. The glue addition in reducing the peak current density makes the deposited zinc more stable and this is illustrated by the deposit morphologies shown in Figures 26 and 27. The deposits were obtained by scanning past point D to -0.785 V vs S.H.E. and holding at this potential for 1 minute. The deposit obtained using the electrolyte containing cobalt alone shows marked signs of zinc dissolution. The platelet edges are rounded and indistinct. Significant portions of the aluminum substrate are plainly visible. With glue added, the deposit is greatly improved. The platelet edges are relatively sharp and much more zinc remains on the aluminum substrate. The structure of the deposit is similar to that obtained for electrolytes containing glue alone. The zinc deposit morphologies for electrolytes containing germanium with and without glue are similar.

It is considered significant that the combination of glue and germanium which gives the lowest peak current density was found to correspond to the optimum level of glue addition for this level of germanium by 12 hour current efficiency studies which were conducted prior to the cyclic tests (1). This may mean that the cyclic voltammetry technique is useful in optimizing the level of glue addition for electrolytes containing germanium and cobalt types of impurities.

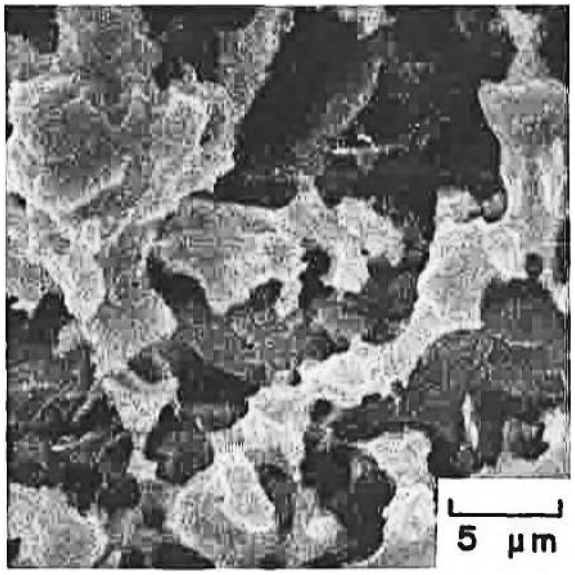

Figure 26. Zinc Deposit Obtained for Electrolyte Containing 65 g/ℓ Zn, 200 g/ℓ H_2SO_4, and 8 mg/ℓ Co. Potential Held at -0.785 V vs S.H.E. for 1 Minute. (3000x)

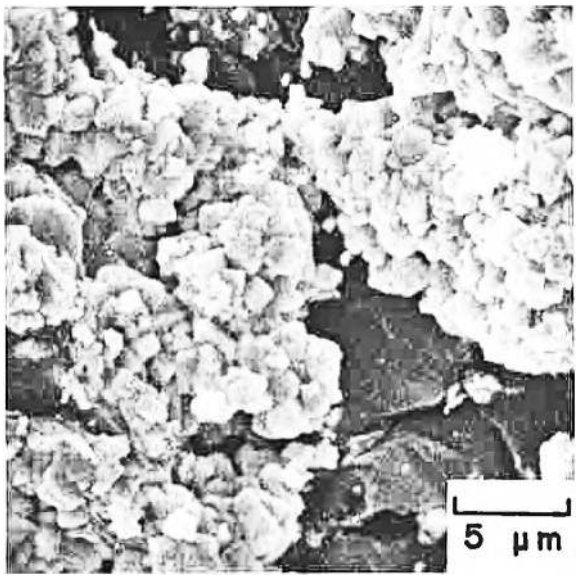

Figure 27. Zinc Deposit Obtained for Electrolyte Containing 65 g/ℓ Zn, 200 g/ℓ H_2SO_4, 8 mg/ℓ Co, and 10 mg/ℓ Glue. Potential Held at -0.785 V vs S.H.E. for 1 Minute. (3000x)

If short term electrochemical characterizations could be used for evaluating solution effects, it would be of use in routine industrial process control and in more basic laboratory studies as well.

The action of glue in counteracting the effects of the impurities is not well understood. Some explanations have been offered to account for the results. Investigators believe that glue adsorption causes more nucleation and hinders crystalline growth resulting in a finer grained and more unform deposit (3,30,31). A more uniform deposit hinders the formation of local cells, and the effects of the impurities are therefore reduced. Another factor which has been mentioned is that the organic additive lowers the surface tension at the cathode surface and promotes removal of adsorbed gas bubbles which hinder zinc deposition (32). Removal of the gas bubbles also promotes a more uniform deposit. For a hydride former such as antimony, the organic additive may hinder formation of the hydride by adsorbing onto the deposited metal and thus blocking hydrogen access to the metal. This assumes that the hydride formation takes place on the cathode surface and not in the double layer. It has been found that the amount of antimony in the deposit increases upon addition of glue to the solution (29,34). Further work is necessary to confirm the mechanism of glue interaction.

Although the addition of glue is beneficial for electrolytes containing germanium or cobalt, the glue seems to be more effective in the case of germanium. The peak current density and potential changes are greater for the germanium-containing electrolytes. This may be due to the levels of impurities used in the two cases. If one assumes that the main benefit of the glue is to minimize local cell formation by making the deposit more uniform, as described

above, then this effect should be stronger if there are less sites for the formation of local galvanic cells. The number of sites formed is proportional to the amount of impurity in the solution. Since the cobalt level is significantly higher than the germanium level, more cobalt sites are available to form the local cells and the beneficial action of the glue may be less because of this.

Possible Applications of this Technique

The use of cyclic voltammetry techniques in glue addition optimization has already been discussed. Other possible applications also exist. It may be possible to classify common impurities such as nickel, iron, copper, arsenic, etc. and their mode of interaction by comparison of various reference voltammograms. This could lead to a more definitive understanding of the reasons for the effects observed for different impurities. This might also prove to be an effective method for screening possible remedial treatments for improving process efficiency. A basic voltammogram could be run on purified plant solution prior to release of the solution to the tank house. Low levels of impurity are detected using this technique and some process control may be possible by comparing the voltammogram obtained for the purified solution with that obtained for a solution which is known to have given good current efficiencies. If they are similar, then further analytical tests on the solution would be unnecessary. If they differ, then further action dictated by the type of impurity causing the change in the voltammogram can be undertaken. The technique can also be used to determine what types of effects will occur when some process parameters such as temperature, acid concentration, zinc concentration, glue concentration, or impurity concentration are

altered. The test time is very short and good correlation with longer time current efficiency studies have been obtained.

Conclusions

1. The use of cyclic voltammetry techniques allows evaluation of the effects of such factors as impurity concentration, zinc concentration , acid concentration, temperature, and glue concentration. These short term test results have proven to be correlatable with the classical long term efficiency tests.
2. The polarization behavior of acid zinc sulfate electrolyte is very sensitive to the type and concentration of impurity and/or additive present.
3. The actual mechanism of impurity interaction is more clearly delineated using this technique. Germanium and cobalt appear to form local galvanic cells, however, antimony does not.
4. Low levels of certain impurities can be detected. Levels of Ge and Co as low as 0.02 and 0.10 mg/l, respectively, can be determined.
5. Changes in the polarization behavior can be used to optimize the amount of glue needed to counteract harmful impurities.

Acknowledgements

The authors wish to acknowledge the financial assistance provided by the AMAX Foundation, New York, NY, and the technical assistance provided by Cominco, Ltd., Trail, British Columbia, Canada, and AMAX Zinc Company, Sauget, IL. We would also like to thank ASARCO, Inc., Hillsboro, IL, for providing the French process zinc oxide used in this study. Without the continued interest and help of the above this work would not have been possible.

We would also like to thank Dr. Yar-Ming Wang, formerly Assistant Research Professor at MRC, UMR, Rolla, MO, for his helpful advice and assistance concerning this study.

References

1. D. R. Fosnacht and T. J. O'Keefe: paper presented at 107th Annual Meeting, A.I.M.E., Denver, CO, 1978.
2. D. J. MacKinnon and J. M. Brannen: J. Appl. Electrochem., 1977, 7, No. 5, 451-459.
3. D. J. Robinson and T. J. O'Keefe: J. Appl. Electrochem., 1976, 6, 1-7.
4. B. A. Lamping and T. J. O'Keefe: Met. Trans. B, 1976, 7B, No. 12, 551-558.
5. Reiner Liebscher: Neue Heutte, 1969, 14, No. 11, 651-3.
6. R. C. Kerby, H. E. Jackson, T. J. O'Keefe, and Y. Wang: Met. Trans. B, 1977, 8B, No. 4, 661-668.
7. D. R. Fosnacht: Masters Thesis, Columbia University, New York, 1975.
8. I. W. Wark: Proc. Australian Conf. Electrochem., 1st., Sydney, Hobart, Austalia, 1963, 889-900.
9. M. Maja: Electrochim Metal., 1967, 2, No. 4, 469-72.
10. M. Maja and S. Pozzoli: Chim. Ind., 1969, 51, No. 2, 133-8.
11. Ignazio R. Bellobono: Ind. Chem. Belge, 1967, 32, 305-8.
12. A. G. Pecherskaya and V. V. Stender: J. Appl. Chem. U.S.S.R., 1950, 23, 975-989.
13. U. F. Turomshina and V. V. Stender: J. Appl. Chem. U.S.S.R., 1954, 27, 1019-1025.
14. Giovanni Scacciati: Industria mineraria, 1953, 4, 511-16.
15. U. F. Turomshina and V. V. Stender: J. Appl. Chem. U.S.S.R., 1955, 28, 447-452.

16. G. Z. Kir'yakov: Zhur. Fiz. Khim., 1958, 32, 2561-4.

17. A. F. Nikiforov: J. Appl. Chem. U.S.S.R., 1964, 37, No. 2, 360-363.

18. Kurt Peukert and Willy Schreiter: Metallurgie u. Gressereitech, 1954, 4, 397-401.

19. A. I. Levin, et al.: J. Appl. Chem. U.S.S.R., 1958, 31, 569-576.

20. Y. Wang, T. J. O'Keefe, and W. J. James: paper presented at 107th Annual Meeting, A.I.M.E., Denver, CO, 1978.

21. A. F. Nikiforov: J. Appl. Chem. U.S.S.R., 1964, 37, 360-363.

22. M. Yunus, C. Capel-Baute, and C. Decroly: Electrochim. Acta, 1965, 10, No. 9, 885-900.

23. B. P. Yur'ev: Tr. Leningr. Politekhn. Inst., 1963, 223, 87-96.

24. G. C. Bratt: Electrochem. Technol., 1964, 2, No. 11-12, 323-6.

25. A. M. Ezrokhina and B. P. Yur'ev: J. Appl. Chem. U.S.S.R., 1969, 42, No. 12, 2697-2699.

26. A. M. Ezrokhina, et al.: J. Appl. Chem. U.S.S.R., 1972, 45, No. 1, 96-100.

27. Niro Matsuura: J. Chem. Soc. Japan, Pure Chem. Sect., 1953, 74, 239-42.

28. Niro Matsuura: Sci. Papers Coll. Gen. Educ. Univ. Tokyo, 1953, 3, 13-18.

29. Z. A. Sheka: Ukrain. Khim. Zhur., 1956, 22, 394-400.

30. Willibald Machu: Österr. Chem. Ztg., 1939, 42, 244-7.

31. A. Riesenkampf: Prace Inst. Hulniczych, 1962, 14, No. 1, 27-36.

32. Ivan Enchev and I. A. Pishkunov: God. Nauchnovzsled. Inst. Tsvet. Met., Plovdiv., 1967, 5, 51-9.

33. Toshmichi Fukumoto, et al.: Denki Kagaku Oyabi Kogyo Butsuri

Kagaku, 1975, 43, No. 2, 94-9.

34. Z. A. Sheka and K. F. Karlysheva: Doklady Akad. Nauk S.S.S.R., 1956, 108, 126-9.

List of Figures

Figure 1. Schematic of Equipment Used for the Cyclic Voltammetry Experiments. [C = Working Electrode (Al); R = Mercurous Sulfate Reference Electrode; A = Auxiliary Electrode (Pt); V = Voltage Monitoring Terminals; and I = Current Supply Terminals].

Figure 2. Voltammogram for No-Addition Electrolyte. T = 45°C; Scan Rate = 0.5 mV/sec.

Figure 3. Hydrogen Current Density vs Electrode Potential for Electrolytes Containing 200 g/ℓ H_2SO_4 and the Indicated Additions. T = 45°C; Scan Rate = 0.5 mV/sec.

Figure 4. Voltammogram Obtained for Electrolytes Containing Germanium or Cobalt Additions. T = 45°C; Scan Rate = 0.5 mV/sec.

Figure 5. Sequence of Changes that Occur at Points i and ai as the Impurity Concentration Increases for Electrolytes Containing Germanium or Cobalt Additions.

Figure 6. Peak Current Density vs Cobalt Content. Scan Rate = 0.5 mV/sec.

Figure 7. Zinc Deposit Obtained for Electrolyte Containing 65 g/ℓ Zn and 200 g/ℓ H_2SO_4. Potential Held at Point D for 1 Minute. (3000x)

Figure 8. Zinc Deposit Obtained for Electrolyte Containing 65 g/ℓ Zn, 200 g/ℓ H_2SO_4, and 100 ppb Ge. Potential Held at Point D for 1 Minute. (3000x)

Figure 9. Zinc Deposit Obtained for Electrolyte Containing 65 g/ℓ Zn, 200 g/ℓ H_2SO_4, and 8 mg/ℓ Co. Potential Held at Point D for 1 Minute. (3000x)

List of Figures (Continued)

Figure 10. Peak Current Density vs Zinc Concentration. Scan Rate = 0.5 mV/sec; T = 45°C.

Figure 11. Peak Current Density vs Acid Concentration. Scan Rate = 0.5 mV/sec; T = 45°C.

Figure 12. Hydrogen Current Density vs Electrode Potential for Electrolytes Containing 6.5 g/ℓ Zn and Various H_2SO_4 Concentrations. Scan Rate = 0.5 mV/sec; T = 45°C.

Figure 13. Peak Current Density vs Cobalt Concentration for Working Electrodes Having Different Surface Preparation. Scan Rate = 0.5 mV/sec; T = 45°C.

Figure 14. Peak Current Density vs Germanium Concentration. Scan Rate = 0.5 mV/sec; T = 45°C.

Figure 15. Peak Current Density vs Cobalt Concentration for Various Temperatures. Scan Rate = 0.5 mV/sec.

Figure 16. Peak Current Density vs Cobalt Concentration. Fast Scan (5 mV/sec) to Point D then Slow Scan (0.5 mV/sec) back to Starting Potential.

Figure 17. Voltammogram Obtained for Electrolytes Containing Antimony Additions. T = 45°C; Scan Rate = 0.5 mV/sec.

Figure 18. Zinc Deposit Obtained for Electrolyte Containing 65 g/ℓ Zn, 200 g/ℓ H_2SO_4, and 104 ppb Sb. Potential Held at Point D for 1 Minute. (3000x)

Figure 19. Voltammogram Obtained for Electrolytes Containing Glue Additions. T = 45°C; Scan Rate = 0.5 mV/sec.

List of Figures (Continued)

Figure 20. Zinc Deposit Obtained for Electrolyte Containing 65 g/ℓ Zn, 200 g/ℓ H_2SO_4, and 10 mg/ℓ Glue. Potential Held at Point D for 1 Minute. (3000x)

Figure 21. Voltammogram Obtained for Electrolytes Containing Glue and Cobalt or Germanium Additions. T = 45°C; Scan Rate = 0.5 mV/sec.

Figure 22. Potential at Point X vs Glue Concentration for Electrolytes Containing Germanium Additions. T = 45°C; Scan Rate = 0.5 mV/sec.

Figure 23. Potential at Point X vs Glue Concentration for Electrolytes Containing Cobalt Additions. T = 45°C; Scan Rate = 0.5 mV/sec.

Figure 24. Peak Current Density vs Glue Concentration for Electrolytes Containing Germanium Additions. T = 45°C; Scan Rate = 0.5 mV/sec.

Figure 25. Peak Current Density vs Glue Concentration for Electrolytes Containing Cobalt Additions. T = 45°C; Scan Rate = 0.5 mV/sec.

Figure 26. Zinc Deposit Obtained for Electrolyte Containing 65 g/ℓ Zn, 200 g/ℓ H_2SO_4, and 8 mg/ℓ Co. Potential Held at -0.785 V vs S.H.E. for 1 Minute. (3000x)

Figure 27. Zinc Deposit Obtained for Electrolytes Containing 65 g/ℓ Zn, 200 g/ℓ H_2SO_4, 8 mg/ℓ Co, and 10 mg/ℓ Glue. Potential Held at -0.785 V vs S.H.E. for 1 Minute. (3000x)

VITA

Donald Ralph Fosnacht was born on December 10, 1950 in Chicago, Illinois. He received his primary education in Chicago and his secondary education in Evanston, Illinois. He received a Bachelor of Science degree in Chemistry from MacMurray College, Jacksonville, Illinois in May, 1973 and a Bachelor of Science degree in Mineral Engineering from Columbia University, New York, New York in May, 1974. In May, 1975 he was awarded the degree of Master of Science in Mineral Engineering from Columbia. While at Columbia he was awarded the Robert Peele Prize and given a commendation for Outstanding Achievement for his graduate work.

He has been enrolled in the Graduate School of the University of Missouri-Rolla since August, 1975 and has held the AMAX Foundation Fellowship for the period August, 1975 to May, 1978.

APPENDIX A

Literature Review

A. Importance of the Zinc Electrowinning Process

Electrowinning from zinc sulfate solutions today accounts for about 60% of the world production of zinc. In the United States, this proportion was 36% in 1973.[1] This percentage will increase significantly in the future as nearly all facilities presently under construction or in the planning stages are electrolytic plants. New electrolytic facilities with a combined capacity of 340,000 tons per year are scheduled to become operational during 1977-1979.[2-3] The proportion of zinc produced electrolytically will also increase due to future closing of horizontal and vertical retort recovery plants caused by obsolescence or environmental restrictions. The net result will be an ever increasing amount of zinc produced by electrolytic means.

The electrolytic zinc process was developed around the turn of the century and has evolved very rapidly to its present state where electrolytic zinc of 99.99+ percent grade is produced routinely.[4]

B. Effects of the Main Process Parameters

The effects of the main process variables: acidity, zinc concentration, temperature, current density, agitation, and deposit thickness, have been the subject of many investigations.[5-18] At current densities up to 100 mA/cm^2, the current efficiency falls with increased acid content, with reduced zinc concentration, with reduced current density and with increased temperature.[10] In the region of high current densities (>100 mA/cm^2) increased temperature

and sulfuric acid content were found to have a somewhat favorable effect on zinc electrolytes.[10]

1. Acid and Zinc Levels. The ratio of zinc to acid concentration was found to be a critical factor.[16] Investigators found that zinc concentrations that are too high or too low can lead to losses in zinc current efficiency.[16] They reported that a zinc to acid ratio of 0.47 to 0.51 was best (ratio expressed in g Zn^{++}/ℓ to g H_2SO_4/ℓ). At high zinc to acid ratios, nodular growth occurred on the zinc surface. These nodules caused electrode shorting and reduced the current efficiency. The authors attributed the effects at high zinc to acid ratios to high viscosity and low conductivity which lead to depletion of the zinc ions in the immediate area of the electrode. Depletion of zinc ions at the electrode interface increases the potential difference between the peaks and valleys which develop on a growing deposit. The zinc ions deposit preferentially at the high potential peaks, accelerating nodular growth. At low zinc to acid ratios, an insufficient amount of zinc ions arrive at the deposition sites and hydrogen as well as impurity ions can compete more effectively for sites on the cathode surface; this in turn reduces the current efficiency. The authors found that residual levels of zinc in the spent electrolyte should be above 48 g/ℓ in order to maintain reasonable current efficiencies.[16] Other authors have reported conditions which they think are the optimum for the process.[11,14,17,18] The actual levels of zinc and acid used also depend on other factors such as solution storage capacity for the plant, acid level needed for the

leaching stage, power consumption, etc. Currently, zinc concentrations of 47 to 80 g/ℓ and acid concentrations of 95 to 200 g/ℓ are being used in the plants.[16,19-20]

2. Temperature and Current Density. The general effects of temperature and current density have already been noted, but a more detailed discussion of these effects is warranted. Increasing the current density causes the hydrogen current to fall, because the over-voltage for discharging hydrogen ions on zinc increases more rapidly than does the over-voltage for zinc deposition.[10] Thus the net result of increasing the current density is an increase in the current efficiency. There are, however, limitations to the current density effect. First, when sufficient zinc can no longer diffuse to the electrode to meet current density requirements, concentration polarization occurs, and the hydrogen yield on the cathode increases. Second, since the power loss due to resistance of the solution is directly proportional to the square of the current ($P = i^2R$), an optimum current density exists which will give the best energy efficiency for the process. The current density employed is a function of the conductivity of the solution and the production rate for zinc set by the plant operators. The conductivity of the electrolyte is largely dependent on the zinc and acid concentrations in the solutions. Since the operating parameters vary widely, a range of current densities of 40 to 75 ma/cm^2 is found in current practice.[16,19-22] Another reason for the use of increased current density is to minimize the effects of impurities; this will be discussed later. Temperature effects are also very

important. Increases in temperature for the range of current density noted above usually cause a decrease in current efficiency. This reduction in current efficiency is attributed to the decrease in the hydrogen over-voltage requirement as the temperature is increased.[23] This is especially true for solutions which contain significant levels of impurity. Temperature increases do provide some beneficial effects at high current density (>200 ma/cm^2). First, the electrolyte resistance is reduced and second, the diffusion coefficient for the zinc ion increases with increasing temperature.[10] In the ranges of current density presently employed in industry, the factors just mentioned are not as important as the reduction in the energy barrier for hydrogen discharge.

3. Agitation. Agitation in the electrolysis bath is provided by circulation of the electrolyte and by bubble formation on the electrodes. Fairly good natural mixing of the solution occurs and external agitation is rarely employed.[16,19-22] The flow of electrolyte past the electrodes is usually started from the bottom of the cell and exits at the top. One investigator found that the best agitation of the electrolyte resulted from a "channel" type circulation.[18] The type of circulation employed and the volume of solution circulated depend on the operating parameters of the various plants. When concentration polarization effects are important (i.e. high current density), some external form of agitation may be required.[8,17] Higher acid levels and temperature also are of importance at high current density operations due to the need

for high conductivity solutions.[10]

C. Importance of Solution Purity

1. General Characteristics. It was discovered quite early in the development of the process that, even when the operation was being done at the design levels of the major process parameters, the current efficiency was often inexplicably low. This difficulty was traced to the presence of metallic impurities in the electrolyte.[24-28] Impurity levels as low as parts per billion were found to drastically reduce the current efficiency. Many of the early investigations examined the effects of single impurities on the electrolysis process. These studies were largely empirical in nature and dealt mostly with finding the levels of impurities that could be tolerated for a given composition of zinc and acid in plant electrolytes. The results of these investigations have been summarized in textbooks and monographs.[5,22] Of all the factors involved in the electrodeposition process, electrolyte purity has been found to be the most significant.[29]

Metallic impurities which are either more active or more noble than zinc have been shown to affect the zinc electrodeposition process. Some effects are quite beneficial, e.g., the presence of cobalt in solution has been shown to lower the anode overvoltage and to lessen the corrosion rate of the lead electrode.[90] Unfortunately, cobalt also interacts at the cathode and causes a reduction in current efficiency.[90] Accordingly, the effects that impurities have on the process are varied. Some impurities show their effects at both electrodes

and in the solution, e.g., for manganese.[108,127-139] Some impurities exhibit no effect individually, but exert considerable influence on the process when they act in concert with other impurities.[54]

The effects exhibited by antimony, arsenic, cadmium, cobalt, copper, germanium, iron, manganese, nickel, the alkali metals and alkaline earth metals will now be reviewed. The effects of additives used to counteract the effects of the impurities will also be discussed. In order to better understand the role that impurities play at the cathode, especially in terms of reducing the current efficiency of the process, the mechanisms of interactions that would lead to a decrease in current efficiency will first be examined.

For an electrolyte containing 50 g/ℓ zinc and 150 g/ℓ sulfuric acid, investigators[159] have reported a cell feed as indicated in Table I. Reversible potentials for the reduction of the various impurities to the metallic state are given in Table II. The estimated values are based on thermodynamic data and activity coefficients from Latimer[160] and Garrels and Christ.[161] The concentrations used have been adjusted to reflect a zinc concentration of 50 g/ℓ zinc.[159] From Table II, it can be seen that of the impurities found in the zinc electrolyte, most should be reduced at the reduction potential for zinc. Manganese is the only exception. Certain restraints are exhibited which can limit the amount of deposition. Activation and concentration overvoltage make deposition of some of the impurities much more difficult. Assuming that some of the impurities do plate out on the

cathode, several effects can occur causing a decreased current efficiency for zinc reduction.

2. Mechanisms of Impurity Interaction. First, simultaneous reduction of the impurity ion with the zinc ion may occur at the cathode. This will reduce the zinc current efficiency by consuming some of the current for reduction of the impurities. Such reduction need not be to the solid phase. Oxidation and reduction couples (i.e. Fe^{++}/Fe^{+++}) can often consume significant quantities of current by cycling between the electrodes. The oxidized form is reduced at the cathode and then subsequently oxidized at the anode. The cycle can continue indefinitely.[120] Such effects can be minimized by keeping the impurity concentration at low levels or by increasing the zinc concentration. The presence of zinc ions has been shown to inhibit the nucleation of cobalt and thus decrease the amount of current consumed by the cobalt. Similar effects have been reported for nickel and iron.[86,88,89,92,93,100-103,106]

Second, the adsorption of positive ions has been shown to change the deposition over-voltage of zinc ions. This may occur by hindering the migration of zinc ions to the cathode[32,125] by their accumulation in the double layer or by being adsorbed on the cathode surface, blocking sites for crystal growth.[137] The presence of these ions may thus require additional expenditures in electrical energy. The adsorption of sodium, calcium and magnesium ions may also cause some depolarization of the cathode by lessening the inhibiting effects of adsorbed hydrogen ions on the zinc deposition process.[143] These investigators attribute

Table I. Composition of Cell Feed for a Zinc Electrolysis Circuit as Reported in the Literature.[159]

Feed Constituent	Concentration (mg/ℓ)
Zn	117,000
Mn	6,300
Cd	0.36
Cu	0.05
Ni	0.25
Co	2.1
Fe	0.57
As + Sb	0.01
F^-	8
Cl^-	55

Table II. Estimated Reversible Potentials Based on Concentrations Approximating Commercial Practice.[159] pH = 0.

	Reaction	$E_{R,298K}$ --- V_{SHE}
1.	$Cu^{++}(aq) + 2e = Cu(s)$	0.10
2.	$HAsO_2(aq) + 3H^+(aq) + 3e = As(s) + 2H_2O(\ell)$	0.10
3.	$SbO^+(aq) + 2H^+(aq) + 3e = Sb(s) + H_2O(\ell)$	0.06
4.	$2H^+(aq) + 2e = H_2(g)$	0.0
5.	$Co^{++}(aq) + 2e = Co(s)$	-0.46
6.	$Ni^{++}(aq) + 2e = Ni(s)$	-0.46
7.	$Cd^{++}(aq) + 2e = Cd(s)$	-0.62
8.	$Fe^{++}(aq) + 2e = Fe(s)$	-0.64
9.	$Zn^{++}(aq) + 2e = Zn(s)$	-0.81
10.	$Mn^{++}(aq) + 2e = Mn(s)$	-1.26

the decrease in cathodic polarization to a weakening of the hydrogen-electrode bond which reduces the blockage of zinc deposition resulting in a lower expenditure of energy.[143] These investigations have shown that even impurities more electronegative than zinc (i.e. Mn^{++}, Na^{+}, Ca^{++}, and Mg^{++}) may have a noticeable influence on the deposition process.

Third, studies have shown that the specific resistance of the electrolyte can be increased by the presence of metal sulfates such as sodium, magnesium, or aluminum. Increasing the resistance of the electrolyte also causes a reduction in the energy efficiency.[32,126]

Fourth, galvanic cells can be set up on the electrode surface at sites of localized potential difference. Such cells can be initiated by surface roughness or dendrite formation. When impurities more electropositive than zinc are present, the impurity ions can be deposited and cause corrosion of the already deposited zinc. The reaction is given below:

$$Zn\ (s) + n\ M^{+}\ (aq) = Zn^{++}\ (aq) + n\ M\ (s)$$

Such microcells can exist on pure zinc cathode surfaces, especially at low current densities. At low current densities, cathodic protection of the zinc may be marginal and in acid solution, local variations in potential caused by surface roughness may set up localized anodic areas. The zinc in these areas will dissolve and hydrogen ions will be discharged on the local cathodic zinc areas. Hydrogen current yields based on comparison with hydrogen polarization data have been found to be greater

than 100% for such situations.[10] Increasing the zinc content or decreasing the level of impurity and acid content has been shown to reduce the action described above. Increasing the current density increases the cathodic polarization and, consequently, the cathodic protection of the zinc.[10]

Fifth, a mechanism directly related to that above will be discussed. When the amount of impurity is quite small, the deposition rate of the impurity will be diffusion-controlled, and therefore quite slow when compared with the rate of zinc deposition. The amount of impurity depositing at the electrode is insufficient to cause much corrosion due to the replacement reaction mentioned previously. However, the small areas of the electrode covered by the impurity metal may have significantly different hydrogen evolution characteristics than the zinc. Under conditions of fixed overvoltages, area, and temperature, the ratio of hydrogen evolved on a platinum surface to a zinc surface is about 10^5.[70] Thus, even small fractions of cathode area covered by platinum can have drastic effects on the rate of hydrogen evolution. Other metals can exhibit similar effects.[32,57,70,76,107,144,175] As the deposition process starts, both the impurity and zinc are deposited over the whole electrode surface. The deposition rate of the impurity will be proportional to its concentration in the electrolyte. The surface remains generally smooth during the initial deposition period, and a uniform cathode potential exists without the presence of any extensive mixed potential regions. After a certain time, activation of the co-deposited impurity begins due

to changes in the surface morphology[72] or surface roughness. When the surface becomes rough, the specific cathode current density for zinc decreases at the recessed areas. A local potential difference is created, and this can initiate zinc corrosion. As the zinc corrodes, more impurity is exposed, and it tends to agglomerate since it is cathodically protected. Hydrogen evolution increases, because more sites favorable to hydrogen discharge are uncovered. The re-solution of the zinc proceeds at an ever increasing rate. The pH at the corrosion site can also be higher due to a deficiency in H^+ ions which are reduced to hydrogen. Thus the potential differences between the corroding and non-corroding areas are accentuated, thereby increasing the driving force of the reaction. When the corrosion of zinc proceeds far enough to expose the Aℓ substrate, hydrogen evolution can occur at both the corrosion sites and on the Aℓ cathode. At this stage, a drastic decrease in the current efficiency is observed.[90] The current density on the aluminum surface can be higher than in the bulk areas where the zinc is depositing due to further agglomeration of impurities. This also strengthens the corrosion driving force. Once the process is initiated, it can become somewhat autocatalytic. Factors which would reduce the effects of impurities acting in this fashion would include: operation at lower temperatures; reduction in hydrogen ion concentration; reduction in the amount of impurity in the solution; use of higher zinc concentrations; the use of higher current densities; and maintenance of level or uniform deposits. Various addition agents which might counteract

the effects of impurities which act in this manner have been investigated.[33,36,40,46,56,68,73-75,145-156] The use of higher current densities aids in several ways. First, the relative proportion of impurity to zinc in the deposit is reduced because the impurity deposition is diffusion-controlled. Second, increased current density causes increased cathodic polarization and more zinc is cathodically protected from corrosion. At very high current densities, "anodic protection" is thought to occur.[32] What this means is that sufficiently high current densities are used which cause the polarization on the cathode areas to reach the point where zinc deposits on top of the impurity sites.

Finally, a decrease in the zinc current efficiency can occur through the formation of hydrides at the cathode surface. Germanium and antimony are thought to act in this fashion.[32,35] The impurities may interact with hydrogen ions in the double layer to form hydrides or may deposit cathodically on the zinc and then form a hydride. The actual site where the hydride forms is questionable. In either case, hydrogen evolution can occur by the formation of a stable hydride in the vicinity of the electron surface (i.e. the double layer). The hydride diffuses out into the bulk solution and becomes unstable because of the lower pH and the lack of cathodic protection. The hydride would then decompose. Hydrogen gas would be evolved, and the metal cation would be freed to participate in another identical sequence of chemical steps. The hydrogen evolution reaction would not have to take place directly on the zinc electrode, since the hydride could be formed in the double layer without

depositing on the zinc.[72] An example of this is as follows:

In the double layer:

$$x\ M^{+} + y\ H^{+} + (x+y)e^{-} = Mx\ Hy$$

In bulk solution:

$$Mx\ Hy = xM^{+} + 1/2y\ H_2(g) + xe^{-}$$

Impurities of this type could act as hydrogen depolarizers (allow easier hydrogen evolution) and their effective concentrations could be orders of magnitude lower than impurities which actually deposit with zinc, since they are not consumed by the reaction.

3. Cathodic Polarization and Deposit Morphology. A factor arising from the influence of impurities at the electrode surface is the degree of cathodic polarization. Impurities in the electrolyte can cause alternative reactions to take place at the cathode as has been discussed above, and these reactions result in the passage of more current at a given potential than would occur in their absence (i.e. more hydrogen evolution). The measured cathodic potential may be less electronegative for the same applied current density. Investigators have shown that impurity interaction may cause the cathode potential to become more electropositive.[32,72-75,108,142]

The structure, orientation, and morphology of the zinc deposit may be influenced by the interaction of impurities at the cathode. Studies have shown that the crystal orientations of the deposit depend on the over-voltage of nuclei formation.[166]

The main causes for the potential differences between crystallographic planes have been related to the reticular densities of the different crystallographic planes.

Single crystal studies performed on a zinc crystal have confirmed the variation of electrode potential with crystallographic plane.[165] Other studies have shown similar effects.[167,168]

The change in cathodic polarization caused by the interaction of the impurities can cause certain preferred orientations to develop for the zinc deposit. Investigators have found that increasing concentrations of most cationic impurities tend to produce a preferred (00·2) orientation for zinc. Organic additives, which generally cause increased cathodic polarization, were found to shift the orientation to (10·1).[72,170,171] It is also reported that certain inorganic impurities can interact with the organic additives and counteract or cancel out each other's effects on the metal deposition.[73-75] Changes in the overpotential and orientation are noted. In the investigation of antimony in combination with glue, the orientation and polarization were found to go through the sequence as shown in Table III.[172] It is also found that the crystal size is affected by the presence of impurities.[73,75,162] The morphology obtained with additives or impurities which depolarize cathodic discharge of hydrogen is characterized by large crystal facets which appear to have a slight preferred orientation to the aluminum substrate compared to that for the addition-free zinc electrolytes.[172] The formation of hydrides (i.e. by antimony, germanium) can depolarize the cathode by providing an alternative path for

Table III. Effect of Antimony and Glue Additions on Crystal Orientation and Polarization.

Excess Antimony	Addition-free or Sb-Glue Combination	Excess Glue
(00·2) (10·3) ---------	(11·2) (11·4) (10·2) -------	(10·1) (11·0)
Decreasing ————	Overpotential ————	Increasing

hydrogen discharge. The presence of impurity at the electrode may also cause depolarization by interfering with adsorption of hydrogen ions on the various zinc crystal planes. The decreased polarization leads to a reduction in zinc nucleation, and this leads to an increase in the size of the observed zinc platelets.[172] Organic additives, which appear to increase cathodic polarization, decrease the crystallite size. Increased polarization favors increased nucleation and a finer crystalline size, because more energy is available to cause nucleation at the more electronegative potential. Adsorption of the organic also can act to block sites for crystal growth. The net effect is decreased crystallite size.[145,153,156] In general, the effects of additives and impurities on the structure and orientation of the zinc deposit and the degree of cathodic polarization are very significant.

4. Review of General Impurity Effects. In summary, the interactions of the impurities at the cathode can greatly affect the deposition process. Changes in crystalline orientation, cathodic polarization, current efficiency, and/or power consumption may occur. Reduction of the current efficiency may occur by a number of different mechanisms. The levels of impurity necessary to influence the process are not very large and the effects can be quite pronounced.

5. Individual Impurity Characteristics.

   a. Antimony. Antimony levels as low as 0.02 mg/ℓ noticeably lower the current efficiency. The dissolution of zinc becomes quite high for antimony additions approaching

0.05 mg/ℓ and nodular deposits of zinc are sometimes observed.[31-34,45-48,55,58-61,67] Dendrite formation has also been found for antimony-containing solutions.[50,52,63] The influence of antimony on the electrode processes increases with acid concentration and temperature.[31-34,45-48,55,58-61,67] The cathode potential becomes increasingly electropositive for solutions containing increasing amounts of antimony.[32,37,47,72-75,172] A (00·2) type of preferred orientation has been found for zinc electrodeposited from antimony-bearing electrolytes.[72,74,172]

Radiotracer studies indicate that the amount of antimony deposition depends on the amount of antimony in the electrolyte.[30,39,164] The rate of antimony deposition is controlled by the diffusion rate to the electrode interface.

Various studies attribute the interaction of antimony at the electrode to local cell action and hydride formation.[32,35,39,40,43,48,50-53,55,57,66,69,70] Several studies have been done to determine the exchange current for hydrogen on zinc and other Tafel characteristics.[57,70,144] The exchange current for hydrogen evolution on zinc is reported to be 1.26×10^{-8} A/cm^2.[70] The value on antimony ranges from 2.63×10^{-8} to 1×10^{-8} A/cm^2.[70,144] Comparison of the exchange current values above indicates that hydrogen evolution characteristics on zinc and antimony are quite similar. This would tend to cast some doubt on the premise that local cell action is involved. More work is

necessary to determine what mechanism governs the electrochemical behavior of antimony additions.

The addition of antimony to some solutions has facilitated the stripping of zinc from the cathode substrate. Investigators feel that changes in the deposit structure caused by the influence of antimony may be responsible.[42-44]

Various additives appear to counteract the influence of antimony. Glue, gelatin, gum arabic, agar-agar, quaternary ammonium salts, uranin, diethylbutynediol, dimethylvinylethyynylcarbinol, sucrose, levulose, tannic acid, and sodium and potassium tartrates are some of the organic additives which have been shown to be beneficial.[33-34,38-41,46,49,56,63,72-75,172] Oxidizing agents, such as potassium permanganate, sodium peroxide, manganese dioxide, and hydrogen peroxide are also commonly added to the electrolyte and they have been found to reduce the influence of antimony.[56]

The addition of combinations of glue and antimony to electrolytes containing other active impurities is sometimes beneficial.[38,73-75,172] Balancing the proper amount of antimony with glue is quite important, and new techniques are being tested to enable the proper amount of addition to be made. The deposits obtained from solutions containing balanced additions of glue and antimony are smooth and uniform, and this may lessen the influence of impurities which act through the local cell action type of mechanism.[73]

Antimony deposition increases for electrolytes containing glue.[39,40] The amount of hydrides formed during electrolysis for solutions containing both antimony and glue appears to be less.[39-40]

Combinations of antimony with other impurities (i.e., manganese, cobalt, arsenic, and B-naphthol) exhibit larger influences on the electrode processes than when the other impurities are absent.[36,49,54] Such synergism often occurs, but is not very well understood.

b. Arsenic. The level of arsenic reported to affect the process varies from 50 mg/ℓ to 0.1 mg/ℓ.[31,34,35,40,45,47,58,60,67] The most recent study[67] indicates that levels up to 5 mg/ℓ cause virtually no current efficiency loss. Other studies indicate that arsenic levels between 1-3 mg/ℓ lead to decreased cathodic polarization and spongy zinc deposits.[37,58] Corrosion of the zinc deposit is accelerated more by antimony or germanium, than by equal concentrations of copper, cadmium, cobalt, or nickel, and the action of these metals is greater than arsenic.[31] The investigators who reported the high value for arsenic (50 mg/ℓ) observed that hydrogen evolution at the cathode was reduced. They attribute this to poisoning of the catalytic centers for hydrogen evolution by deposited arsenic.[35] The actual amount of arsenic deposition was low when compared to other impurities.[107] The interactions of arsenic at the electrode for

electrolytes containing high acid concentrations and at elevated temperature have not been closely studied. Most of the available data are for one acid level and one temperature. More data are needed to ascertain the acceptable levels of arsenic in solution, especially for the conditions of high acidity and temperature. Most industrial zinc operations try to maintain arsenic levels below 0.1 mg/ℓ.[159,19-20]

Organic reagents, manganese dioxide, and aluminum sulfate are often beneficial additives for arsenic containing electrolytes.[34,40,47,56,77,107] Hydrated manganese dioxide formed at the anode during zinc electrolysis provides a large surface of strong oxidizing power and adsorptive capacity and helps decrease the amount of arsenic in the solution. Similar effects are found for germanium and antimony.[40]

More studies are needed to see what influence arsenic has on the zinc morphology and crystallographic orientation. Arsenic may interact at the electrode by forming stable hydrides as arsine can form in acid solution.[173] If arsenic does form stable hydrides, the effects on morphology and orientation may be quite similar to those attributed to antimony.

Antimony and arsenic have been reported to exhibit some synergism.[54] The arsenic interactions were enhanced by the presence of antimony.

c. Cadmium. The presence of cadmium does not cause the pronounced decrease in current efficiency associated with many other impurities. An exchange current of 1.26×10^{-12} A/cm^2

is found for cadmium in acid solution, and for zinc the value is 1.26×10^{-8} A/cm^2.[70] Since the exchange current of hydrogen reduction on the cadmium is lower than on the zinc, the zinc sites should be favored for hydrogen reduction. Local action cell formation should not occur.

The main influence of cadmium on reducing the current efficiency is through codeposition with zinc. Cadmium levels are kept sufficiently low to prevent this effect.

A separate cadmium recovery circuit is usually associated with zinc recovery and as much cadmium as is economically feasible is removed from the zinc bearing solutions.[159,19-20]

The effects of cadmium on the morphology of the zinc deposit have been investigated.[72] Mixed orientations were found for zinc deposits obtained from a solution containing 5 mg/ℓ. Other studies have been done to determine the presence of cadmium in the deposit[35] and the levels that can be tolerated in the solution.[31,34,40,60,65] Operators usually require cadmium levels below 1 mg/ℓ.

d. Cobalt. Cobalt can cause severe losses in current efficiency, and the removal of cobalt from solution by purification is quite difficult.[91,174]

Depending on the current density, zinc concentration, and acidity, cobalt levels as high as 10 mg/ℓ have been tolerated in commercial zinc electrolytes.[21] Usually, levels below 1 mg/ℓ are used.[159,19-20]

Difficulties in purification sometimes cause higher

levels of cobalt than desired to enter the electrolysis circuit. The difficulties can be traced to the interaction of zinc ions with cobalt ions. Small amounts of zinc ion in solution (6 g/ℓ Zn) can inhibit cobalt deposition for solutions containing as high as 1 M cobalt sulfate.[86,92-93,98,100-103] At high zinc levels, significant overpolarization, as high as 300 to 350 mV, can occur.[92,100,101] Some investigators attribute this effect to the formation of zinc-cobalt alloys which hinder cobalt nucleation.[100-101] Others do not observe alloy formation, but still find overpolarization. The deposits obtained by these investigators have a layered structure.[86] They attribute the inhibition of cobalt nucleation to the specific adsorption of zinc ions at the electrode. They also find that hydrogen evolution is favored over cobalt deposition.[92] The specific adsorption of the zinc ions may block active sites for cobalt nucleation and displace the cobalt ions from the dense portion of the double layer, therefore hindering their discharge at the electrode. Similar effects have been reported for nickel and iron.[88] The hindering effect has been observed to decrease as the rate of discharge of the zinc ion increases.[88] Even though the presence of zinc hinders the deposition of cobalt, it does not stop some deposition. Radiotracer studies show that some cobalt deposition does occur and that the amount deposited depends on its concentration and the zinc concentration.[79,80,82,96] Increasing the zinc concentration in the electrolyte decreases the amount of cobalt in the deposit.[102]

Increasing the acid content also is found to decrease the amount of cobalt deposition.[82] The cobalt is uniformly distributed in the deposit.[32,63]

Cobalt also deposits at the anode and in amounts much higher than at the cathode.[79,80-85,90] Deposition at the anode causes a lowering of the anodic potential[81,90] and lowers the extent of anode corrosion.[83-85,90] Investigators consider cobalt to be deposited at the anode as a Co_2O_3 film.[80] The extent of cobalt deposition at the anode depends on the acidity of the solution.[80] Corrosion of the anode is also smaller for lead-cobalt anodes.[105]

The beneficial effects of cobalt at the anode must be balanced against the deleterious effects produced at the cathode. Severe current efficiency losses occur at the cathode when cobalt is present in solution.[21,32,90] The current efficiency losses are found to depend on the cobalt content of the electrolyte and upon the duration of electrolysis. Investigators find that initial current efficiency for solutions containing cobalt is quite close to that obtained for solutions without the impurity.[90,94] The current efficiency, however, decays with time. The induction period depends on the acidity and the impurity concentration.[41,82,90,94,99,104] Increases in acidity are especially important. Temperature increases also increase the corrosion of zinc for cobalt-containing solutions.[61,62,78,82,90,99] The cathode potential

becomes less electronegative as the cobalt content of the electrolyte increases.[32,96,108]

The current efficiency loss is attributed to local cell action, and a marked increase in hydrogen evolution is found.[32,48,50-52,69,87,90,94-96,108] Cycles of zinc formation-redissolution occur.[94,95] The exchange current for hydrogen deposition on cobalt (4.5×10^{-7} A/cm^2) is significantly higher than for zinc.[70] Therefore, hydrogen evolution should occur more readily on cobalt sites.

A concentration level of 5 mg/ℓ cobalt produces a (00.2) preferred orientation for the zinc deposit.[72] At lower concentrations, the orientation is quite similar to that obtained from cobalt-free electrolytes.[43,72]

The addition of glue and other organics to cobalt containing electrolytes is often beneficial in improving current efficiency and deposit appearance.[61,62,97] Similar results occur for the addition of glue with antimony. The use of B-naphthol with glue increases the current efficiency.[33,38,46,90] B-naphthol is thought to complex with the cobalt and reduce its possible interaction at the electrode.[46] Ammonium sulfate and gelatin additions also help increase the current efficiency. Oxidizing agents, such as permanganate, sodium peroxide, manganese dioxide, and hydrogen peroxide are also useful additives.[56,90,108] The oxidizing agents may oxidize cobaltous ion to cobaltic and cobaltic is reported to have less effect on the cathodic process.[83]

In the absence of glue, cobalt combinations with antimony and B-naphthol lower the current efficiency more than the individual impurities.[54] Other combinations, such as copper and cobalt give similar effects.[36] Accordingly, a proper balance of additives is very important.

Higher current density, lower acid concentration, higher zinc concentration, and lower temperature also aid in decreasing the interaction of cobalt at the cathode.[90,108] Lower acid levels permit the use of cobalt concentrations as high as 10 mg/ℓ.[21,90]

e. Copper. Copper appears to interact in much the same way as do cobalt and nickel. More copper is found to deposit with the zinc than any of the other impurities (based on equivalent concentrations).[107] Copper is uniformly distributed in the zinc deposit.[32,40] Concentration levels greater than 1 mg/ℓ cause a considerable drop in current efficiency and hydrogen over-voltage.[34,45,66,109] This is attributed to local cell action.[32,35,43,50,51,57,67,109] The exchange current for hydrogen evolution on copper is reported to be 1.7×10^{-7} A/cm^2.[70] This is somewhat lower than that of cobalt or nickel, but higher than that of zinc. However, much less copper can be tolerated in the electrolyte than cobalt, because more copper plates out than cobalt and this provides more sites for hydrogen evolution at the cathode.

Similarly as with cobalt additions, the cathode potential and current efficiency are a function of the copper concentration. The cathode potential becomes more

electropositive, and the current efficiency decreases with increasing copper concentrations in the electrolyte.[32,37,109]

The current efficiency and cathode potential also show a time effect.[109] Initially, the values are steady, but after a certain induction period, they begin to change significantly. The current efficiency decreases, and the cathode potential becomes more electropositive. Increases in temperature and acid content enhance the interaction of copper at the cathode.[32,48,51,69]

Dendrite formation is observed for solutions containing copper[50,52,62,63] and spongy deposits of zinc are obtained for solutions containing high levels of this impurity.[37,47,58] A preferred orientation of (00.2) is observed for zinc deposited from a solution containing 5 mg/ℓ.[72]

Addition agents, such as glue and gelatin improve the current efficiency, but the additions are only mildly effective.[32,33,68] The appearance of the deposit and the current efficiency are improved when glue is added in conjunction with antimony.[38]

f. Germanium. Electrolytes containing germanium show severe current efficiency losses at concentration levels as low as 0.02 mg/ℓ.[31,34,114,116,117] The concentration levels are similar to those of antimony.[32,35,67] Radiotracer studies indicate that germanium deposition is low.[112,113,164] The amount deposited is lower than the amount of antimony deposited under similar conditions.[164]

The interaction of germanium at the cathode has

noticeable effects on the morphology.[113] At concentrations as low as 0.01 mg/ℓ a preferred (00·2) orientation is obtained for the zinc deposit.[72] The interaction at the cathode is enhanced by low current densities,[65,111,113] increased temperature,[61-62] and increasing acid concentration.[35] The action of germanium is attributed to hydride formation by some[32,35] and to local cell action by others.[53,113] The effects may be caused by a combination of the two mechanisms. Studies show that elemental iron reduces germanium oxide to the elemental state.[118] If iron reduces germanium, zinc probably should also, and thus germanium should be deposited. The exchange current value of hydrogen deposition on germanium is 1×10^{-5} A/cm^2.[70] This value is quite high when compared to that of zinc. Hydrogen evolution on germanium sites should therefore be easier than on the zinc sites and local cell action may be quite significant. Future studies are needed to determine which mechanism is the major contributor to the behavior of germanium additions during zinc plating.

The presence of manganese dioxide and silica reduce the amount of germanium in solution by adsorption[110,115] and current efficiencies are often improved by making these additions. Organic reagents and oxidizing agents reduce the influence of germanium at the cathode and cause some increase in current efficiency to be obtained.[111] The effects of these additives are less than for nickel or cobalt.[111] Sugar, pyridine and triethanolamine are also

useful addition agents.[111]

g. Iron. The presence of iron in small quantities has been shown to lower the current efficiency for zinc, but not to the extent exerted by cobalt and nickel.[35] At equal concentration levels in the electrolyte, less iron codeposits with zinc than do copper, nickel, antimony, or cobalt.[107] Zinc ions have been found to hinder the deposition of iron, cobalt, and nickel.[88-89] This may be caused by alloy formation[53] or by the specific adsorption of zinc ions at the electrode. The effect increases with increasing zinc ion concentration.

Some studies have indicated that iron levels as high as 100 mg/ℓ have little effect on the zinc process,[67] but other studies show that the process is affected at much lower concentrations (10-30 mg/ℓ).[34,119] Generally, concentration levels below 10 mg/ℓ are maintained in industry.[159,19-20]

The sensitivity of the zinc deposition process to interactions with iron impurities is greater at increased levels of temperature and acid concentration.[61,62,121] Increasing the concentration of iron increases the amount of hydrogen evolution[122] and causes the cathode potential to become more electropositive.[121] Increases in current density have been reported to increase the zinc current efficiency.[121]

The effects of iron have been attributed to local cell action and to ferrous/ferric oxidation and reduction.[35,122] The exchange current for hydrogen evolution on iron is

reported to be 1.2×10^{-6} A/cm^2.[70] This suggests that hydrogen reduction should be enhanced on the iron sites in the zinc deposit, since the value of the exchange current for zinc is lower. It has been found that the current efficiency drops with time.[122] This is due to the formation of the local action cells and to the buildup of ferric ions formed at the anode.

The effects of iron are weakened by additions of organic compounds and oxidizing agents.[49,56,107] These additives appear to be more effective in reducing the effects of iron than for cobalt.[97]

h. Manganese. Manganese has been shown to interact with the zinc electrolysis system in many ways and the interactions exhibited depend on the chemical species of manganese in the electrolyte. Manganese (II) has been reported to have little influence on the current efficiency obtained for zinc deposition,[128,132] and is reported to aid in reducing anode corrosion.[135]

Manganese dioxide at levels below 10 g/ℓ has little effect on the current efficiency.[128,129,130,134,136] In many cases, increases in current efficiency have been observed for solutions containing suspended manganese dioxide particles. Manganese dioxide has been found to reduce the dissolution of zinc and to improve the quality of the cathodic deposit.[129] The degree of lead contamination in zinc cathodes is less for solutions containing MnO_2.[108,113,123,127,131,136] The improvements in current efficiency caused by MnO_2 in the

electrolyte are believed to be due to the oxidizing power and adsorptive capacity of the MnO_2 particles,[40,56,139,188,189] which lower the amount of other active impurities in the electrolyte. Some investigators also believe that MnO_2 forms a low conductivity film at the cathode which acts as a barrier to hydrogen ions and the dissolution of zinc.[129] Some investigators believe that the high surface activity of the MnO_2 particles reduces the effects of suspended lead dioxide and sulfate through adsorption of the lead species onto the suspended MnO_2 particles.[113,123,127] The MnO_2 eventually settles to the bottom of the cells and collects as slime. The slime (or mud) gathers at the bottom of the cell and is flushed out periodically.[16] Increases in the cell temperature and acid content cause desorption of the collected impurities in the mud and current efficiency problems have arisen when fluctuations in acidity or temperature occur.[16]

Permanganate ion has been reported to be produced at the anode during zinc electrolysis.[124] The corrosion rate of zinc increases with increasing permanganate concentration. The permanganate ion is thought to be reduced stepwise to manganese (II).[124,139,188] The cathode potential is observed to become more electropositive with increasing MnO_4^- concentrations.[124,128] The amount of permanganate formed in the electrolyte is lessened by interaction with manganese (II) and manganese dioxide, and by the interaction with other impurities.[108,134] The latter has been found to reduce the effects of the impurities at the cathode.[56,139,188,189]

Some investigators have reported that permanganate can react with Mn^{2+} to form Mn^{3+} which also lowers the current efficiency[130] but not to the extent of MnO_4^-.

The levels of manganese that can be tolerated in solution depend largely on its oxidation state. Initial concentrations up to 4 g/ℓ of Mn^{2+} do not seriously affect the current efficiency.[108] Increasing temperatures are found to have little effect for solutions containing manganese species other than permanganate.[134]

i. Nickel. The behavior of nickel is similar to that of cobalt and iron. The current efficiency decreases markedly as the concentration of nickel is increased from 0 to 5 mg/ℓ.[61,67,140,163] Levels below 1 mg/ℓ are usually sought in commercial practice.

The effects of nickel can be seen at lower concentration levels than cobalt or iron. On an equal concentration basis, more nickel than cobalt is deposited with the zinc.[140,163] The deposition of nickel like the other iron-based metals is hindered by zinc ions.[88] Whether this occurs by alloy formation or by specific zinc ion adsorption remains open to question.[53,88,89]

Temperature and acid concentration increases have been shown to increase the action of nickel impurities.[32,35,48,61,62,95,140,163] Investigators have also found that an induction period occurs where the initial current efficiency is close to that for the solution containing no nickel, but then decays with time.[94,95,140,163]

The induction time depends on the nickel concentration, acid concentration and temperature. The effects of nickel are more pronounced at lower current densities.[51,93,95,99] The cathode potential becomes more electropositive as the concentration of nickel in the electrolyte increases.[32,140,163]

The effects of nickel in zinc electrodeposition have been attributed to the formation of local action cells.[32,87,140-142] Nickel has a low hydrogen overvoltage[140,70] and the exchange current value reported for hydrogen evolution on nickel is 4×10^{-6} A/cm^2.[70] This is significantly higher than that reported for zinc and indicates that hydrogen reduction on the nickel sites should be easier than on the zinc sites. Investigators, using scanning electron microscopy, report that nickel agglomerates near the zinc corrosion sites.[70,141] Furthermore, a preferred (00.2) orientation is developed by the zinc layer for solutions containing 5 mg/ℓ nickel.[70]

A recent investigation, using cyclic voltammetry, found that the amount of hydrogen evolved and the rate of zinc corrosion greatly increased in the presence of nickel. Nickel levels as low as 0.5 mg/ℓ are reported to affect the zinc deposition process for a solution containing 60 g/ℓ zinc and 200 g/ℓ H_2SO_4. Lowering the zinc concentration enhanced the effect of nickel.[142] These investigations lend support to the local action mechanism as being responsible for the effect of nickel on the zinc deposition process.

j. Action of Additives. The use of various addition agents to counteract the effects caused by impurities has already been mentioned. The mechanisms of additive-impurity interaction are not well understood. Some organic agents act to improve the current efficiency, whereas others act to promote corrosion.[149] The proper choice of an addition agent and its concentration are very important factors in the maintenance of high current efficiencies. Glue, gelatin and organic amines have been found to be useful addition agents.[146] The effectiveness of the organic agent used often depends on the length of the organic radical.[75,147] New techniques which allow evaluation of the effectiveness of various additives have been demonstrated.[75] The use of polarization studies (i.e., cyclic voltammetry), scanning electron microscopy, and x-ray diffraction permit characterization of some of the effects exhibited by the presence of impurities and addition agents in terms of cathode polarization and deposit morphology.[72-75,142,172] Some investigations have shown that these techniques may allow the control of addition agent usage by indicating what the optimum level of addition should be.[72-75,172]

The use of polarization analysis using potentiodynamic scan curves for determining the amount of active glue in solution has also been tried for copper and lead production.[157-158] The proper level of organic addition is very important, because excess glue or other organics may lead to current efficiency reduction, deposit brittleness,

difficulties in melting, increased power consumption, etc.[73,151-152]

The addition of glue to a relatively impurity-free electrolyte generally decreases the zinc current efficiency.[151-152] Investigators attribute this to the inhibition of both zinc and hydrogen discharge with the former being inhibited to a higher degree. The overvoltage of zinc deposition from electrolytes containing additives is found to be higher than those free of additives.[73,74,156,172] The benefit of addition agents lies in their ability to reduce the effects of other impurities. The current efficiency even at optimum levels of addition agent is still found to be below that obtained for a pure addition-free electrolyte.[73-74,172]

Although the interactions between addition agents and impurities are not well understood, some explanations have been offered to account for the results. It has been reported that organic colloids are deposited with the zinc,[145,150] and that the cathode potential increases with the concentration and molecular weight of the surface active additives.[153] Investigations have also shown that the grain size of the deposit is reduced and more uniform deposits are obtained from solutions containing organics.[145] Investigators believe that the adsorption of the addition agents at the cathode causes more nucleation and hinders crystalline growth resulting in a finer grained and more uniform deposit. A more uniform deposit

hinders the formation of local cells, and the effect of the impurities are therefore reduced. Another factor which has been mentioned is that an organic additive lowers the surface tension at the cathode surface and promotes the removal of adsorbed gas bubbles which hinder zinc deposition.[153] Removal of the gas bubbles also promotes a more uniform deposit. Another possibility for the interaction of organics with impurities may be due to complex formation,[46] but more research is necessary to confirm if this does occur. For a hydride former such as antimony, the organic additive may hinder formation of the hydride by adsorbing onto the deposited metal and thus blocking hydrogen ion access to the metal. This assumes that the hydride formation takes place on the cathode surface and not in the double layer. It has been found that the amount of antimony in the deposit increases upon addition of glue to the solution.[39-40] More tests are needed to confirm the actual mechanism of interaction.

The effects of the addition agents are complex in nature. The use of new techniques hopefully will allow a better understanding of their interaction at the electrode and a determination of the optimum level for a given amount of impurity. Basic research which characterizes the effects on the basis of deposit orientation, morphology, and polarization appears to be a step in the right direction. Other methods which allow control of electrolyte quality have been proposed.[64,190] These methods compare the anodic to

cathodic deposition times and give an index of electrolyte quality. More research is necessary in this area also.

k. Lead and Anode Factors. The main source of lead contamination in the zinc cathode is the deterioration of the lead alloy anodes. The amount of lead incorporated in the cathode has been found to be proportional to the amount of suspended PbO_2 and dissolved lead in the solution. The amount of dissolved lead (Pb^{++} and lead sulfate) is usually low, but not negligible (3-6 mg/ℓ).[178]

Increases in acid concentration and temperature increase the amount of lead in suspension and in solution.[179,181] The form of lead contamination varies with the current density. At low current density, deposition of Pb^{++} has been reported to be the primary source, whereas, at high current density (where there is increased bubbling and mixing of the electrolyte), PbO_2 is the major source of contamination.

Lead has been reported to affect the structure and morphology of the deposited zinc.[172] Lead dioxide formed at the anode and deposited as sponge at the cathode lowers the current efficiency by roughening the surface.[182] Deposition of metallic lead has been reported to have little effect on the current efficiency other than consuming a small amount of the current in its deposition. The exchange current value for hydrogen evolution on lead is 2×10^{-13} A/cm^2.[70] This is much lower than zinc and local cell action on lead sites should not occur.

The amount of lead contamination is attributed to the amount of anode deterioration. The amount of lead contamination in the cathode has been reduced through the use of addition agents which lower the amount of lead in solution and by use of more stable anodes.

Investigators have found that lead contamination is reduced by the addition of Cr^{+++}, V^{+++}, Mo^{+++}, or Co^{++}.(85) Strengthening of the PbO_2 film on the anode is thought to lower the amount of suspended PbO_2. Addition of alkaline earth and rare earth (La, Ce and Nd) sulfates to the electrolyte appear to decrease lead contamination.(177,183,184) Investigators report that the action of strontium compounds removes lead ions from the solution by incorporation of the lead ions into growing strontium sulfate crystals.(185) These investigators found that the presence of chloride ions has a marked effect on the rate of lead removal by strontium carbonate. When slurries containing strontium (1 kg $SrCO_3$/ ton cathode Zn) are added to the acid zinc electrolyte, the lead contamination at the cathode was lowered from 0.0037% to 0.0015%.

As an alternative to modifications of the electrolyte, stabilization of the anode has been attempted through alloying. Lead-silver alloys exhibit a much better corrosion resistance than lead alone.(176,184) The presence of silver improves the chemical resistance of the anode, lowers the anode voltage, and reduces the amount of lead in the zinc. It has also been found that addition of a third component to the

alloy, such as Sn, Tl, or Ca also enhances corrosion resistance.[81,176] The mechanical strength of the anode is also improved by the addition of silver and calcium. Not all alloying additions have been found to be beneficial. The addition of arsenic or antimony to the lead has been found to increase corrosion of the lead anode.[71]

Another method employed to reduce lead contamination is pretreatment of the anode in a fluoride solution. The oxide film becomes more stable, and the anode life is increased by this pretreatment.[186] The stabilized oxide film reduces the amount of suspended PbO_2 and accordingly the amount of lead contamination.

Alternative anode materials may also avoid the problem of lead contamination. The use of a titanium anode coated with MnO_2 has been reported to reduce the anode potential and anode weight.[138]

The problem of anode corrosion and lead contamination is quite serious. Poor quality zinc and excessive anode loss can lead to poor economy of operation. Fortunately, methods of coping with the problem have been developed.

D. Commentary on Past and Future Research

The results of the various investigations show the importance of impurity interaction on the zinc electrodeposition process. Many of the results are not directly comparable, because the experimental conditions, such as acid concentration, zinc concentration, current density, temperature, time of electrolysis, and impurity content vary from investigator to investigator. As a result, there remain

many unresolved contradictions concerning the degree of harm caused by the presence of a given impurity as well as the maximum acceptable level of the impurity in the electrolyte. Some effects of the impurities are beneficial, but most are not. Balancing the levels of addition reagents with the impurity content of the electrolyte is still largely done on an empirical basis. New techniques, such as cyclic voltammetry, scanning electron microscopy, and x-ray diffraction hold promise in this area, but much more work is needed using these techniques.

In addition, it has often been found that some electrolytes which contain more than one impurity encounter a much greater drop in cathode current efficiency than expected. This synergistic effect of one impurity with another is well recognized, but it is not well understood. Also, quantitative guidelines for allowable concentrations of mixed impurities are not very reliable. More research is needed to study the combined effects of the impurities and to observe how the main process parameters interact with changes in the impurity content. The use of factorially designed experiments has only recently been applied to studying the zinc electrolysis system.[17,104] Such experiments may be of great help in sorting out the combinations of impurities which act synergistically. Process modeling of the factors involved in the zinc electrolysis also would be possible using statistically designed experiments. This would allow some predictability on the effects of changing impurity concentrations and process parameters.

Progress has been made towards a better understanding of the mechanisms by which impurities interact at the cathode. It is only recently that the newer techniques have been applied to this problem

and much of the older research only provides limited evidence to support the various hypotheses of interaction. The use of cyclic voltammetry and morphology studies should be of particular help in confirming past ideas of impurity interaction.

In view of the large amounts of electrical energy consumed by the electrowinning process, a better understanding of the influence of the impurities and additives is important in achieving a more efficient use of energy resources. Because the effects of the impurities are exhibited at low levels, most of the research and development effort has been aimed at improving the purification process and the reliability of the analytical control of the final purity of the electrolyte. Since any decrease in cathodic current efficiency results in a corresponding increase in electrical power consumption, the cell operator asks for an electrolyte as free as possible of harmful impurities. The cost of the purification, however, should not be neglected, since it requires heating solutions to high temperatures and consumes large quantities of zinc powder in the purification. If the interactions of the major process parameters and impurities were better understood, perhaps less thorough purification could be used and an overall energy saving realized. As an example, at times of poor purification, bad current efficiencies are usually obtained. If the major process parameters could be adjusted during this time (i.e., stripping time, acid concentration), some improvement in the current efficiency could probably be obtained. Once the mechanism of interaction is understood, more process control should be possible.

Overall, the research done thus far has helped point out which impurities are the most harmful and give a general range of

concentration that is critical for the impurity interaction to be significant. The ways the impurities may interact has also been proposed, but in many cases not fully confirmed. Of the various impurities discussed, antimony and germanium seem to be the most harmful, followed by nickel, copper, cobalt, iron, arsenic, cadmium, lead, and then manganese. The first two have significant effects at concentrations in the ppb range, whereas, the others in the ppm (mg/ℓ) range. Substantial work is still necessary to confirm the mechanisms of interaction; determine what synergism exists; and to obtain ways to better characterize a given electrolyte so that the current efficiency and the type of zinc deposit obtained may be better predicted.

APPENDIX B

Bibliography

1. Minerals Yearbook, 1974, Vol. I, U.S.B.M.

2. J. Metals, 1974, 26, No. 8, 6.

3. Min. Eng., 1974, 26, No. 12, 19.

4. A. Zentner: Trans. A.I.M.E., 1936, 121, 453.

5. D. M. Liddell: Handbook of Non-Ferrous Metallurgy, 1st edition, Vol. II, p. 1129, McGraw-Hill Book Co., New York, 1926.

6. D. McIntosh: Trans. Roy. Soc. Canada, 1917, 2, No. 3, 113-9.

7. P. Röntgen and R. Buchkremer: Metallwirtschaft, 1931, 10, 931-6.

8. I. Y. Ogawa: J. Mining Inst. Japan, 1932, 48, 1289-96.

9. O. A. Esin and A. Levin: J. Gen. Chem. U.S.S.R., 1936, 6, 1539-48.

10. U. F. Turomshina and V. V. Stender: J. Appl. Chem. U.S.S.R., 1954, 27, 1019-1025.

11. O. A. Khan, et al.: Trudy Altaisk. Gorno-Met. Nauch. - Issledovatel. Inst., 1957, 5, 76-81.

12. P. V. Sergeev: Tsvetnye Metal., 1959, 32, No. 9, 35-8.

13. O. A. Khan, et al.: Trudy Chetvertogo Soveshchaniya po Elektrokhimii, Moscow, 1956, 558-60.

14. Petur Mechenov, et al.: Rudodobiv Met., 1966, 21, No. 3, 21-4.

15. A. A. Salin and M. R. Syrgabaev: Vestn. Akad. Nauk Kaz. S.S.R., 1971, 27, No. 6, 64-8.

16. A. R. Ault, et al.: paper presented at Aus. I.M.M. Conference, South Australia, July, 1975.

17. R. C. V. Boas and T. Balberyszski: paper presented at 102nd Annual Meeting, A.I.M.E., Feb., 1973.

18. I. D. Enchev: Khim. Ind., 1968, No. 5, 217-19.

19. D. I. J. Evans and R. S. Shoemaker: International Symposium on Hydrometallurgy, 770-805, A.I.M.E., New York, 1973.

20. C. H. Cotterill and J. M. Cigan: World Symposium on Mining and Metallurgy of Lead and Zinc, Vol. II, 177-328, A.I.M.E., New York, 1970.

21. Mining Magazine, 1975, No. 12, 426-435.

22. C. L. Mantell: Electrochemical Engineering, 4th ed., 211-244, McGraw-Hill Book Co., New York, 1960.

23. G. N. Znamenskii and V. V. Stender: Zhur. Priklad. Khim., 1960, 33, 2728-30.

24. U. C. Tainton: Trans. Electrochem. Soc., 1922, 41, preprint.

25. P. Röntgen and R. Buchkremer: Metallwirtschaft, 1931, 10, 963-7.

26. G. D. Scholl: Chem. Met. Eng., 1922, 26, 595-602.

27. F. Laist, et al.: Trans. A.I.M.E., 1921, 64, 699.

28. J. T. Ellsworth: Trans. Electrochem. Soc., 1922, 42, 187-202.

29. A. A. Salin: Tsvetnye Metal., 1961, 34, No. 8, 28-33.

30. Niro Matsuura: J. Chem. Soc. Japan, Pure Chem. Sect., 1952, 73, 291-2.

31. Giovanni Scacciati: Industria mineraria, 1953, 4, 511-16.

32. A. G. Pecherskaya and V. V. Stender: J. Appl. Chem. U.S.S.R., 1950, 23, 975-989.

33. V. S. Kolevatova and A. I. Levin: Zhur. Priklad. Khim., 1954, 27, 456-60.

34. Kurt Peukert and Willy Schreiter: Metallurgie u. Giessereitech, 1954, 4, 397-401.

35. U. F. Turomshina and V. V. Stender: Zhur. Priklad. Khim., 1955, 28, 372-87.

36. U. F. Turomshina and V. V. Stender: Zhur. Priklad. Khim., 1955, 28, 467-74.

37. N. T. Kudryavtsev and A. G. Atanasyants: Zhur. Fiz. Khim., 1955, 29, 1227-35.

38. A. I. Levin, et al.: Ural. Politekh. Inst. im. Kirova, Korroziya i Metallopokrytiya, Sbornik Statei, 1953, No. 43, 24-55.

39. Z. A. Sheka: Ukrain. Khim. Zhur., 1956, 22, 387-93.

40. Z. A. Sheka and K. F. Karlysheva: Doklady Akad. Nauk S.S.S.R., 1956, 108, 126-9.

41. Z. A. Sheka and L. A. Kotorlenko: Ukrain. Khim. Zhur., 1956, 22, 691-6.

42. A. I. Levin and V. S. Kolevatova: Tsvetnye Metal., 1956, 29, No. 9, 28-34.

43. V. L. Klimenko: Zhur. Priklad. Khim., 1957, 30, 533-46.

44. V. L. Klimenko: Tsvetnye Metal., 1956, 29, No. 9, 35-43.

45. G. N. Pakhomova and S. I. Orlova: Sbornik Nauch. Trudov Gosudarst. Nauch. - Issledovatel. Inst. Tsvetn. Metal., 1955, No. 10, 183-99.

46. A. I. Levin, et al.: Zhur. Priklad. Khim., 1958, 31, 581-9.

47. N. T. Kudryavtsev and A. G. Atanasyants: Trudy Moskov. Khim. - Tekhnol. Inst. im. D. I. Mendeleeva, 1956, No. 22, 143-57.

48. A. V. Pomosov, et al.: Zhur. Priklad. Khim., 1958, 31, 734-42.

49. A. I. Zhurin and S. P. Pyunnenen: Trudy Leningrad. Politekh. Inst. im. M. I. Kalinina, Elektromet. Tsvetnykh Metal., 1957, No. 188, 204-11.

50. G. Z. Kir'yakov: Zhur. Fiz. Khim., 1958, 32, 2561-4.

51. A. F. Nikiforov and V. V. Stender: Ukrain. Khim. Zhur., 1959, 25, 18-24.

52. G. Z. Kir'yakov and F. K. Bainietova: Trudy Inst. Khim. Nauk, Akad. Nauk Kazakh. S.S.R., 1958, 3, 64-71.

53. D. P. Zosimovich and N. E. Nechaeva: Trudy Chetvertogo Soveshchaniya Elektrokhim., Moscow, 1956, 541-6.

54. Georg Steintveit and Hans Holtan: J. Electrochem. Soc., 1960, 107, 247-8.

55. K. N. Kovalenko, Yu. P. Ivanova, and S. P. Vorab'eva: Uchenye Zapiski Rostov.-na-Donu Univ., 1958, No. 41, 27-38.

56. P. Guareschi: Industria Chimica, 1933, 8, 704-8.

57. P. V. Sergeev: Vestnik Akad. Nauk Kazakh. S.S.R., 1960, 16, No. 12, 26-35.

58. N. T. Kudryavtsev: Trudy Soveshchaniyapo Voproson Vliyaniga Poverkhn. Aktiv. Veshchestv na Elektroosazhdenie Metal, 1958, 113-21.

59. Miroslav Kett: Hutnicke Listy, 1961, 16, 660-71.

60. Isao Kushima, et al.: Suiyokaishi, 1956, 13, 67-79.

61. A. A. Salin and V. S. Volkova: Sb. Nauchn.-Tekhn. Tr. Nauchn.-Issled. Inst. Met. Chelyab. Sovnarkhoza, 1961, No. 4, 139-43.

62. A. A. Salin, et al.: Tsvetnye. Metal., 1962, 35, No. 12, 13-18.

63. V. G. Bundzhe and G. Z. Kir'yakov: Tr. Inst. Khim. Nauk, Akad. Nauk Kaz. S.S.R., 1962, 9, 3-17.

64. A. A. Salin, G. G. Rannev, and I. M. Kogol: Tsvetnye. Metal., 1964, 37, No. 1, 31-5.

65. A. Lange: Arch. Hutnictwa, 1964, 9, No. 1, 3-30.

66. A. G. Brandt and G. Z. Kir'yakov: Tr. Inst. Khim. Nauk, Akad. Nauk Kaz. S.S.R., 1967, 15, 37-44.

67. Reiner Liebscher: Neue Huette, 1969, 14, No. 11, 651-3.

68. G. Z. Kir'yakov and A. G. Brandt: Tr. Inst. Khim. Nauk, Akad. Nauk Kaz. S.S.R., 1969, 24, 41-9.

69. G. Z. Kir'yakov and Yu. D. Dunaev: Tr. Inst. Khim. Nauk, Akad. Nauk Kaz. S.S.R., 1969, 24, 32-40.

70. G. C. Bratt: Electrochem. Technol., 1964, 2, No. 11-12, 323-6.

71. N. A. Novikova, et al.: J. of Appl. Chem. U.S.S.R., 1969, 44, No. 10, 2518-2522.

72. H. H. Fukubayashi, T. J. O'Keefe, and W. C. Clinton: R. I. 7966, U. S. Bureau of Mines, 1974.

73. D. J. Robinson and T. J. O'Keefe: J. of Appl. Electrochem., 1976, 6, 1-7.

74. B. A. Lamping and T. J. O'Keefe: Met. Trans. B, 1976, 7B, No. 12, 551-558.

75. R. C. Kerby, H. E. Jackson, T. J. O'Keefe, and Y. Wang: paper presented at 106th Annual Meeting, A.I.M.E., Atlanta, GA, 1977.

76. G. Z. Kir'yakov: Zhur. Priklad. Khim., 1962, 35, 2661-6.

77. L. Cambi and G. G. Monselise: Rend. ist. lombardo sci., 1936, 69, 392-6.

78. V. P. Bogatskii and A. N. Zhurin: Trans. Leningrad Ind. Inst., Sect. Met., 1940, No. 4, 86-9.

79. Niro Matsuura: J. Chem. Soc. Japan, Pure Chem. Sect., 1953, 74, 239-42.

80. Niro Matsuura: Sci. Papers Coll. Gen. Educ. Univ. Tokyo, 1953, 3, 13-18.

81. G. Z. Kir'yakov and V. V. Stender: Izvest. Akad. Nauk Kazakh. S.S.R., 1953, 120, Ser. Khim. No. 5, 91-101.

82. Z. A. Sheka: Ukrain. Khim. Zhur., 1956, 22, 394-400.

83. Takeshi Tsuruoka: Nippon Kogyo Kaishi, 1958, 74, 177-82.

84. Takeshi Tsuruoka: Nippon Kogyo Kaishi, 1959, 75, 93-6.

85. Isao Kushima and Giroku Miyatani: Suiyokaishi, 1959, 14, 43-6.

86. M. Yunus, C. Capel-Boute, and C. Delcroly: Mem. Sci. Rev. Met., 1962, 59, 131-46.

87. A. F. Nikoforov: Zhur. Priklad. Khim., 1964, 37, No. 2, 348-52.

88. B. P. Yur'ev: Tr. Leningr. Politekhn. Inst., 1963, 223, 87-96.

89. B. P. Yur'ev: Tr. Leningr. Politekhn. Inst., 1964, 239, 175-92.

90. I. W. Wark: Proc. Australian Conf. Electrochem., 1st Sydney, Hobart, Australia, 1963, 889-900.

91. Alfred Lange: Z. Erzbergbau Metallhuettenw., 1965, 18, No. 5, 242-52.

92. M. Yunus, C. Capel-Boute, and C. Decroly: Electrochim. Acta, 1965, 10, No. 9, 885-900.

93. G. N. Znamenskii and V. M. Serebritskii: Ukrain. Khim. Zhur., 1965, 31, No. 7, 703-8.

94. M. Maja: Electrochim. Metal., 1967, 2, No. 4, 469-72.

95. Mario Maja and S. Pozzoli: Chim. Ind., 1969, 51, No. 2, 133-8.

96. Ignazio R. Bellobono: Ind. Chim. Belge, 1967, 32, 305-8.

97. G. Z. Kir'yakov, et al.: Tr. Inst. Khim. Nauk, Akad. Nauk Kaz. S.S.R., 1969, 24, 50-6.

98. Carmen Capel-Boute and J. Vereecken: Metallurgie, 1970, 10, No. 1, 3-17.

99. St. Karaivanovr and Sn. Magaeva: Nauch. Tr. Vissh. Pedagog. Inst., Plovdiv, Mat., Fiz. Khim., Biol., 1970, 8, No. 2, 147-54.

100. A. M. Ezrokhina and B. P. Yur'ev: J. of Appl. Chem. U.S.S.R., 1969, 42, No. 12, 2697-2699.

101. A. M. Ezrokhina, B. P. Yur'ev, and S. N. Shpol'nikov: J. of Appl. Chem. U.S.S.R., 1972, 45, No. 1, 96-100.

102. B. P. Yur'ev and A. M. Ezrokhina: Zhur. Priklad. Khim., 1974, 47, No. 6, 1424-5.

103. T. S. Mazur, A. F. Nikiforov, and V. V. Repka: Yop. Khim. Khim. Tekhnol., 1973, 30, 102-6.

104. R. C. V. Boas and C. M. S. Coelho: Met. ABM, 1973, 29, No. 192, 689-96.

105. A. Aleksandrov: Metalurgiya, 1974, 29, No. 1, 19-22.

106. R. Collee: Trib. CEBEDEAU, 1975, 28, No. 375, 65-80.

107. G. N. Pakhomova: Tsvetnye Metal., 1965, 38, No. 9, 33-6.

108. D. R. Fosnacht: Masters Thesis, Columbia University, New York, NY, 1975.

109. G. N. Znamenskii, V. V. Kardashevskii, and V. V. Stender: J. of Appl. Chem. U.S.S.R., 1961, 34, 1235-1241.

110. Harald Lundin: Trans. Electrochem. Soc., 1933, 63, 149-153.

111. Pietro Guareschi: Industria Chimica, 1934, 9, 1466-76.

112. Niro Matsuura, Masuo Kojima, and Watae Furusawa: J. Chem. Soc. Japan, Pure Chem. Sect., 1953, 74, 337-41.

113. Christa Fischer Bartelk: Freiberger Forschungsh, 1960, B47, 21-40.

114. Isao Kushima, et al.: Suiyokaishi, 1956, 13, 67-79.

115. D. S. Nadezhdin and I. B. Kovaleva: Tsvetnye Metal., 1965, 38, No. 11, 99-100.

116. Peyu Bechev, et al.: Rudodobiv Met., 1966, 21, No. 8, 28-30.

117. S. T. Ross and J. L. Bray: J. Metals, 1951, 3, 465-7.

118. O. V. Zakolodyazhnaya and R. L. Magunov: J. of Appl. Chem. U.S.S.R., 1971, 44, No. 10, 2358-2359.

119. O. A. Khan and L. S. Dukhankina: J. of Appl. Chem. U.S.S.R., 1959, 32, 823-6.

120. O. A. Khan and L. S. Dukhankina: Trudy Altaisk. Gorno-Met. Nauch.-Issledovatel. Inst., Akad. Nauk Kazakh. S.S.R., 1961, 11, 65-75.

121. L. S. Dukhankina and V. D. Ponomarev: Met. i Khim. Prom. Kazakhstana, Nauchn.-Tekhn. Sb., 1962, No. 5, 52-6.

122. L. S. Dukhankina and V. D. Ponomarev: Tr. Inst. Met. i Obogashch. Akad. Nauk Kaz. S.S.R., 1964, 11, 114-18.

123. O. C. Ralston: Eng. Mining Journal, 1930, 130, 606-8.

124. V. Yu. Zaidler, V. D. Ponomorev, and V. V. Stender: J. Appl. Chem. U.S.S.R., 1944, 17, 282-3.

125. U. F. Turomshina and V. V. Stender: J. Appl. Chem. U.S.S.R., 1955, 28, 151-8.

126. Yu B. Kletenik: J. Appl. Chem. U.S.S.R., 1950, 30, 1320-2.

127. G. Z. Kir'yakov, F. K. Bainietova, and R. S. Vakhidov: Trudy Inst. Khim. Nauk, Akad. Nauk S.S.R., 1958, 3, 72-81.

128. R. S. Vakhidov and G. Z. Kir'yakov: Izvest. Vysshikh. Ucheb. Zavedenii, Khim. i Khim. Tekhnol., 1959, 2, 238-43.

129. R. S. Vakhidov and G. Z. Kir'yakov: Izvest. Akad. Nauk Kazakh. S.S.R., Ser. Khim., 1959, No. 1, 44-6.

130. Takeshi Tsuruoka: Nippon Kogyo Kaishi, 1960, 76, 311-18.

131. Takeshi Tsuruoka: Nippon Kogyo Kaishi, 1960, 76, 633-8.

132. Mehdi Ghodsi, Carmen Capel-Baute, and Claude Decroly: Compt. Rend., 1961, 253, 2962-4.

133. Takeshi Tsuruoka: Nippon Kogyo Kaishi, 1961, 77, 995-1003.

134. R. S. Vakhidov and G. Z. Kir'yakov: Met. i Khim. Prom. Kazakhstana, Nauchn. Tekhn. Sb., 1961, No. 1, 56-8.

135. G. N. Pakhomova and L. M. Marenkova: Tsvetnye Metal., 1966, 39, No. 8, 38-41.

136. Reiner Liebscher: Neue Huetee, 1969, 14, No. 10, 597-602.

137. Miguel Saloma and Hans Holtan, Jr.: Acta. Chem. Scand., 1974, 28, No. 1, 93-8.

138. N. I. Ful'man, et al.: Tsvetnye Metal., 1974, No. 5, 22-4.

139. V. V. Stender, G. Z. Kir'yakov, and R. S. Vakhidov: Zhur. Priklad. Khim., 1960, 33, 2238-45.

140. G. N. Znamenskii and B. N. Bez'yazykov: J. Appl. Chem. U.S.S.R., 1965, 38, No. 2, 355-358.

141. Don Cottey: Masters Thesis, Columbia Univ., New York, NY, 1976.

142. Yar-Ming Wang and T. J. O'Keefe: paper presented at 107th Annual Meeting, A.I.M.E., Denver, CO, 1978.

143. Miguel Saloma and Hans Holtan, Jr.: Acta Chem. Scand., 1974, 28, No. 1, 86-92.

144. A. B. Kilimnik and A. L. Rotinyan: J. Appl. Chem. U.S.S.R., 1972, 45, No. 5, 1137-1139.

145. Willibald Machu: Österr. Chem. Ztg., 1939, 42, 244-7.

146. N. P. Diev and L. E. Gurevich: Tsvetnye Metal., 1938, No. 10, 75-84.

147. J. L. Bray and F. R. Morral: Trans. Electrochem. Soc., 1940, 78, preprint.

148. D. I. Derkachev and V. N. Rozov: Tsvetnye Metal., 1938, No. 6, 46-58.

149. V. G. Bundzhe and G. Z. Kir'yakov: Izvest. Akad. Nauk Kazakh. S.S.R., Ser. Khim., 1959, 18-25.

150. A. Riesenkampf: Prace Inst. Hutniczych, 1962, 14, No. 1, 27-36.

151. G. Z. Kir'yakov: Izv. Akad. Nauk Kaz. S.S.R., Ser. Khim., 1962, No. 2, 41-6.

152. F. O. El Kashif, J. Gerlach, and J. Osterwald: Metall., 1968, 22, No. 8, 792-5.

153. Ivan Enchev and I. N. Pishkunov: God. Nauchnovzsled. Inst. Tsvet. Met., Plovdiv, 1967, 5, 51-9.

154. O. S. Stepanova: Sb. Tr. Molodykh. Uch., Tomsk. Politekh. Inst., 1973, No. 1, 21-3.

155. G. Z. Kir'yakov and A. G. Brandt: Izv. Akad. Nauk Kaz. S.S.R., Ser. Khim., 1970, 20, No. 3, 77-9.

156. Toshmichi Fukumoto, et al: Denki Kagaku Oyabi Kogyo Butsuri Kagaku, 1975, 43, No. 2, 94-9.

157. T. N. Anderson, R. D. Budd, and R. W. Strachan: Met. Trans. B., 1976, 7B, No. 9, 333-338.

158. C. J. Krauss: J. Metals, 1976, 28, No. 11, 5-9.

159. J. T. Wood, P. L. Kern, and N. C. Ashdown: J. Metals, 1977, 29, No. 11, 7-11.

160. W. M. Latimer: Oxidation Potentials, 2nd Ed., 341-357, Prentice-Hall, New York, 1952.

161. Robert Garrels and Charles Christ: Solutions, Minerals, and Equilibria, 403-429, Freeman, Cooper & Company, San Francisco, 1965.

162. G. H. Turner: Research, 1951, 4, 246-7.

163. G. N. Znamenskii and B. N. Bez'yazykov: Zhur. Priklad. Khim., 1965, 38, No. 2, 361-5.

164. Niro Matsuura and Masuo Kojima: Sci. Papers Coll. Gen. Educ., Univ. Tokyo, 1952, 2, 47-66.

165. R. Bartonicek: Korose e Ochrana Materialu, 1959, 3, 33-6.

166. N. A. Pangarov, St.D. Vitkova and V. Velinov: Tr. Mezhdunar. Kongr. Korroz. Metal., 1966, 3, 307-16.

167. Richard F. Ashton and Malcolm T. Hepworth: Corrosion, 1968, 24, No. 2, 50-3.

168. G. I. Finch, H. Wilman and L. Yang: Discussions Faraday Soc., 1947, 1, 144-58.

169. J. O. M. Bockris and A. K. N. Reddy: Modern Electrochemistry, Vol. 2, 1212-1218, Plenum Press, New York, 1970.

170. R. Sato: J. Electrochem. Soc., 1959, 106, 206.

171. E. R. Cole, Jr.: Ph.D. Thesis, University of Missouri-Rolla, Rolla, MO, 1970.

172. D. J. Mackinnon and J. M. Brannen: J. Appl. Electrochem., 1977, 7, No. 5, 451-459.

173. F. Albert Cotton and Geoffrey Wilkinson: Advanced Inorganic Chemistry, 2nd ed., p. 492, Interscience Publishers, New York, 1966.

174. G. M. Meisel: J. Metals, 1974, 26, No. 8, 25-32.

175. A. A. Salin: Sbornik Nauch.-Tekh. Trudov, Nauch.-Issledovatel. Inst. Met. Chelyabinsk. Sovnarkhoza, 1960, No. 2, 131-9.

176. V. G. Ageenkov and S. L. Sosunov: Tsvetnye Metal., 1934, No. 5, 61-74.

177. Robert P. Yeck and Yurii E. Lebedeff: U. S. 2, 539, 681, Jan. 30, 1951.

178. Masuo Kojima: J. Chem. Soc. Japan, Pure Chem. Sect., 1953, 74, 434-7.

179. Motoo Watanabe and Seitaro Fukushima: Tohoku Daigaku Senko Seiren Kenkyusho Iho, 1957, 13, 13-19.

180. Motoo Watanabe and Seitaro Fukushima: Sci. Repts. Research Inst., Tohoku Univ., 1958, 10, 68-76.

181. Hisashi Ito and Tetsuo Shibano: Nippon Kogyo Kaishi, 1959, 75, 97-100.

182. Takeshi Tsuruoka: Nippon Kogyo Kaishi, 1959, 75, 1037-44.

183. Isao Kushima and Giroku Miyatani: Suiyokaishi, 1959, 13, 785-8.

184. Guenther Haensel: Neue Huette, 1962, 7, No. 6, 356-62.

185. G. C. Bratt and W. N. Smith: Proc. Australian Conf. Electrochem., 1st, Sydney, Hobart, Australia, 1963, 939-48.

186. Frank S. Gaunce: Fr. 1,419,356, Nov. 26, 1965.

187. T. Rogachev, Violeta Karoleva and Deckko Pavlov: Metalloberflaeche, 1970, 24, No. 11, 421-2.

188. R. S. Vakhidov and G. Z. Kir'yakov: Izvest. Akad. Nauk Kazakh. S.S.R., Ser. Khim., 1960, No. 2, 50-60.

189. Z. A. Sheka and K. F. Karlysheva: Ukrain. Khim. Zhur., 1959, 25, 668-73.

190. P. Radhakrishnamurthy and A. K. N. Reddy: J. Appl. Electrochem., 1975, 5, No. 1, 39-41.

APPENDIX C

Experimental Values for the Current Efficiency Tests

Table IV. Current Efficiency Results for the Factorial Design.

Design Reference Number	Factorial Code	Current Efficiency, % Experimental	Current Efficiency, % Calculated
1	1	93.3	92.3
2	t	94.1	92.8
3	a	86.4	84.1
4	ta	70.5	71.5
5	g	88.5	88.6
6	tg	87.0	85.4
7	ag	76.2	70.7
8	tag	52.9	53.2
9	s	91.1	91.8
10	ts	79.5	82.3
11	as	76.6	79.0
12	tas	38.5	43.5
13	gs	81.2	84.4
14	tgs	52.5	60.4
15	ags	28.4	39.9
16	tags	6.0	18.4
17	c	93.0	90.3
18	tc	78.8	81.7
19	ac	40.3	41.1
20	tac	39.6	35.9
21	gc	88.0	86.8

Table IV (Continued)

Design Reference Number	Factorial Code	Current Efficiency, % Experimental	Current Efficiency, % Calculated
22	tgc	83.2	80.5
23	agc	7.6	21.8
24	tagc	0.9	3.8
25	sc	76.8	78.1
26	tsc	66.2,69.0	70.3
27	asc	48.0	55.7
28	tasc	13.3	21.9
29	gsc	45.0	51.7
30	tgsc	32.4	40.6
31	agsc	0.6	18.4
32	tagsc	5.1,2.5	6.5
33	r	93.0	89.9
34	tr	90.4	85.8
35	ar	85.4	76.6
36	tar	66.4,72.8	69.2
37	gr	89.8	87.6
38	tgr	77.7	78.3
39	agr	67.2	66.7
40	tagr	42.4	41.0
41	sr	86.6	88.0
42	tsr	66.7	67.4

Table IV (Continued)

Design Reference Number	Factorial Code	Current Efficiency, % Experimental	Current Efficiency, % Calculated
43	asr	45.0	50.8
44	tasr	10.0	22.4
45	gsr	68.4	73.7
46	tgsr	44.7	50.6
47	agsr	35.0	42.2
48	tagsr	19.6	22.4
49	cr	92.9	91.5
50	tcr	65.3	71.7
51	acr	31.4	33.0
52	tacr	0.0	-0.5
53	gcr	92.2	91.0
54	tgcr	61.6	68.9
55	agcr	4.0	8.6
56	tagcr	0.0	-0.3
57	scr	56.0	61.7
58	tscr	53.8	58.7
59	ascr	17.0	24.4
60	tascr	12.6	9.0
61	gscr	42.8	51.4
62	tgscr	7.5	22.5
63	agscr	0.0	19.2

Table IV (Continued)

Design Reference Number	Factorial Code	Current Efficiency, % Experimental	Current Efficiency, % Calculated
64	tagscr	0.0	-0.1
65	o	86.9,87.3	93.3
66	to	85.0	86.4
67	ao	73.2	75.6
68	tao	72.9	77.0
69	go	85.3	90.4
70	tgo	78.7	80.3
71	ago	50.6	56.2
72	tago	50.6	55.4
73	so	92.4	96.8
74	tso	88.5	85.7
75	aso	83.6	81.3
76	taso	58.6	58.6
77	gso	91.2	93.2
78	tgso	84.8	77.0
79	agso	76.8	65.3
80	tagso	56.1	48.9
81	co	86.3	85.1
82	tco	91.3	87.2
83	aco	43.5	41.5
84	taco	28.9	28.6

Table IV (Continued)

Design Reference Number	Factorial Code	Current Efficiency, % Experimental	Current Efficiency, % Calculated
85	gco	90.0	87.2
86	tgco	69.6	71.1
87	agco	67.5	52.1
88	tagco	20.1	13.3
89	sco	92.8	85.2
90	tsco	74.0	72.3
91	asco	76.4	69.7
92	tasco	60.9	46.0
93	gsco	85.8	72.8
94	tgsco	61.2	54.1
95	agsco	70.8	54.2
96	tagsco	27.4	18.5
97	ro	84.7	86.7
98	tro	82.4	83.0
99	aro	59.0	63.9
100	taro	70.1,76.0	72.3
101	gro	87.4	88.4
102	tgro	90.8	86.2
103	agro	75.6	72.1
104	tagro	43.2	43.4
105	sro	93.1	92.8

Table IV (Continued)

Design Reference Number	Factorial Code	Current Efficiency, % Experimental	Current Efficiency, % Calculated
106	tsro	86.4	79.5
107	asro	87.2	75.0
108	tasro	64.4	53.0
109	gsro	93.2	89.1
110	tgsro	85.6	73.4
111	agsro	81.4	67.9
112	tagsro	33.6	31.9
113	cro	89.8	91.3
114	tcro	72.5	71.3
115	acro	18.1	21.6
116	tacro	0.9	1.5
117	gcro	88.4	89.6
118	tgcro	74.7	72.5
119	agcro	5.1	5.7
120	tagcro	0.0	0.4
121	scro	83.7	78.1
122	tscro	54.9	55.1
123	ascro	29.0	26.7
124	tascro	0.0	3.6
125	gscro	81.4	72.9
126	tgscro	53.7	43.9

Table IV (Continued)

Design Reference Number	Factorial Code	Current Efficiency, % Experimental	Current Efficiency, % Calculated
127	agscro	62.7,66.1	50.4
128	tagscro	0.9	1.1

Table V. Current Efficiencies for the Center Points and Analysis of Variance for the Factorial Design.

Test #	Current Efficiency, %	Avg., CE	Variance
26	66.2, 69.0	67.6	3.92
32	5.1, 2.5	3.8	3.39
35	66.4, 72.8	69.6	20.52
65	86.9, 87.3	87.1	0.08
99	70.1, 76.0	73.1	17.39
127	62.7, 66.1	64.4	2.89
Center Points:	86.8 82.3	79.3	31.36
	84.4 81.3		
	83.7 78.3		
	84.5 78.0		
	70.0 80.2		
	77.6 74.8		
	68.3		

Pooled Variance = 23.58

Pooled Standard Deviation = 4.86

Table VI. Current Efficiency Results for 12 hour Deposits at 45°C from the Base Electrolyte.

Current Density (ma/cm^2)	Current Efficiency (%)	Reference #
40.4	96.7	1-50-1
40.2	97.2	1-71-1
40.7	97.0	2-4-1
40.3	96.6	2-24-1
40.7	96.6	2-52-5
40.6	96.7	2-59-1

Average Current Efficiency, % = 96.8.

Table VII. Current Efficiency Results for 12 hour Deposits at 40°C from Industrial Electrolyte Containing 60 g/ℓ Zn and 200 g/ℓ H_2SO_4.

Current Density (ma/cm^2)	Current Efficiency (%)	Reference #
30	66.6	3-80-1
	53.6	3-86-1
40	79.5	3-84-1
	69.2	3-86-1
50	77.9	3-80-2
	77.7	3-86-2
60	82.2	3-80-4
	80.8	3-86-3
70	86.7	3-80-5
	78.7	3-82-5
	82.9	3-84-4
80	86.3	3-80-6
	85.1	3-84-3

Table VIII. Current Efficiency Results for 12 hour Deposits at 40°C from Industrial Electrolytes Containing 60 g/ℓ Zn and Various Concentrations of H_2SO_4.

Acid Concentration G/ℓ H_2SO_4	Current Density (ma/cm^2)	Current Efficiency (%)	Reference #
0	70.1	94.7	3-82-1
50	70.1	95.9	3-82-2
100	70.1	93.9	3-82-3
150	70.1	90.8	3-82-4
200	70.1	86.7	3-80-5
	70.1	78.7	3-82-5
	70.1	82.9	3-84-4
250	70.1	54.7	3-82-6

Table IX. Current Efficiency Results for 12 hour Deposits at 45°C from Electrolytes Containing Antimony and 100 g/ℓ H_2SO_4.

Antimony Concentration PPB, Sb	Current Density (ma/cm^2)	Current Efficiency (%)	Reference #
7	39.7	95.0	2-10-1
	40.8	95.0	2-11-1
	40.6	93.4	2-59-2
13	40.3	92.5	2-63-6
14	39.7	92.6	2-10-2
	40.8	92.3	2-11-2
21	39.7	91.6	2-10-3
	40.8	91.0	2-11-3
28	40.4	87.7	2-61-1
	40.2	79.8	2-85-3
35	40.4	86.4	2-12-1
42	40.4	83.9	2-12-2
52	40.4	80.4	2-61-2
78	40.4	72.4	2-61-3
104	40.4	61.1	2-61-4
130	40.4	56.7	2-61-5
156	40.4	48.7	2-61-6

Table X. Current Efficiency Results for 12 hour Deposits at 45°C from Electrolytes Containing Antimony and 150 g/ℓ H_2SO_4.

Antimony Concentration PPB, Sb	Current Density (ma/cm^2)	Current Efficiency (%)	Reference #
0	40.3	94.8	2-70-1
6.5	40.3	92.6	2-71-1
13	40.3	88.9	2-71-2
26	40.3	83.3	2-71-3
39	40.3	79.9	2-71-4
52	40.3	72.9	2-71-5
65	40.3	66.0	2-71-6

Table XI. Current Efficiency Results for 12 hour Deposits at 45°C from Electrolytes Containing Arsenic and 100 g/ℓ H_2SO_4.

Concentration PPB, As	Current Density (ma/cm^2)	Current Efficiency (%)	Reference #
20	40.4	96.3	2-81-4
	40.5	96.3	2-82-2
40	40.4	96.5	2-81-5
	40.5	96.0	2-82-3
60	40.5	94.7	2-82-4
80	40.4	96.2	2-81-6
	40.5	93.8	2-82-5
100	40.5	93.8	2-82-6

Table XII. Current Efficiency Results for 12 hour Deposits at 45°C from Electrolytes Containing Arsenic and Varying Acid Concentrations.

Concentration PPB, As	Concentration G/L, H_2SO_4	Current Density (ma/cm^2)	Current Efficiency (%)	Reference #
80	100	40.4	96.2	2-81-6
		40.5	93.8	2-82-5
		40.4	92.2	2-90-1
80	150	40.4	73.7	2-90-2
80	200	40.4	55.9	2-90-3

Table XIII. Current Efficiency Results for 12 hour Deposits at 45°C from Electrolytes Containing Cobalt and 100 g/ℓ H_2SO_4.

Cobalt Concentration PPM, Co	Current Density (ma/cm^2)	Current Efficiency (%)	Reference #
1	39.5	97.4	1-59-4
	40.6	96.4	2-14-1
3	40.5	95.8	2-16-1
	40.0	95.3	2-60-5
5	39.1	95.5	1-61-1
	40.7	94.0	2-4-4
10	39.6	94.2	1-63-2
	40.5	92.7	1-92-3
	39.2	92.4	1-72-1
	39.6	91.7	1-45-1
15	40.0	91.2	1-73-1
	40.7	90.3	2-4-5
	40.0	92.9	2-60-6
20	40.5	85.2	1-93-1
	39.8	86.4	1-91-2
	39.8	80.8	1-91-1
	42.1	79.7	1-74-1
25	40.0	62.8	1-73-2
	40.5	81.5	1-92-1
	40.5	72.7	1-93-2
35	40.5	45.9	1-92-2
	40.5	29.8	1-93-3
	40.0	18.5	1-73-3

Table XIV. Current Efficiency Results for 12 hour Deposits at 45°C from Electrolytes Containing Cobalt and 150 g/ℓ H_2SO_4.

Cobalt Concentration PPM, Co	Current Density (ma/cm^2)	Current Efficiency (%)	Reference #
0	40.3	94.8	2-70-1
3	40.5	93.5	2-68-1
5	40.5	92.5	2-68-2
10	40.5	64.8	2-68-3
15	40.5	51.5	2-68-4
20	40.5	41.4	2-68-5

Table XV. Current Efficiency Results for 12 hour Deposits at 45°C from Electrolytes Containing Germanium and 100 g/ℓ H_2SO_4.

Germanium Concentration PPB, Ge	Current Density (ma/cm^2)	Current Efficiency (%)	Reference #
10	40.2	95.9	2-2-1
	40.7	96.2	2-4-2
20	40.2	94.9	2-2-2
	40.0	94.3	2-3-2
	40.5	95.2	2-58-1
	40.5	94.7	2-58-2
	40.5	94.7	2-58-3
40	40.2	93.8	2-2-3
	40.0	91.7	2-3-3
	40.5	91.3	2-58-4
	40.5	91.0	2-58-5
	40.5	90.3	2-58-6
60	40.2	90.4	2-2-4
	40.0	87.9	2-3-4
	40.6	86.9	2-59-4
	40.6	86.1	2-59-5
	40.6	86.2	2-59-6
	40.6	86.5	2-55-1
80	40.2	88.4	2-2-5
	40.0	85.7	2-3-5
	39.5	88.4	1-59-3
	39.4	87.0	1-65-1
	40.3	83.0	1-67-1
	39.2	83.8	1-70-1
	39.2	83.3	1-70-3
	39.2	80.9	1-70-2
	40.4	86.2	2-56-1

Table XV (Continued)

Germanium Concentration PPB, Ge	Current Density (ma/cm^2)	Current Efficiency (%)	Reference #
80	40.4	85.5	2-56-2
	40.4	82.5	2-56-3
	40.4	84.0	2-56-4
	40.4	82.8	2-56-5
100	40.4	79.0	2-56-6
	40.4	81.8	2-57-1
	40.4	76.5	2-57-2
	40.4	76.4	2-9-3
	40.4	74.6	2-9-4
	40.5	81.6	2-39-1
	40.5	78.2	2-39-2

Table XVI. Current Efficiency Results for 12 hour Deposits at 45°C from Electrolytes Containing Germanium and 150 g/ℓ H_2SO_4.

Germanium Concentration PPB, Ge	Current Density (ma/cm^2)	Current Efficiency (%)	Reference #
0	40.3	94.8	2-70-1
10	40.3	93.2	2-70-2
20	40.3	92.0	2-70-3
30	40.3	88.7	2-70-4
40	40.3	88.4	2-70-5
	40.5	86.9	2-39-3
60	40.3	83.8	2-70-6

Table XVII. Current Efficiency Results for 12 hour Deposits at 45°C from Electrolytes Containing Glue and 100 g/ℓ H_2SO_4.

Glue Concentration PPM, Glue	Current Density (ma/cm^2)	Current Efficiency (%)	Reference #
1.0	40.5	96.7	1-88-1
1.7	40.5	96.5	1-88-2
3.4	40.5	96.3	1-88-3
5.2	40.0	97.1	1-89-1
6.9	40.0	96.0	1-89-2
8.6	40.0	95.5	1-89-3
10.3	40.3	94.8	2-18-1
20.6	40.3	92.3	2-18-2
41.3	40.3	88.9	2-18-3
82.6	40.3	84.9	2-18-4

Table XVIII. Current Efficiency Results for 12 hour Deposits at 45°C from Electrolytes Containing Gum Arabic and 100 g/ℓ H_2SO_4.

Gum Arabic Concentration PPM, Gum Arabic	Current Density (ma/cm^2)	Current Efficiency (%)	Reference #
22	40.6	92.6	2-26-3
33	40.1	91.3	2-31-1
44	40.1	89.7	2-31-2
55	40.6	88.8	2-26-4
66	40.1	87-9	2-31-3
77	40.1	87.7	2-31-4
88	40.6	86.2	2-26-5

Table XIX. Current Efficiency Results for 12 hour Deposits at 45°C from Electrolytes Containing Chloride and 100 g/ℓ H_2SO_4.

HCl Concentration PPM, HCl	Current Density (ma/cm^2)	Current Efficiency (%)	Reference #
99	40.6	96.3	2-28-1
198	40.6	96.4	2-82-2
297	40.6	95.7	2-28-3
396	40.6	95.5	2-28-4
495	40.6	95.6	2-28-5

Table XX. Current Efficiency Results for 12 hour Deposits at 45°C from Electrolytes Containing Antimony and Germanium and 100 g/ℓ H_2SO_4.

Impurity Concentration PPB, Sb	PPb, Ge	Current Density (ma/cm^2)	Current Efficiency (%)	Reference #
13	20	40.3	87.8	2-63-1
		40.4	84.0	2-66-1
13	40	40.3	81.0	2-63-2
		40.4	73.0	2-66-2
13	60	40.3	74.4	2-63-3
		40.4	65.8	2-66-3
13	80	40.3	72.3	2-63-4
		40.4	52.5	2-66-4
13	100	40.3	57.4	2-63-5
		40.4	47.3	2-66-5

Table XXI. Current Efficiency Results for 12 hour Deposits at 45°C from Electrolytes Containing Antimony and Glue and 100 g/ℓ H_2SO_4.

Impurity Concentration PPB, Sb	PPM, Glue	Current Density (ma/cm^2)	Current Efficiency (%)	Reference #
7	20.6	40.4	94.3	2-35-1
14	20.6	40.4	94.2	2-35-2
21	20.6	40.4	93.5	2-35-3
28	20.6	40.4	93.3	2-35-4
35	20.6	40.4	93.1	2-35-5
104	1	40.3	68.4	2-69-1
104	3	40.3	71.6	2-69-2
104	6	40.3	74.4	2-69-3
104	10	40.3	75.2	2-69-4
104	13	40.3	79.0	2-69-5
104	18	40.3	85.3	2-69-6

Table XXII. Current Efficiency Results for 12 hour Deposits at 45°C from Electrolytes Containing Antimony and Gum Arabic and 100 g/ℓ H_2SO_4.

Impurity Concentration PPB, Sb	Impurity Concentration PPM, Gum Arabic	Current Density (ma/cm^2)	Current Efficiency (%)	Reference #
7	22	40.7	94.8	2-32-1
14	22	40.7	94.4	2-32-2
21	22	40.7	93.6	2-32-3
28	22	40.7	93.3	2-32-4
35	22	40.7	92.5	2-32-5

Table XXIII. Current Efficiency Results for 12 hour Deposits at 45°C from Electrolytes Containing Cobalt and Antimony and 100 g/ℓ H_2SO_4.

Impurity Concentration PPM, Co	PPB, SB	Current Density (ma/cm^2)	Current Efficiency (%)	Reference #
1	7	40.6	94.4	2-14-2
1	14	40.6	92.4	2-14-3
1	21	40.6	90.3	2-14-4
1	28	40.6	89.0	2-14-5
3	7	40.5	94.0	2-16-2
3	14	40.5	91.6	2-16-3
3	21	40.5	88.7	2-16-4
3	28	40.5	86.3	2-16-5
5	7	40.5	87.0	2-13-1
5	14	40.5	84.6	2-13-2
5	21	40.5	79.3	2-13-3
5	28	40.4	65.8	2-12-3
		40.5	71.2	2-13-4
10	28	40.4	52.5	2-12-4
15	28	40.4	27.1	2-12-5

Table XXIV. Current Efficiency Results for 12 hour Deposits at 45°C from Electrolytes Containing Cobalt, Antimony, and Glue and 100 g/ℓ H_2SO_4.

Impurity Concentration PPM, Co	PPB, Sb	PPM, Glue	Current Density (ma/cm^2)	Current Efficiency (%)	Reference #
5	7	20.6	40.8	91.2	2-25-2
5	14	20.6	40.8	91.5	2-25-3
5	21	20.6	40.8	89.4	2-25-4
5	28	20.6	40.8	88.4	2-25-5
			41.2	85.2	2-22-2

Table XXV. Current Efficiency Results for 12 hour Deposits at 45°C from Electrolytes Containing Cobalt and Germanium and 100 g/ℓ H_2SO_4.

Impurity Concentration PPM, Co	PPB, Ge	Current Density (ma/cm^2)	Current Efficiency (%)	Reference #
1	100	40.4	81.7	2-43-1
3	100	40.4	78.7	2-43-2
5	20	40.8	92.0	2-27-1
		40.8	92.0	2-27-1
5	40	40.2	84.5	2-30-2
		40.8	89.8	2-27-2
5	60	40.2	77.4	2-30-3
		40.8	80.0	2-27-3
5	80	40.2	69.2	2-30-4
		40.8	73.5	2-27-4
5	100	40.2	67.4	2-30-5
		40.8	67.5	2-27-5

Table XXVI. Current Efficiency Results for 12 hour Deposits at 45°C from Electrolytes Containing Cobalt, Germanium, and Glue and 100 g/ℓ H_2SO_4.

Impurity Concentration PPM, Co	PPM, Glue	PPB, Ge	Current Density (ma/cm^2)	Current Efficiency (%)	Reference #
5	3	100	40.3	87.9	2-42-1
			40.7	82.1	2-48-1
5	6	100	40.3	90.9	2-42-2
			40.7	90.4	2-48-2
5	9	100	40.3	92.9	2-42-3
			40.7	92.7	2-48-3
5	12	100	40.3	93.1	2-42-4
			40.7	92.6	2-48-4
5	15	100	40.3	92.6	2-42-5
			40.7	93.3	2-48-5

Table XXVII. Current Efficiency Results for 12 hour Deposits at 45°C from Electrolytes Containing Cobalt and Glue and 100 g/ℓ H_2SO_4.

Impurity Concentration PPM, Co	PPM, Glue	Current Density (ma/cm^2)	Current Efficiency (%)	Reference #
5	10	40.3	93.5	2-24-2
5	20	40.3	92.3	2-24-3
		40.8	91.8	2-25-1
5	40	40.3	88.6	2-24-4
5	80	40.3	84.9	2-24-5

Table XXVIII. Current Efficiency Results for 12 hour Deposits at 45°C from Electrolytes Containing Germanium and Glue and 100 g/ℓ H_2SO_4.

Impurity Concentration PPB, Ge	PPM, Glue	Current Density (ma/cm^2)	Current Efficiency (%)	Reference #
20	20	40.0	92.4	2-36-1
40	20	40.0	91.9	2-36-2
60	20	40.0	91.4	2-36-3
80	20	40.0	91.6	2-36-4
100	1	40.5	81.2	2-67-1
100	3	40.5	86.4	2-67-2
100	6	40.5	90.8	2-67-3
100	10	40.5	92.2	2-67-4
100	13	40.5	92.3	2-67-5
100	18	40.5	91.1	2-67-6
100	20	40.0	91.5	2-36-5

Table XXIX. Current Efficiency Results for 12 hour Deposits at 45°C from Electrolytes Containing Glue and Chloride and 100 g/ℓ H_2SO_4.

Impurity Concentration PPM, Glue	PPM, HCl	Current Density (ma/cm^2)	Current Efficiency (%)	Reference #
10	198	40.7	93.2	2-34-1
20	198	40.7	93.7	2-34-2
40	198	40.6	92.6	2-26-1
		40.7	91.6	2-34-3
50	198	40.7	91.0	2-34-4
80	198	40.7	88.0	2-34-5

Table XXX. Current Efficiency Results for 12 hour Deposits at 45°C from Electrolytes Containing Gum Arabic and Chloride and 100 g/ℓ H_2SO_4.

Impurity Concentration PPM, Gum Arabic	PPM, HCl	Current Density (ma/cm^2)	Current Efficiency (%)	Reference #
11	198	40.3	95.8	2-33-1
22	198	40.3	94.7	2-33-2
44	198	40.3	92.3	2-33-3
		40.6	92.0	2-26-2
66	198	40.3	90.9	2-33-4
88	198	40.3	88.6	2-33-5

Table XXXI. Current Efficiency Results for 24 hour Deposits at 45°C from Electrolytes Containing Various Impurities and 100 g/ℓ H_2SO_4.

Impurity Concentration PPM, Co	PPB, Ge	PPB, Sb	Current Density (ma/cm^2)	Current Efficiency (%)	Reference #
0	0	0	40.4	95.7	2-72-1
5	0	0	40.4	94.8	2-72-2
0	40	0	40.4	88.6	2-72-3
0	0	20	40.4	88.5	2-72-4
5	20	0	40.4	86.4	2-72-5
5	0	13	40.4	84.5	2-72-6

Table XXXII. Current Efficiency Results for 12 hour Deposits at 45°C from Electrolytes Containing Arsenic and Other Impurities and 100 g/ℓ H_2SO_4.

Impurity Concentration				Current Density	Current Efficiency	
PPB, As	PPM, Co	PPB, Ge	PPB, Sb	(ma/cm^2)	(%)	Reference #
80	4	0	0	40.4	41.7	2-90-6
80	0	20	0	40.4	74.9	2-90-4
80	0	0	13	40.4	59.3	2-90-5

Table XXXIII. Current Efficiency Results for 12 hour Deposits at 35°C from Electrolytes Containing Various Impurities and 100 g/ℓ H_2SO_4.

Impurity Concentration	Current Density (ma/cm^2)	Current Efficiency (%)	Reference #
20 PPM Glue	60.1	86.9	3-11-1
40 PPB As	60.1	86.4	3-11-2
40 PPB Ge	60.1	83.0	3-11-3
2.4 PPM Co	60.1	91.5	3-11-4
20 PPB Sb	60.1	79.9	3-11-5
No addition	60.1	93.8	3-11-6

Table XXXIV. Current Efficiency Results for 12 hour Deposits at 35°C from Electrolytes Containing Various Impurities and 200 g/ℓ H_2SO_4.

Impurity Concentration	Current Density (ma/cm^2)	Current Efficiency (%)	Reference #
20 PPM Glue	60.2	73.2	3-13-1
40 PPB As	60.2	76.8	3-13-2
40 PPB Ge	60.2	58.1	3-13-3
2.4 PPM Co	60.2	30.2	3-13-4
20 PPB Sb	60.2	64.2	3-13-5
No addition	60.2	86.4	3-13-6
	60.2	88.1	3-29-1

APPENDIX D

Calculated Factor Effects for the Factorial Design

Table XXXV. Factors and Factor Effects for the Factorial Design.

Factor	Calculated Factor Effect
mean	58.99
t	-16.475
a	-37.275
ta	-3.275
g	-11.322
tg	-2.481
ag	-2.587
tag	0.378
s	-9.190
ts	-4.844
as	5.106
tas	-1.059
gs	-2.703
tgs	0.263
ags	3.094
tags	1.497
c	-23.603
tc	-2.188
ac	-11.287
tac	2.541
gc	0.109
tgc	0.106

Table XXXV (Continued)

Factor	Calculated Factor Effect
agc	2.125
tagc	0.784
sc	1.972
tsc	1.850
asc	9.437
tasc	0.291
gsc	-1.028
tgsc	-1.719
agsc	1.150
tagsc	-1.341
r	-9.631
tr	-1.941
ar	-3.884
tar	1.031
gr	3.744
tgr	-0.372
agr	2.028
tagr	-0.738
sr	-1.744
tsr	0.147
asr	1.153
tasr	-0.569

Table XXXV (Continued)

Factor	Calculated Factor Effect
gsr	1.894
tgsr	-1.922
agsr	2.066
tagsr	-1.062
cr	-6.331
tcr	-0.509
acr	-3.041
tacr	1.744
gcr	1.144
tgcr	1.137
agcr	0.434
tagcr	2.125
scr	0.262
tscr	0.097
ascr	1.053
tascr	-0.813
gscr	1.125
tgscr	-3.009
agscr	0.403
tagscr	-1.406
o	13.284
to	-0.688

Table XXXV (Continued)

Factor	Calculated Factor Effect
ao	3.119
tao	-2.478
go	6.678
tgo	-3.100
ago	0.637
tago	-4.166
so	13.815
tso	-2.506
aso	2.100
taso	-1.884
gso	2.497
tgso	-0.381
agso	-2.381
tagso	-2.397
co	2.591
tco	-4.525
aco	-0.569
taco	-2.122
gco	1.909
tgco	-1.375
agco	2.262
tagco	-0.534

Table XXXV (Continued)

Factor	Calculated Factor Effect
sco	-2.184
tsco	-2.037
asco	-2.844
tasco	1.803
gsco	0.597
tgsco	0.300
agsco	-1.737
tagsco	-1.434
ro	-0.475
tro	0.072
aro	-3.641
taro	-1.469
gro	-0.331
tgro	0.684
agro	-2.272
tagro	-1.931
sro	0.075
tsro	-3.003
asro	-0.566
tasro	-1.581
gsro	-1.019
tgsro	-0.103

Table XXXV (Continued)

Factor	Calculated Factor Effect
agsro	-0.097
tagsro	0.956
cro	-4.125
tcro	0.966
acro	-3.509
tacro	0.869
gcro	0.531
tgcro	2.953
agcro	0.509
tagcro	0.694
scro	-0.694
tscro	-1.666
ascro	-0.203
tascro	-1.775
gscro	4.375
tgscro	0.434
agscro	4.316
tagscro	-0.325

APPENDIX E

Statistical Evaluation of the Fit of the Model to the Experimental System for the Factorial Design and Determination of Curvature

Using an F test, the "goodness of fit" of the model derived using the calculated factor effects from the factorial study can be evaluated. The variance of the calculated versus experimental values of the current efficiencies is 42.45. The calculated F ratio is 1.80. The F statistic for 127 and 18 degrees of freedom respectively and a probability level of 0.95 is 1.95.* Since the calculated value is less than this, the model provides a reasonable representation of the data within the limits of the experimental error.

In order to test for curvature, thirteen center point tests were conducted. The conditions employed were half-way between the high and low levels reported for the statistical design. The average of the center points is 79.3. The calculated mean for the factorial study is 58.99. The difference between these two values is 20.3. Since this exceeds the curvature statistic (4.1), significant curvature exists for the system and at least one variable has non-zero curvature associated with it. The model will not fit as well at other values of the factors used in the design.

---

*Sylvain Ehrenfeld and Sebastian B. Littauer: Introduction to Statistical Method, p. 523, McGraw-Hill Book Company, New York, 1964.

APPENDIX F

Method of Computation Used to Determine the Factor Effects and Calculated Current Efficiencies for the Statistically-Designed Experiment

A computer program based on the "Table of Signs" Computation technique was used to determine the factor effects and calculated current efficiencies for the various factors used in this design.

The main effect of a factor is found by determining the average of the differences between the responses at the high and low levels of the factor. This average value is the calculated factor effect. The interaction effects are determined by calculating the average of differences of diagonally opposite pairs of points. For a simple 2-factor design, this interaction is given by:

$$\text{Interaction} = \frac{(Y_{LL} + Y_{HH})}{2} - \frac{(Y_{LH} + Y_{HL})}{2}$$

where Y_{AB} = Response Value

A = Factor level of factor 1

B = Factor level of factor 2.

The calculation of interaction effects for more complex designs is similar, but much more involved.

Seven factors are considered in the experimental design used in this study. The main effects of each factor were calculated as described above. The interactions of the various factors were determined by adding the various response values according to the table of signs generated for the particular combination of factors. A

computer program was used to generate the table of signs and to calculate the factor effects for all the 128 factors and interactions that were possible.

After the factor effects were computed, they were placed in a statistical model and current efficiencies were calculated for the various factor levels used in the design. The calculated and experimental current efficiencies were compared and the variability between the generated and experimental values determined.

A copy of the program used for calculating the factor effects and a program deck are available at the Metallurgy Department Office and at the Materials Research Center. The program contains instructions explaining its use. Subroutine MULT of the program generates the tables of signs used in subsequent calculations. The actual calculation of the factor effects is done using Subroutine BOZO. The program as written can handle up to 7 factors. Slight modification would be required if more than 7 factors are considered.

Reference: Strategy of Experimentation, E. I. du Pont de Nemours & Co., Wilmington, Delaware, 1975.

APPENDIX G

Determination of Zinc Concentration by EDTA Titration

Zinc concentrations for the neutral purified solutions were detected by direct titration with EDTA, using Eriochrome Black T as the indicator. The procedure followed is given below.

Procedure:

1. Prepare a 0.01 M solution of EDTA from the di-sodium salt. The solution is prepared by first drying the salt to remove surface moisture and then weighing 3.72 g of the salt and placing this in a 1000 mℓ flask. Distilled water is then added to dissolve the EDTA. The solution is then standardized using a solution of known zinc concentration.
2. An Eriochrome Black T indicator solution is prepared by dissolving 200 mg of the solid in 15 mℓ of Triethanolamine and 5 mℓ of absolute alcohol.
3. A pH 10 buffer is prepared by mixing 570 mℓ of aqueous NH_3 and 70 g of $NH_4C\ell$ with distilled water using a 1000 m volumetric flask.
4. Using the above reagents, a sample of the neutral solution is then titrated. A 10 mℓ sample of the neutral solution is placed in a 500 mℓ volumetric flask and diluted to 1/50 of its original concentration using distilled water. A 5 mℓ aliquot is taken from the diluted solution and placed in the titrating vessel. 10 to 15 mℓ of the pH 10 buffer and 3 to 4 drops of the

indicator are then added to this vessel. The sides of the container are washed with distilled water. The contents are then titrated with the standardized EDTA solution until the purple color of the solution completely disappears and a deep blue color is found. The volume of the titrant used is then noted and the zinc concentration of the original solution calculated using the relation below. The titration is then repeated.

$$g/l\ Zn = \text{vol. titrant} \times M\ EDTA \times 50 \times 65.37/5$$

Reference: Douglas A. Skoog and Donald M. West: Fundamentals of Analytical Chemistry, 2nd ed., pp. 352-357, Holt, Rinehart and Winston, Inc., New York, 1969.

APPENDIX H

Analysis of Zinc Oxide Powder Used to Prepare Neutral Purified Solution

The zinc oxide powder used to prepare the neutral purified zinc sulfate solutions was obtained from ASARCO, Inc., P. O. Box 538, Hillsboro, Illinois, 62049. Two different lots of comparable composition were used. The physical and chemical characteristics of the zinc oxide powder are given below.

Lot No.	91-5935	71-5542
Date Produced	5-14-69	3-6-77
% Zn	80.25	80.25
% ZnO	99.89	99.89
% Pb	0.0019	0.0019
% Cd	0.0024	0.0014
% H_2O	0.097	0.008
% +325 mesh	0.0008	0.0008
Specific Surface Area - m^2/g	3.33	3.23
Average Particle Diameter - Calorimeter, Microns	0.324	0.330
Average Particle Diameter - Air Permeability, Microns	0.323	0.333

APPENDIX I

Possible Future Research

The results of this investigation show the importance of impurity interaction on the zinc electrodeposition process. Changes in current efficiency, morphology, and polarization are caused by low concentrations of impurity. The techniques used in the present study should be applied in the future to measure the effects of other impurities such as nickel, iron, manganese, and copper. Cyclic voltammetry investigations on these impurities may allow classification of their effects according to their mechanism of interaction at the cathode. Constant current electrolyses should also be conducted on electrolytes containing the above impurities and for combinations of these impurities with the impurities (Ge, As, Sb, and Co) considered in the present investigation. The additional process parameters of electrolysis time and current density should be examined in conjunction with the impurity behavior. Both classical and statistically-designed experiments should be conducted.

Cyclic voltammetry techniques which measure the anodic to cathodic areas should be studied in relation to electrolyte purity. A factorial design using the a/c ratio instead of the current efficiency may lead to a rapid method of electrolyte characterization. Long-time electrolyses using the same levels and factors as the a/c ratio tests should also be conducted to see if a correlation between the two testing procedures can be found. If a correlation is obtained, a practical means of electrolyte characterization may result.

The results of this investigation and that of other investigations

(see literature review) indicate that synergism among impurities can be very significant. Further studies should be conducted to see if the mechanisms of joint impurity interaction can be explained. Some of the combinations of impurities which warrant further study include: Co, Ni, Fe, Cu, and Ge with Mn; As with Co; Ni, Fe, Cu with glue; and, antimony and glue with Co, Fe, Ni, Cu, and Ge. The effects of the various combinations of impurities and additives on current efficiency, deposit morphology, and polarization should be examined using both cyclic voltammetry and long-time electrolyses.